University
of Ljubljana
Faculty
for Civil and Geodetic Engineering

SYEDA KHUSHNUMA WASIM

PREDICTABILITY OF FLASH FLOODING IN SLOPING DUTCH CATCHMENTS

(RUR, NIERS AND SWALM RIVERS)

MASTER'S THESIS

MASTER STUDY PROGRAMME FLOOD RISK MANAGEMENT

Univerza *v Ljubljani*

UNESCO IHE DELFT

TECHNISCHE UNIVERSITÄT DRESDEN

UNIVERSITAT POLITÈCNICA DE CATALUNYA BARCELONATECH

Deltares

Ljubljana, 2022

University
of Ljubljana
Faculty
*for Civil and Geodetic
Engineering*

Candidate

SYEDA KHUSHNUMA WASIM

PREDICTABILITY OF FLASH FLOODING IN SLOPING DUTCH CATCHMENTS

(RUR, NIERS AND SWALM RIVERS)

Mentor:
Prof. Dr. Albrecht Weerts (Deltares)
Dr. Matthijs den Toom (Deltares)

Supervisor:
Assist. Prof. Simon Rusjan, Ph.D.
Commission member:
Dr. Schalk Jan van Andel (IHE Delft)

Chairman of the Commission:
Assist.Prof. Simon Rusjan, Ph.D.

Ljubljana, 22. August. 2022

Univerza *v Ljubljani*

"This page is intentionally blank"

I, (Syeda Khushnuma Wasim), registration number (26125063), author of the written thesis of the study entitled: Predictability of flash flooding in sloping Dutch Catchments (Rur, Niers and Swalm Rivers).

I DECLARE

1. Circle one of variants a) or b)
    a) that the written final work of the study is the result of my independent work;

    b) that the written final work of the study is the result of the own work of several candidates and meets the conditions set out in the UL Statute for joint final work of the study and is in the required proportion the result of my independent work;

2. that the printed form of the written final part of the study is identical to the electronic form of the written final part of the study;

3. that I have obtained all the necessary permissions for the use of data and copyrighted works in the written final part of the study and clearly marked them in the written final part of the study;

4. that in preparing the written final part of the study I acted in accordance with ethical principles and, where necessary, obtained the consent of the ethics commission for the research;

5. I agree that the electronic form of the written final part of the study is used to check the similarity of the content with other parts with the software for checking the similarity of the content related to the study information system of the member;

6. to transfer to UL free of charge, non-exclusively, spatially and indefinitely the right to store the author's work in electronic form, the right to reproduce and the right to make the written final part of the study available to the public on the World Wide Web through the UL Repository;

7. dissertations. UL consents enable free, non-exclusive, space and time unlimited storage of the author's work in electronic form and reproduction and making the dissertation available to the public on the World Wide Web through the UL Repository;

8. that I allow the publication of my personal data, which are stated in the written final part of the study and this statement, together with the publication of the written final part of the study.

V / Na:

Date:22/08/2021
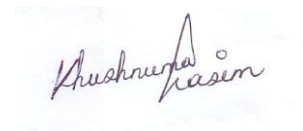
Student's signature / -to:

"This page is intentionally blank"

Wasim, S.K. 2022. Predictability of Flash Flooding in Sloping Dutch Catchments (Rur, Niers and Swalm Rivers)

Ljubljana, UL FGG, Masters of Science Thesis in Flood Risk Management.

ERRATA

Error page	Error bar	Instead	Let it be

ACKNOWLEDGEMENTS

Wasim, S.K. 2022. Predictability of Flash Flooding in Sloping Dutch Catchments (Rur, Niers and Swalm Rivers)

III

Ljubljana, UL FGG, Masters of Science Thesis in Flood Risk Management.

BIBLIOGRAPHIC-DOCUMENTALISTIC INFORMATION AND ABSTRACT

Abstract

The Dutch province Limburg is characterized by sloping terrain and is therefore prone to serious damages during flash floods. This was also the case for the July 2021 flood event. The study focuses on a detailed hydrological analysis and the generation of deterministic flood forecasts of the tributaries of the Meuse River in Limburg (i.e. Rur, Niers and Swalm rivers). For hydrological modeling, the wflow_sbm model was used which is a distributed hydrological model and its parameters were estimated with the Iterative Hydrography Upscaling (IHU) method and from Pedo Transfer Functions (PTFs). The horizontal hydraulic conductivity fraction (KsatHorFrac) parameter for the Rur catchment was calibrated to generate deterministic forecasts. Due to the significant difference between the observed and the simulated discharges of the Niers and Swalm catchments it was not possible to calibrate their hydrological models. Probable reasons for this difference can be the effects of ground water abstractions for pit mining and other purposes, frequent mowing management in the Niers catchment etc. Therefore forecasts were generated only for the Rur catchment by coupling the wflow model with Delft-FEWS. The forecasts generated using the DWD ICON dataset showed substantial error when compared to the observed discharge. However, for the flood event of 2021, the model predicted high flows 5-6 days ahead of the flood. There was a large overestimation of the peak for the forecast in downstream of the Rur catchment. The sensitivity of the forecast performance by changing KsatHorFrac was also analysed in the end. The findings of the study show several scopes of improvements in the wflow hydrological modeling and flood forecasting of the Meuse tributaries. Future studies based on these recommendations could aid in providing a more accurate flood prediction in this region.

BIBLIOGRAFSKO – DOKUMENTACIJSKA STRAN IN IZVLEČEK

Izvleček:

Območje Limburga na Nizozemskem z relativno strmo topografijo terena je med poplavami julija 2021 utrpelo veliko poplavno škodo. Magistrska naloga se osredotoča na podrobne hidrološke analize in izdelavo deterministične napovedi poplav pritokov reke Meuse na območju Limburga (prispevna območja rek Rur, Niers in Swalm). Za potrebe hidrološkega modeliranja je bil uporabljen prostorsko distribuiran hidrološki model wflow_sbm, parametri modela so bili ocenjeni z metodo Iterative Hydrography Upscaling (IHU) in s pomočjo Pedo Transfer Function (PTF). Parameter horizontalne hidravlične prevodnosti (KsatHorFrac) v hidrološkem modelu prispevnega območja reke Rur je bil umerjen in na podlagi tega so bile izdelane deterministične hidrološke napovedi. Zaradi znatnih razlik med opazovanimi in simuliranimi pretoki rek Niers in Swalm ni bilo mogoče detajlno umeriti hidroloških modelov za prispevni območji teh dveh rek. Najverjetnejši vzroki za ugotovljena razhajanja med merjenimi in modeliranimi pretoki so velike količine odvzete vode za različne rabe ter izvaje regulacijskih in vzdrževalnih del v strugi reke Niers. Zato so bile hidrološke napovedi izdelane za prispevno območje reke Rur z združeno uporabo modelov wflow in Delft-FEWS. Hidrološke napoved, ustvarjena z uporabo nabora vhodnih hidrometeoroloških podatkov iz baze DWD ICON, so se izkazale kot precej nenatančne. Navkljub slabšim rezultatom simulacij je bil model sposoben za poplavni dogodek, ki se je zgodil leta 2021, napovedal visokovodne razmere 6 dni pred dejanskim pojavom poplavnega dogodka. Simulirane vrednosti pretoka so bile precenjene predvsem v spodnjem delu prispevnega območja reke Rur. Na koncu smo analizirali tudi občutljivost hidroloških napovedi na spremenjene vrednosti parametra KsatHorFraca. Izsledki študije nakazujejo možnosti izboljšav pri hidrološkem modeliranju z uporabo programa wflow in napovedovanju poplav hudourniških pritokov reke Meuse. Nadaljnje študije, ki temeljijo na naših ugotovitvah, bi lahko zagotovile natančnejšo napoved poplav v obravnavani regiji.

Wasim, S.K. 2022. Predictability of Flash Flooding in Sloping Dutch Catchments (Rur, Niers and Swalm Rivers)

V

Ljubljana, UL FGG, Masters of Science Thesis in Flood Risk Management.

TABLE OF CONTENTS

Wasim, S.K. 2022. Predictability of Flash Flooding in Sloping Dutch Catchments (Rur, Niers and Swalm Rivers)

VII

Ljubljana, UL FGG, Masters of Science Thesis in Flood Risk Management.

LIST OF FIGURES

LIST OF TABLES

Wasim, S.K. 2022. Predictability of Flash Flooding in Sloping Dutch Catchments (Rur, Niers and Swalm Rivers)

IX

Ljubljana, UL FGG, Masters of Science Thesis in Flood Risk Management.

ABBREVIATIONS

NAP	Normaal Amsterdams Peil or Amsterdam Ordnance Datum
IHU	Iterative Hydrography Upscaling
PTFs	PedoTransfer Functions
PBias	Percent Bias
RMSE	Root Mean Squared Error
MAE	Mean Absolute Error
NSE	Nash-Sutcliffe Efficiency
Log NSE	Logarithmic Nash-Sutcliffe Efficiency
KGE	Kling Gupta Efficiency
KGE_{NP}	Non-Parametric Kling Gupta Efficiency
E-OBS	European daily high-resolution gridded dataset
DWD	Deutscher Wetterdienst (German Weather Service)
ICON	ICOsahedral Nonhydrostatic model
ERA5	Fifth generation ECMWF atmospheric reanalysis of the global climate
KsatHorFrac	Horizontal Hydraulic Conductivity Parameter
AET	Actual Evapotranspiration
PET	Potential Evapotranspiration
ECMWF	European Centre for Medium-Range Weather Forecasts

Wasim, S.K. 2022. Predictability of flash flooding in sloping Dutch Catchments (Rur, Niers and Swalm Rivers)

Ljubljana, UL FGG, Masters of Science Thesis in Flood Risk Management.

1

1   INTRODUCTION

1.1   Problem Statement

The Netherlands and surrounding nations were hit by a flood in mid-July 2021 that was described as a once-in-a-millennium disaster. Heavy rainfall in neighboring mountainous sections of Germany, Belgium's Ardennes region, and Belgian Limburg caused serious flooding in various parts of western Germany, Belgium's East, and the Netherlands' southernmost province Limburg. On July 16, 2021, the Meuse River shattered all previous records dating back to the 17th century, with a flow of 3168 m^3/s, 20 times the mean flow (Sharma, 2021). The highest water level in the Meuse River was observed near Sint Pieter which was 48.00 meters above the NAP (the true Amsterdam water level used for measuring across Europe) ("Hoogwater", 2021). There were at least 220 documented injuries, with damage estimates ranging from 300-600 million EUR in the Netherlands, 350 million EUR in Belgium, and 17 billion EUR in Germany (Report Task Force, 2021). The flooding was the worst the Netherlands had experienced in decades.

The Meuse's peak discharge in Eijsden and a number of tributaries was the greatest ever recorded. Low-lying areas of Liège, as well as several Maastricht neighborhoods, Roermond, Venlo, Valkenburg, and other communities along the Meuse, had to be evacuated quickly. The flood in Valkenburg, a tiny town in the Netherlands, was one of the worst in the country, with almost 700 households affected and water damage downtown estimated at 400 million EUR. Valkenburg is situated at the foot of a valley, making it an ideal site for severe flooding. The water rose so swiftly, according to fire chief Leon Houben, that the evacuation of nursing homes in Valkenburg was severely hindered, and people spent the night in fear and anguish. He also stated that a disaster plan existed for flooding from the Meuse, but not for smaller rivers such as the Geul and Gulp, which impacted Valkenburg and others ("Limburg flood", 2022).

It isn't the first time that Limburg has been flooded as a result of severe rainfall. Flooding in the provinces of Limburg, North Brabant, and Gelderland in January 1926 is remembered as one of the most devastating floods of the twentieth century. Limburg had to contend with significantly more water in the 1990s, and far bigger areas of the province were inundated. The Meuse flooded its banks once more in December 1993, submerging 8% of the land of the province. The overall cost of the damage was 254 million guilders. The dangerously high levels of the Meuse, Rhine, Waal, and IJssel rivers led to one of the greatest evacuations (250,000 people) in recent Dutch history a little over a year later, in January 1995 (Sharma, 2021).

As a result of these floods, national and municipal governments developed new mitigation measures aimed at preventing future harmful consequences. The 'Maaswerken' programs were first introduced in 1997. The 'Grensmaas' project, which was implemented as part of the 'Maaswerken' surrounding the Maas in South-Limburg, deepened and widened the river, broadened floodplains, repositioned and elevated dikes, and constructed sluices along the river's course. However, according to Kreienkamp et al. (2021), a flood event like 2021 can be expected every 400 years given the current climatic condition. The study also states that the severity of a 1-day or 2-day event like 2021 would rise by 0.8 -6 % in a climate 2°C warmer than in preindustrial times. So, there is a high probability that the increasing

frequency and intensity of rainfall and snowmelt might affect the volume of river flow in the Meuse and its tributaries resulting in similar or bigger floods in the Limburg region in near future. Therefore, it's important to review and improve the flood protection measures in this region before another disaster hits it.

Although the high water spared most damage in the Netherlands during the 2021 flood event, it created new issues, notably in terms of the interplay between the Meuse and its tributaries. From the standpoint of operational forecasting, only a little amount of work has been put into the modeling and forecasting of these tributaries. Simple statistical connections are often employed in these catchments. There is a high probability that floods of the same or greater size may occur more frequently in the future as a result of climate change. That might bring severe damage to provinces like Limburg with relatively steep valleys. Detailed hydrologic and forecasting modeling of the Meuse River's tributaries will be extremely beneficial in reducing the future flood risk of these regions.

1.2   Motivation

Following the flood disaster of 2021, it was discovered that the Meuse River's minor tributaries have an important role in producing flash floods in the Limburg Province by adding decimetres to the river's water level. The main motivation of the study is the lack of research and application of modeling and forecast in these small tributaries of Meuse. The study is focused on determining the predictability of flash flooding in the sloping catchments of Niers, Rur, and Swalm by generating deterministic forecast using a distributed hydrological model wflow_sbm. The study will aid in determining the tributaries' contribution to the Meuse's water level and provide a more accurate flood prediction than basic statistical estimates.

1.3   Objectives

The objectives of this study are as follows:
1. Evaluate the performance of wflow_sbm model for the Niers, Rur and Swalm River basins and calibrate the horizontal hydraulic conductivity fraction parameter (KsatHorFrac).

2. Generate deterministic hydrological forecast by using DWD ICON forecasts and evaluate the forecast performance.

3. Determine the sensitivity of the forecast to the model parameter KsatHorFrac.

1.4   Research Questions

The study has tried to answer the following research questions-
1. How much improvement in the results does the calibration of the horizontal hydraulic conductivity bring?

2. What is the predictability of (flash) floods in the sloping catchment (Rur)? What is the effect of model on the predictability?

3. What is the sensitivity of predictions to model parameters?

Wasim, S.K. 2022. Predictability of flash flooding in sloping Dutch Catchments (Rur, Niers and Swalm Rivers)

3

Ljubljana, UL FGG, Masters of Science Thesis in Flood Risk Management.

2 LITERATURE REVIEW

2.1 Description of wflow_sbm model

The hydrological model for the study has been developed by Deltares by using the wflow_sbm model software. It is a conceptual rainfall-runoff model used in the geographically distributed wflow modelling platform, which is built on Julia. The conceptual bucket model wflow sbm (Figure 1) is based on topog sbm (Vertessy & Elsenbeer, 1999) and employs a kinematic wave approach for lateral subsurface, overland, and river flow processes. The model calculates the water balance at each point in each time step using gridded topography, forcing data, soil, and land use. The kinematic wave is used to calculate the hydrological routing for channel, overland, and lateral subsurface flow (Schellekens et al., 2021). The one-dimensional model is based on an eight-flow-direction grid cell network (D8) for surface and subsurface flow routing, including both vertical and lateral flows (Wannasin, 2021). It consists of four main routines: i) a precipitation-snow routine based on the HBV model (Lindstrom et al., 1997), (ii) a rainfall interception routine based on the modified Rutter model (Rutter et al., 1971, 1975) or the Gash model (Gash, 1979), (iii) a soil water routine based on topog sbm, and (iv) a flow generation routine with the kinematic wave function.
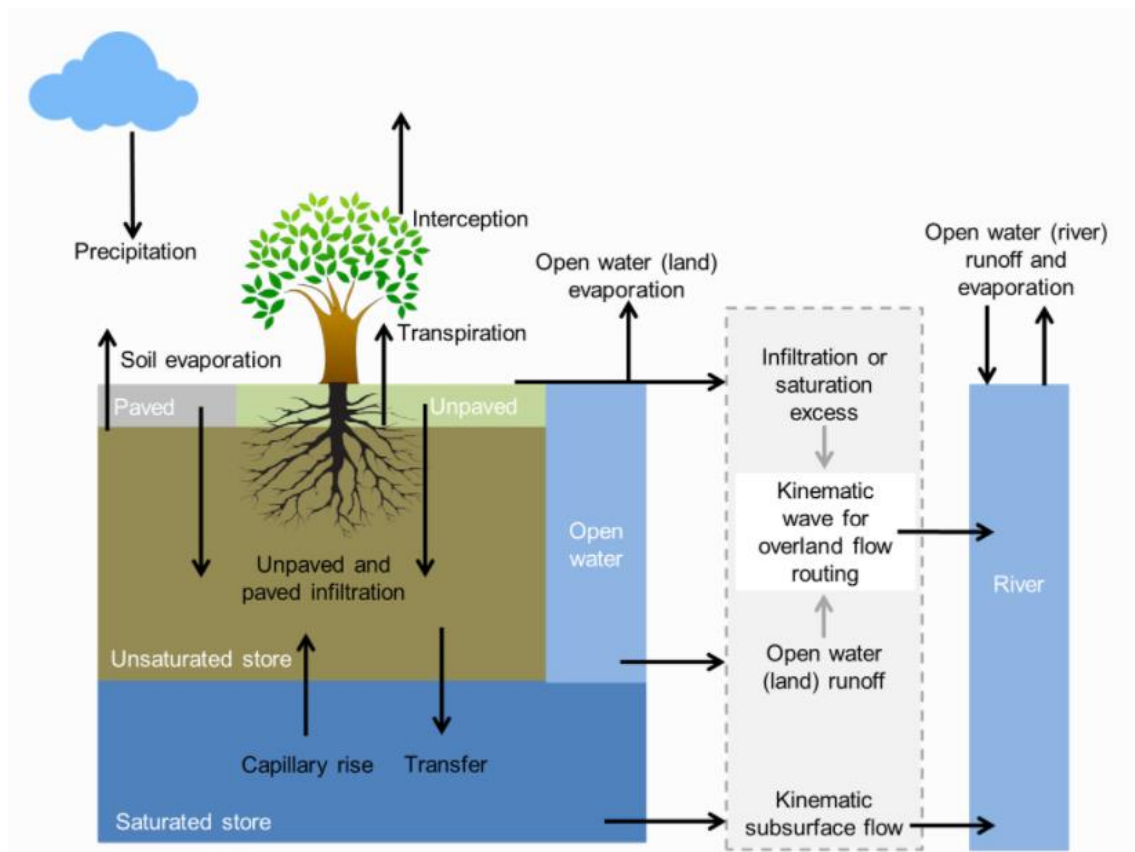
Figure 1 Overview of processes and fluxes in the wflow_sbm model
(Schellekens et al., 2021)

4   Wasim, S.K. 2022. Predictability of flash flooding in sloping Dutch Catchments (Rur, Niers and Swalm Rivers).

Ljubljana, UL FGG, Masters of Science Thesis in Flood Risk Management.

2.2 Horizontal Hydraulic Conductivity Fraction Parameter (KsatHorFrac)

The wflow model's needed parameters were calculated using a hydrography upscaling approach or (pedo) transfer functions (PTFs) based on available spatial data. In a distributed hydrological model, hydrography upscaling algorithms are used to upscale flow direction data from high-resolution to coarser resolutions. The Iterative Hydrography Upscaling (IHU) approach, as reported by Eilander et al. (2020), was applied in this situation. The PTFs, as noted by Imhoff et al. (2020), are functions created from laboratory studies that relate the parameters to physical features of the soil in the catchment and have the benefit of not requiring additional calibration. Before generating the hydrological forecasts, just one parameter, the Horizontal Hydraulic Conductivity Fraction (KsatHorFrac) had to be calibrated because there is no pedo-transfer function for this parameter due to the difficulties in estimating it. The KsatHorFrac has been proven to be a particularly sensitive parameter in the model and is connected to geological features of the soil. The ease with which water may move through the soil is influenced by the hydraulic conductivity, which is a function of soil texture. Compared to compacted soils with a variety of particle sizes, loose, coarse, homogeneous soils have a higher horizontal hydraulic conductivity. The horizontal hydraulic conductivity is usually greater than the vertical hydraulic conductivity of soil as reported by Dabney and Selim (1987). Therefore, the KsatHorFrac has to be multiplied with the Vertical Hydraulic Conductivity (KsatVer) (mm/day) to generate the Horizontal Hydraulic Conductivity (KsatHor) (mm/day). This parameter significantly influences how discharge is divided between rapid runoff and baseflow. Higher baseflow, smaller peaks, and a little slower recession following a discharge peak are the results of higher KsatHorFrac values (Imhoff et al., 2020).

2.3 Description of Delft-FEWS

Delft-FEWS is an operational forecasting platform introduced in 2002-2003 by Deltares. It is a free software that quickly manages huge amounts of forecast data, integrates the most recent observations with the latest meteorological forecasts, and ensures data quality, uniform work processes, visualization, and reporting (Delft-FEWS, 2022). There are four steps consisted in the flood forecasting and warning process, which are- (i) Detection, (ii) Forecasting, (iii) Dissemination and Warning, and (iv) Response (Haggett, 1998 as cited in Werner et al., 2013). Among these steps, Delft-FEWS is mostly associated with the second one, forecasting where it provides additional lead time by predicting future hydro-meteorological conditions in the short term. Meteorological forecast data are imported and processed by the Delft-FEWS forecasting system to use it as future input data for hydrological and hydraulic models (Werner et al., 2013). Figure 2 shows the schematic diagram of the link between Delft-FEWS and other primary system within the operational environment.

Delft-FEWS is made up of multiple layers, including a data storage layer, a data access layer, and components for importing, altering, displaying, and exporting data. This forecasting system provides a framework for bringing model codes into the operational domain, where they may subsequently be coupled with data from operational networks and developments in adjacent disciplines.

Wasim, S.K. 2022. Predictability of flash flooding in sloping Dutch Catchments (Rur, Niers and Swalm Rivers)

5

Ljubljana, UL FGG, Masters of Science Thesis in Flood Risk Management.
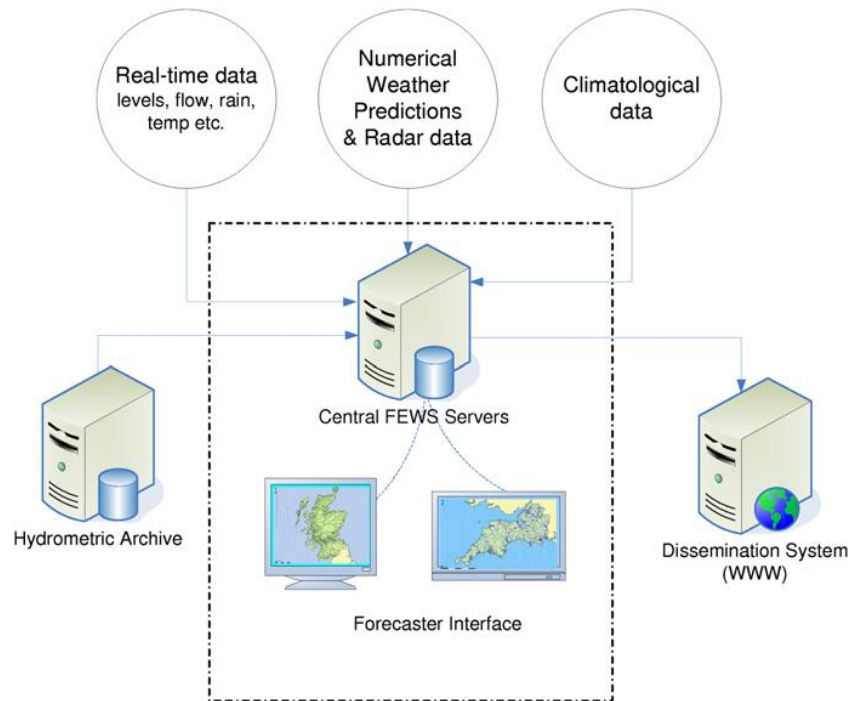
Figure 2 Schematic diagram of the connection between the forecasting system to real time data acquisition (Werner et al., 2013)

2.4   Indicators for Assessing Hydrological Model and Forecast Performance

It is important to initially assess the performance of the hydrological model to ensure high-quality hydrological forecasts. Again, one of the main objectives of this study is to evaluate the forecast performences. For evaluation of the hydrological model and the forecast performences, the matrices listed in

Table 1 were used.

Table 1 Indicators used for assessing hydrological model performance

Indicator	Range	Ideal Value	Evaluation for
Percent Bias (Pbias)	-∞ to + ∞	0	Hydrological model and forecast
Root Mean Squared Error (RMSE) (m^3/s)	0 to + ∞	0	Hydrological model and forecast
Mean Absolue Error (MAE) (m^3/s)	0 to + ∞	0	Forecast
Nash-Sutcliffe Efficiency (NSE)	-∞ to 1	1	Hydrological model
Logarithmic Nash-Sutcliffe Efficiency (Log NSE)	-∞ to 1	1	Hydrological model
Kling Gupta Efficiency (KGE)	-∞ to 1	1	Hydrological model
Non-Parametric Kling Gupta Efficiency (KGE_{NP})	-∞ to 1	1	Hydrological model

6   Wasim, S.K. 2022. Predictability of flash flooding in sloping Dutch Catchments (Rur, Niers and Swalm Rivers).

Ljubljana, UL FGG, Masters of Science Thesis in Flood Risk Management.

These indicators were computed with the help of Python Package Spotpy and Hydroeval developed by Houska et al. (2015) and Hallouin (2021) respectively. The following sub-sections describe the details of these indicators.

2.4.1   Percent Bias

According to Moraisi (2007), percent bias (PBias) quantifies the average tendency for simulated data to be greater or smaller than their corresponding observed data. The PBias values ranges from infinity to negative infinity, with PBias = 0 being the ideal value and low magnitude values suggesting accurate model simulation. Positive values imply model underestimation bias, while negative values indicate model overestimation bias. The equation for determining PBias is as follows:

$$PBias = \left[\frac{\sum_{i=1}^{n}\left(Y_i^{obs} - Y_i^{sim}\right) * 100}{\sum_{i=1}^{n} Y_i^{obs}} \right] \tag{1}$$

In equation (1), n indicates the number of observations, Y_i^{obs} are the observed and Y_i^{sim} are the simulated values. According to Gupta et al. (1999), PBias is able to identify clearly bad model performance. During dry years, PBias for streamflow tend to fluctuate more among different autocalibration methods than during wet years. This fact must be taken into account when conducting a split-sample evaluation.

2.4.2   Root Mean Squared Error

The root mean squared error (RMSE) demonstrates the model's absolute fit and how closely the predicted values match the actual data points. It provides an objective depiction of the model's predicted accuracy. It is given by the following equation:

$$RMSE = \sqrt{\frac{1}{n}\sum_{i=1}^{n}(Y_i^{sim} - Y_i^{obs})^2} \tag{2}$$

According to Hyndman & Koehler (2006), The RMSE is a decent accuracy metric, but it is scale sensitive, hence it should only be used to evaluate different approaches on the same dataset, not between scales. It is also more sensitive to outliers, which could be the flow peaks in this study. The RMSE's range is 0 to infinity, with 0 being the ideal value, and it uses the same units as the compared variables.

2.4.3   Mean Absolute Error

The mean absolute error (MAE) refers to the mean of the absolute difference between the forecast and the observed value. The MAE represents the average size of the forecast error that can be anticipated. The values of MAE ranges from 0 to ∞. Lower values indicate higher accuracy.

$$MAE = \frac{\sum_{i=1}^{n} |Y_i^{for} - Y_i^{obs}|}{n} \tag{3}$$

Wasim, S.K. 2022. Predictability of flash flooding in sloping Dutch Catchments (Rur, Niers and Swalm Rivers)

7

Ljubljana, UL FGG, Masters of Science Thesis in Flood Risk Management.

2.4.4 Nash-Sutcliffe Efficiency

The Nash-Sutcliffe efficiency (NSE) compares the residual variance (noise) to the measured data variance (information) (Nash and Sutcliffe, 1970). NSE displays how closely the observed versus simulated data graphic corresponds to the 1:1 line. The equation to compute NSE is as follows:

$$NSE = 1 - \left[\frac{\sum_{i=1}^{n}(Y_i^{obs} - Y_i^{sim})^2}{\sum_{i=1}^{n}(Y_i^{obs} - Y^{mean})^2} \right] \tag{4}$$

In equation 3, Y^{mean} corresponds to the mean of observed data for the constituent being evaluated. NSE ranges between $-\infty$ and 1, with the ideal value being 1. Values between 0 and 1 are regarded as acceptable, however values smaller than 0 imply that the mean observed value is a better predictor than the simulated value, indicating unacceptable performance.

2.4.5 Logarithmic Nash Sutcliffe Efficiency

According to Krause et al. (2005), the Nash-Sutcliffe efficiency (NSE) is frequently estimated with logarithmic values of observed and simulated data to decrease the problem of squared differences and the resultant susceptibility to extreme values. The logarithmic conversion of the runoff data flattens the peaks and maintains the low flows at roughly the same level. As a result, the influence of low flow values relative to flood peaks increases, resulting in an increase in Log NSE's sensitivity to systematic model over- or underprediction. Log NSE = 1 is the optimum value, while the range of possible values spans from 1 to negative infinity. The following equation computes the Log NSE:

$$LogNSE = 1 - \left[\frac{\sum_{i=1}^{n}(\log(Y_i^{obs}) - \log(Y_i^{sim}))^2}{\sum_{i=1}^{n}(\log(Y_i^{obs}) - \log(Y^{mean}))^2} \right] \tag{5}$$

2.4.6 Kling Gupta Efficiency

The Kling Gupta Efficiency (KGE) is one of the most modern methodologies for hydrological model calibration and evaluation. It relates the three main components of the NSE, namely the correlation coefficient (r_P), the relative variability of the simulated and observed values (α), and the bias (β), but it is solved with a multi-objective perspective, considering the three components as separate criteria in order to optimize and minimize the Euclidean distance from the ideal point. The equation to compute KGE is:

$$\beta = \frac{\mu_{sim}}{\mu_{obs}} \tag{6}$$

$$\alpha = \frac{\sigma_{sim}}{\sigma_{obs}} \tag{7}$$

$$r_P = \frac{\sum_{i=1}^{n}(Y_i^{obs} - \mu_{obs})(Y_i^{sim} - \mu_{sim})}{\sqrt{(\sum_{i=1}^{n}(Y_i^{obs} - \mu_{obs})^2)(\sum_{i=1}^{n}(Y_i^{sim} - \mu_{sim})^2)}} \tag{8}$$

$$KGE = 1 - \sqrt{(\beta - 1)^2 + (\alpha - 1)^2 + (r_P - 1)^2} \qquad (9)$$

In these equations, μ and σ denote the mean and standard deviation of the data respectively. The optimal value for this indicator is KGE = 1, where all three components equal 1, and it can range from 1 to negative infinity. According to Knoben et al. (2019), a value of KGE = 0 does not indicate that the model has a poor performance, as in the case of NSE = 0; however, if the mean value is used as an indicator, it would result in a value of KGE = -0.41.

2.4.7   Non-Parametric Kling Gupta Efficiency

The calculation of KGE implicitly assumes the linearity and normality of the data, as well as the lack of outliers. However, it is well known that both the discharge time series and model simulation errors are severely skewed, which contradicts the implicit assumptions underlying KGE. As mentioned by Pool (2018), the non-parametric KGE (KGE$_{NP}$) reformulates the correlation and variability terms of KGE in a non-parametric fashion. On the basis of the Flow Duration Curve (FDC), the non-parametric form of the discharge variability (α_{NP}) has been constructed. The FDC describes the relationship between the frequency and magnitude of streamflow and is an indicator of flow variability across all flow magnitudes of a catchment (Vogel and Fennessey, 1995), whereas the standard deviation measures only the variability of flows around the mean flow for non-normally distributed data. Spearman rank correlation (r_s) was used to describe discharge dynamics as a non-parametric alternative to the correlation term Pearson correlation coefficient, which is utilized by KGE. It was calculated by the ranks of observed (R_i^{obs}) and simulated (R_i^{sim}) discharge time series. Spearman rank correlation is less susceptible to extreme values in a time series than Pearson correlation, resulting in a more robust representation of the correlation (Legates and McCabe 1999, Krause et al. 2005). The equations to calculate the KGE$_{NP}$ are as follows:

$$\alpha_{NP} = 1 - \frac{1}{2}\sum_{k=1}^{n}\left|\frac{Y_{sim}(I(k))}{n\overline{Y}_{sim}} - \frac{Y_{obs}(J(k))}{n\overline{Y}_{obs}}\right| \qquad (10)$$

$$r_s = \frac{\sum_{i=1}^{n}(R_i^{obs} - \overline{R}_{obs})(R_i^{sim} - \overline{R}_{sim})}{\sqrt{(\sum_{i=1}^{n}(R_i^{obs} - \overline{R}_{obs})^2)(\sum_{i=1}^{n}(R_i^{sim} - \overline{R}_{sim})^2)}} \qquad (11)$$

$$KGE_{NP} = 1 - \sqrt{(\beta - 1)^2 + (\alpha_{NP} - 1)^2 + (r_S - 1)^2} \qquad (12)$$

2.5   Mann-Kendall Test for Trend Analysis

The Mann-Kendall Trend Test, also known as the MK test, is used to look for patterns that are regularly growing or decreasing in time series data (monotonic trends). It examines how the signals of earlier and later data points differ. According to the theory, if a trend is present, the sign values will tend to continuously increase or decrease.

Wasim, S.K. 2022. Predictability of flash flooding in sloping Dutch Catchments (Rur, Niers and Swalm Rivers)

9

Ljubljana, UL FGG, Masters of Science Thesis in Flood Risk Management.

For this study, the original Mann Kendall analysis was performed to determine the trends in the meteorological conditions in the study area. The original Mann Kendall test is a non-parametric test and the python package pyMannKendall was used to perform this test (Hussain et al., 2019). As input, the data and significance level (default value= 0.05) were provided. The five output parameters- p-value, z-value, tau, Sen's slope, Mann Kendall score were analysed to understand the trend of the data.

p-value- This indicates the p-value of the significance test. p-value < 0.05 indicates a monotonic trend and p-value > 0.05 indicates that there is no monotonic trend in the data.

z-value- At the chosen significance level, the absolute value of Z is compared to the normal cumulative standard distribution to see if a trend exists. A Z number that is positive or negative denotes an upward or downward trend.

Sen's slope- The Sen's slope corresponds to the change in the data per unit time.

Tau- Tau expresses the monotony of the slope. The range of Kendall's Tau is -1 to 1, with positive values for increasing trends and negative values for decreasing trends.

Mann Kendall Score (S)- Each value is compared to all future time period values for the indicator to determine the test statistic, S. If the second number in a comparison pair is higher than the first, a score of "+1" is given. The comparison receives a "-1" score if the latter value is less than the former value. The test statistic, S, is then calculated by adding up all of the results. An increase in the trend is indicated by a positive S value, whereas a decline in the trend is indicated by a negative S value ("Mann-Kendall Test for Trend Overview", 2021).

10   Wasim, S.K. 2022. Predictability of flash flooding in sloping Dutch Catchments (Rur, Niers and Swalm Rivers).

Ljubljana, UL FGG, Masters of Science Thesis in Flood Risk Management.

3 STUDY AREA

The study area for this research consists of three tributaries (Rur, Niers and Swalm) of the Meuse River which are located in the Limburg province of the Netherlands (Figure 3). Parts of France, Luxembourg, Belgium, Germany, and the Netherlands make up the Meuse basin, which spans around 33,000 km². The catchments of the three tributaries Niers, Rur and Swalm cover around 4%, 7% and 1% (de Wit et al., 2007) respectively of the Meuse River basin. The following sections describe the details of each of these catchments.
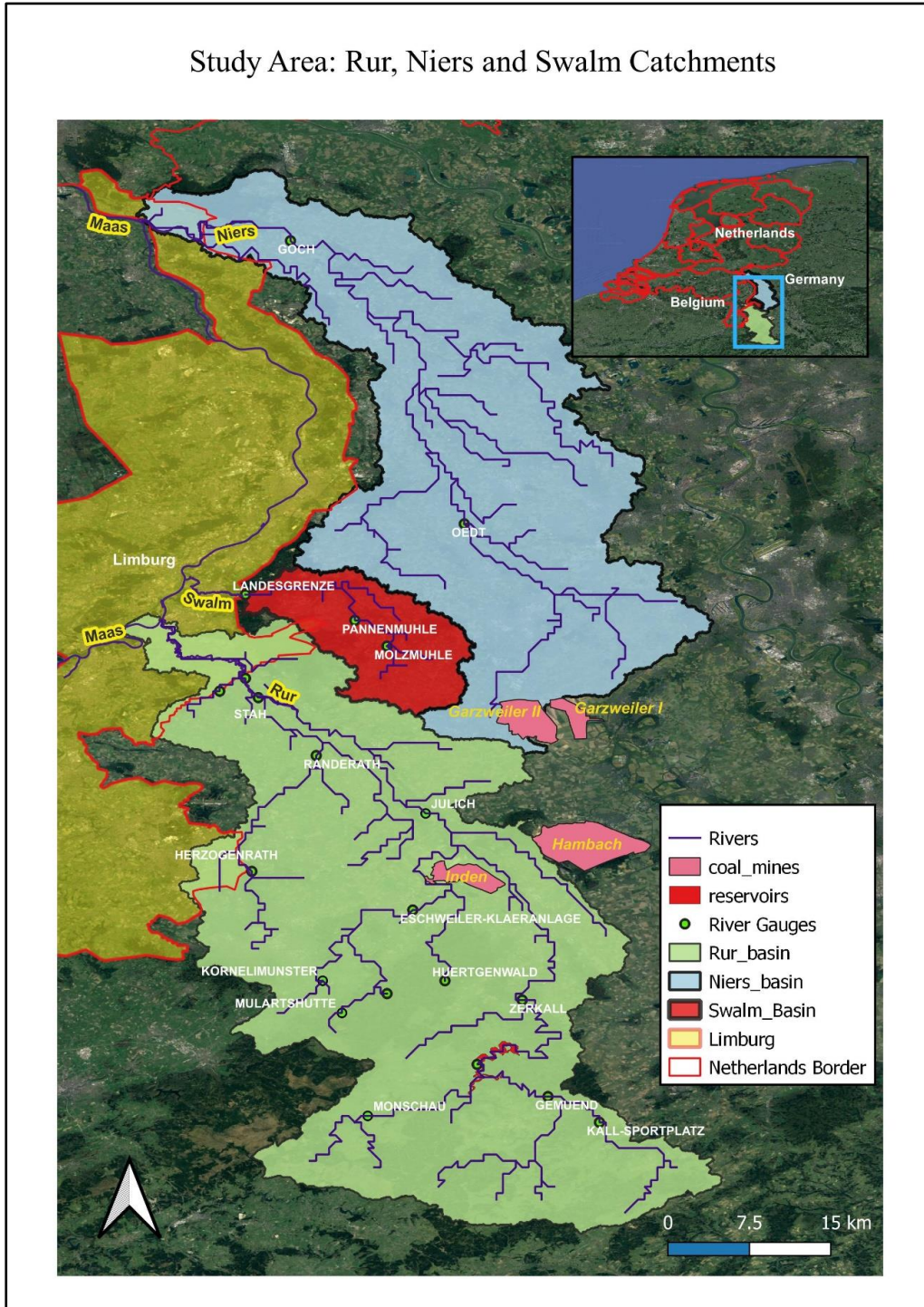
Figure 3 The catchments of Rur, Niers and Swalm rivers

Wasim, S.K. 2022. Predictability of flash flooding in sloping Dutch Catchments (Rur, Niers and Swalm Rivers)

11

Ljubljana, UL FGG, Masters of Science Thesis in Flood Risk Management.

3.1   Rur Basin Area

Parts of Germany, Belgium, and the Netherlands are included in the Rur basin. The majority of the land is in Germany, accounting for 89% of the total. Urft for the higher reaches, Inde for the middle spans, and Wurm for the lower reaches are the principal tributaries of Rur. With the headwaters in Belgium, it falls into the Meuse near Roermond, Netherlands. The river has a total length of 163 km, with 21 km in the Netherlands. The basin has an area of 2,338 km^2 and the yearly mean precipitation is 855 mm. As reported by Drogue et al., 2010, there are two completely distinct landscape zones within the basin. The Rhenish Massif is responsible for the basin's southernmost region, which contains largely cemented rock. The towns of Aachen, Eschweiler, and Düren are along its northern border. The Lower Rhine lowlands include the region with primarily unconsolidated rock to the north of this line. Drinking and industrial water recovery take place here frequently. They have also stated that the mainland uses in the German part of the basin area are arable land (30%), grassland (20%) and forests (30%). Moreover, 57% of the Belgian part of the catchment is used for agriculture. Also, the basin area is mostly utilized for agriculture in the Netherlands (MUNLV, 2005-1, as cited in Drogue et al., 2010).

The Eifel's nine reservoirs and over 50 flood control basins have a significant impact on the discharge behavior of the river. The combined storage volume of the nine reservoirs is over 300 million m^3. They are used for drinking water supply, flood control, low-flow enrichment, power production, and recovery, among other things (Drogue et al., 2010).

The open pit mining industry is another significant land use in this catchment. Open-cast coal mines in the Rur Catchment area have an impact on the groundwater level, but even larger mines in the nearby catchment area have an impact on the groundwater table in the northern Rur region (Vidaurre et al., 2016).

3.2   Niers Basin Area

The Niers basin is located between Germany and the Netherlands. The river falls into the Meuse near Gennep, Netherlands. The Niers has a total length of 118 km, with 8 km in the Netherlands and the basin area is about 1400 km^2 having mean annual precipitation of 708mm. The basin is part of the Lower Rhine lowlands and is dominated by unconsolidated rock. Because of the basin's flat geography, flood control measures are required. Aside from the natural retention in the floodplains, controlled flood retention basins are used. For minor and medium-sized flood occurrences, dikes along rivers provide flood protection (MUNLV, 2005-2, as cited in Drogue et al., 2010).

The original highly wet stream valley floor has been drained for agricultural use by a significant number of water management operations. The stream system was maintained and handled more methodically throughout time. The width and depth of the Niers were fixed (normal profile). Today, aquatic plants are mowed five to six times during the growing season. The Niers in Germany was entirely canalized in the 1920s. The part of Niers along the Dutch border, which makes up the lowest portion of the lower course, was exempted from canalisation, hence this portion still follows a meandering path (Van Den Brink and Lanphen, 1999).

One of the major characteristics of the southern Niers catchment area is the brown coal mine, Garzweiler II, located 15 km east of the Dutch-German border at Roermond and 10 km south of Mönchengladbach. Mining in the 48 km^2 Garzweiler II started in 2006 and is expected to be continued till 2045 ("Garzweiler surface mine", 2022). Overall, brown coal mining significantly disturbs the ecosystem's natural balance. Since brown coal is extracted from dry mines, substantial groundwater lowering, and pumping procedures are required. According to (Meiners, 2002), the groundwater level in Garzweiler II has decreased by more than 200 m, and between 80 and 150 million m^3 of groundwater being removed each year for up to 40 years.

According to Van Den Brink and Lanphen (1999), the urban and agricultural infrastructure and the mowing management are aimed at draining the water to the Meuse as quickly as possible. As a result, the river can no longer handle an extreme supply of precipitation water, such as during prolonged rainfall or torrential downpours, flooding occurs downstream. In the lower reaches, the peak discharges of the Niers usually coincide with high water levels in the Meuse, causing the Niers water to back up, resulting in large-scale flooding.

3.3   Swalm Basin Area

In comparison to the considerably bigger Meuse River, the Swalm is a very minor tributary. Its source is in Wegberg in the district Heinsberg, south-west of Mönchengladbach in North Rhine-Westphalia, and it meanders till its confluence with the Meuse between Venlo and Roermond in the Netherlands. It has a total length of 46 km and a catchment area of 268.7 km^2, about 27 km^2 of which is in the Netherlands.

Wasim, S.K. 2022. Predictability of flash flooding in sloping Dutch Catchments (Rur, Niers and Swalm Rivers)

13

Ljubljana, UL FGG, Masters of Science Thesis in Flood Risk Management.

4   RESEARCH METHODOLOGY

This chapter discusses the datasets, methods, models, and procedure used in this study to determine the predictability of flooding in Niers, Rur, and Swalm catchments.

The general steps for developing this study are data collection, data pre-processing and comparison of datasets, developing wflow_sbm model for the tributaries, calibration and validation of the hydrological model, water balance analysis, generation of deterministic hydrological forecasts by coupling wflow_sbm with Delft FEWS, evaluating the forecast performance and sensitivity analysis of the forecasts to the model parameter KsatHorFrac. A conceptual framework linking the datasets, models, analysis, and findings of this investigation is depicted in Figure 4. In the following sections, the technique and explanation of the methodologies, models, and datasets utilized in this study will be discussed in detail.
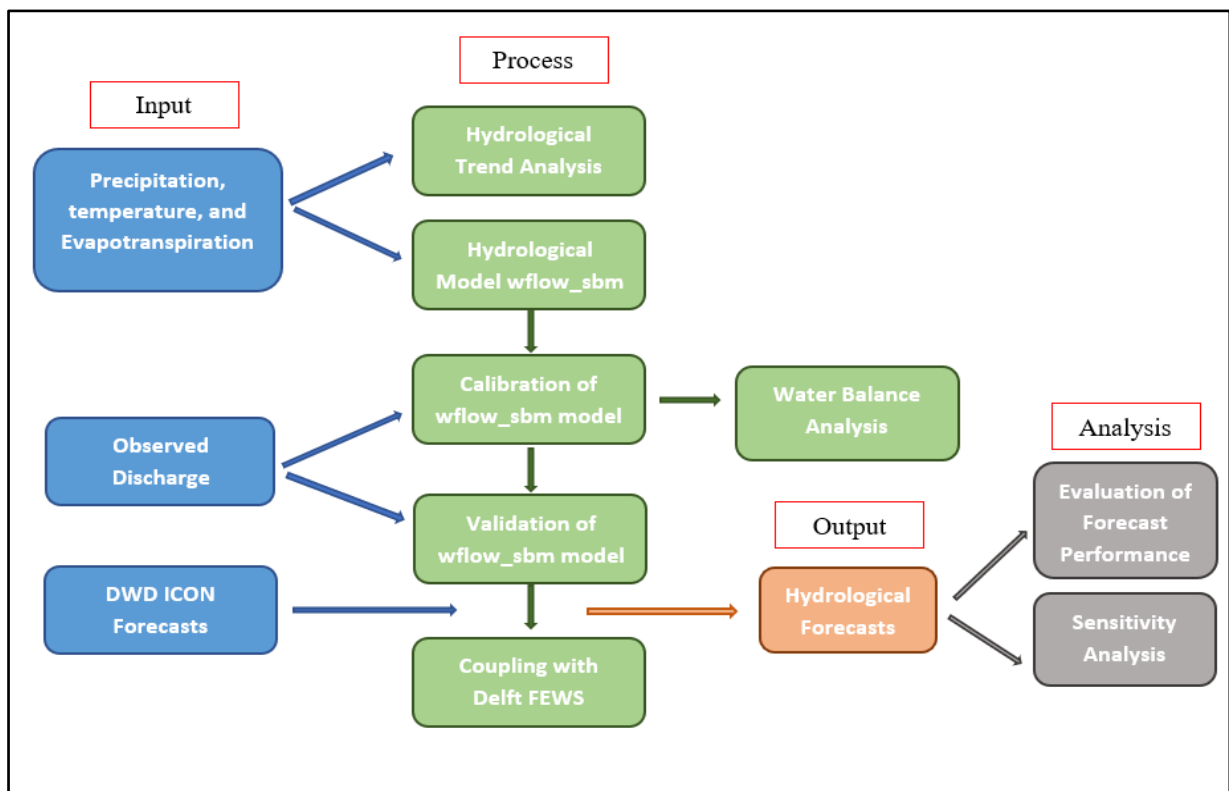
Figure 4 Conceptual framework relating datasets, models, analysis and results in this study

4.1   Data Collection

As input of the hydrological model, precipitation, temperature and evapotranspiration data were collected. Discharge data from various river gauges located in the study area was used for calibration and validation of the hydrological model. Moreover, DWD ICON weather forecasts were used to generate the deterministic forecast from Delft-FEWS.

4.1.1 Precipitation Data

The precipitation dataset was collected from E-OBS which is a daily grided meteorological dataset for Europe. The E-OBS dataset provides daily observation of precipitation from 1950 to 2021. For this study, the precipitation data from 02-01-1979 to 31-12-2021 was derived from E-OBS version 25 with a higher horizontal resolution of $0.1° \times 0.1°$.

4.1.2 Temperature and Evapotranspiration Data

Temperature and potential evapotranspiration are also required as input driving data for the hydrological model employed in this research. Daily temperature (T) and solar radiation (Rs) were collected from the ERA5 which is the fifth generation ECMWF atmospheric reanalysis of the global climate. Estimates of a significant number of atmospheric, land, and oceanic climate variables are provided hourly by ERA5. Daily and monthly data aggregated from hourly fields are also provided. The data span the planet on a grid of 30 km, and they use 137 levels to resolve the atmosphere from the ground up to an altitude of 80 km ("ERA 5: data documentation", 2022). The potential evapotranspiration (ET_{ref}) was calculated using the technique utilizing the temperature (T) and solar radiation (R_s) (Bruin et al., 1987).

$$ET_{ref} = 0.65 \ \frac{s}{s + \gamma} \frac{R_s}{\lambda} \qquad (13)$$

In equation 13, s is the saturated vapor pressure gradient relative to water, γ is the psychrometer constant and λ is the heat of evaporation water.

4.1.3 Forecast Data

DWD ICON forecast from the beginning of 2018 to 25-07-2022 with a resolution of $0.25°$ was used for the generation of hydrological forecasts. Temperature and precipitation were the forecast variables used for this study. The maximum lead time of the forecasts were 7 days with a time step of 3 hours. DWD (German Meteorological Service) is one of the world's fourteen weather services to run a global numerical weather prediction (NWP) model which is recognized as ICOsahedral Nonhydrostatic model (ICON). DWD and the Hamburg-based Max-Planck Institute for Meteorology (MPI-M) collaboratively created the ICON modeling system as a whole and the model became operational at 20-01-2015 (Reinert et al., 2016).

4.1.4 Discharge Data

For the calibration and validation of the hydrological models of the Niers, Rur, and Swalm River basins, daily discharge data from several monitoring stations were collected from Water information system ELWAS from the state of North Rhine-Westphalia, Germany (Table 2).

Wasim, S.K. 2022. Predictability of flash flooding in sloping Dutch Catchments (Rur, Niers and Swalm Rivers)

15

Ljubljana, UL FGG, Masters of Science Thesis in Flood Risk Management.

Table 2 Summary of the river gauges in the study area

Station Name	River	U/S Area (sq.km)	Longitude	Latitude	Period
Rur					
Kall_Sportplatz	Urft	133.5	6.55	50.55	Jan 1979-Jun 2021
Gemund	Urft	345.61	6.48	50.58	Jan 1979-Jun 2021
Monschau	Rur	146.4	6.25	50.55	Jan 1979-Nov 2021
Zerkall	Rur	791.99	6.45	50.70	Jan 1979-Jun 2021
Mulartshutte	Vichtbach	32.09	6.21	50.69	Jun 1984- Jun 2021
Kornelimunster	Inde	64.58	6.18	50.73	Jan 1979-Jun 2021
Eschweiler	Inde	251.18	6.30	50.82	Jan 1979-Jun 2021
Julich	Rur	1463.39	6.35	50.92	Jan 1979-Jun 2021
Herzogenrath	Wurm	132.02	6.10	50.87	Jan 1979-Jun 2021
Randerath	Wurm	301.98	6.18	51.02	Jan 1979-Jun 2021
Stah	Rur	2151.73	6.10	51.10	Jan 1979-Jun 2021
Niers					
Goch	Niers	1403.5	6.15	51.69	Jan 1979-Jun 2020
Oedt	Niers	484.87	6.37	51.32	Jan 1979-Jun 2020
Swalm					
Molzmuhle	Swalm	51.16	6.27	51.16	Nov 1985- Jun 2020
Pannenmuhle	Swalm	128.98	6.23	51.20	Jan 1979-Jun 2020
Landesgrenze	Swalm	244.24	6.09	51.23	Nov 1985- Jun 2020

4.2   Hydrological Trend Analysis

To better understand the catchment response, trend analyses of the input forcing parameters e.g. precipitation, actual and potential evapotranspiration, interception, temperature and observed discharge were done by performing the Mann-Kendall test as described in section 2.5. Moreover, the analysis was also done for the annual mean, maximum and minimum discharges to observe the trend against time. Additionally, the seasonal variation of discharges in various sub-catchments was also demonstrated.

4.3   Hydrological Modelling

The hydrological models of the Rur, Niers and Swalm basins were provided by Deltares for this study. The wflow_sbm model (Van Verseveld et al., 2022) was used for the hydrological modeling as described in section 2.1.

4.3.1   Hydrological Model Parameters

Table 3 lists the variables utilized in the wflow model, together with their units, value ranges [min, max], and how they vary over the Rur catchment. Parameters used for the Niers and Swalm basin models can be found in Appendix B. Among the Eifel's reservoirs, the Olef, Urft and Rur reservoirs were modelled in the Rur catchment using wflow. These three reservoirs were combined as one reservoir at the location of the Rur reservoir in the model. More details on modelling the reservoir in Rur catchment can be found in the ongoing master's report of Hartgring, S. (2022).

Table 3 Parameters used in wflow_sbm model for the Rur catchment

Parameter ID	Parameter Name	Units	Value	Variation
Physiography				
dem	Terrain Elevation	m	[15.6, 660.6]	Spatial
Slope	Terrain Slope	-	[0.002, 0.339]	Spatial
RiverSlope	River Slope	-	[0, 0.05]	Spatial
riverlength	River Length	m	[75.72, 2100.86]	Spatial
RiverDepth	River Depth	m	[1, 2.67]	Spatial
riverwidth	River Width	m	[30, 263.63]	Spatial
Land use and soil properties				
landuse	Land use	-	class	Spatial
soil	Soil Type	-	class	Spatial
N	Manning parameter for overland flow	$s/m^{1/3}$	[0.01,0.6]	Spatial
N_River	Manning parameter for river flow	$s/m^{1/3}$	[0.03,0.05]	Spatial
SoilMinThickness	Minimum soil depth	mm	[600, 2000]	Spatial
SoilThickness	maximum soil depth	mm	[600, 2000]	Spatial
KsatVer	Vertical saturated conductivity at the surface	mm/day	[38.9, 8162.8]	Spatial
M	decrease of KsatVer with depth	mm	[130, 10,000]	Spatial
thetaR	Residual water content	mm/mm	[0.06, 0.195]	Spatial
thetaS	Water content saturation	mm/mm	[0.406, 0.509]	Spatial
KsatHorFrac*	Horizontal saturated conductivity fraction	-	[50, 650]	Constant/Spatial
Infiltration				
c	Brooks-Corey power co-efficient	-	[7.59, 11.03]	Spatial
cf_soil	Infiltration reduction factor	-	0.038	Constant
InfiltCapPath	Infiltration capacity of compacted soil fraction	mm/day	5	Constant
InfiltCapSoil	Infiltration capacity of non-compacted soil fraction	mm/day	600	Constant
MaxLeakage	Maximum Leakage	mm/day	0	Constant
PathFrac	Fraction of compacted area	-	[0, 0.999]	Spatial
Evaporation				
EoverR	Average wet canopy evaporation over precipitation	-	0.11	Constant
LAI	Monthly leaf area index	-	[0, 2.78]	Spatial/Temporal
SI	Specific leaf storage	mm	[0, 0.127]	Spatial
Kext	Light extinction coefficient	-	[0.6,0.8]	Spatial
Swood	"Canopy" capacity of vegetation woody fraction	-	[0, 0.5]	Spatial
RootingDepth	Rooting depth of the vegetation	mm	[0, 431.5]	Spatial
rootdistpar	Root connection with the groundwater table	mm	-500	Constant
Snow				
Cfmax	Ice Melting Factor	mm/(°C/day)	3.75	Constant
TT	Temperature threshold for snow precipitation	°C	0	Constant
TTI	Temperature range for rain and snow mixing	°C	2	Constant
TTM	Temperature threshold for ice melting	°C	0	Constant
WHC	Fraction of water stored in snow volume	-	0.1	Constant
WaterFrac	Water fraction	-	[0, 0.94]	Spatial

4.3.2   Calibration and Validation of Hydrological Model

To determine the optimal value of the KsatHorFrac parameter for each sub-catchment, the wflow model for each river was run keeping the same initial conditions except KsatHorFrac. The whole time period was divided into 4 parts and for each part, the indicators mentioned in section 2.4 were plotted against different KsatHorFrac values for the most upstream stations. From the plots, the best value of KsatHorFrac was selected for each indicator and taking the average KsatHorFrac for all indicators, one value was determined for each time period. After that, taking these KsatHorFrac values, the indicators

Wasim, S.K. 2022. Predictability of flash flooding in sloping Dutch Catchments (Rur, Niers and Swalm Rivers)

17

Ljubljana, UL FGG, Masters of Science Thesis in Flood Risk Management.

were determined for each time period to observe the range of the indicator values. By analysing the extent of the indicators, a suitable KsatHorFrac was selected for the upstream sub-catchments.

The selected KsatHorFrac value was then incorporated into the wflow model for the upstream sub-catchments and the model was run again. After that, the steps described in the previous paragraph were repeated to calibrate the immediate downstream sub-catchments of the initially calibrated upstream sub-catchment. The same procedure was conducted until calibrating the most downstream sub-catchment. After that, the simulated and observed annual mean, maximum, minimum, driest year and wettest year discharges corresponding to the best KsatHorFrac value were compared to check how the selected values represent these hydrographs and annual discharges. In the next step, the models were used to generate and evaluate the hydrological forecasts.

4.4   Water Balance Analysis

While calibrating some sub-catchments, it was observed that the discharge in those sub-catchments was not properly simulated. The values of the indicators especially Pbias, NSE and KGE were very poor. So, water balance analysis was conducted to see if the model simulation agrees with the input forcing parameters. The approximate water balance equation in any catchment is given by:

$$P - AE - I = Q \tag{14}$$
$$\text{(Inflow = Outflow)}$$

Where, P=Precipitation (mm), AE= Actual evapotranspiration (mm), I= Interception (mm) and Q= Mean discharge over the catchment (mm). For comparatively shorter time period, the water storage amount has to be taken into account.

4.5   Hydrological Forecast

The validated wflow_sbm model was coupled with Delft FEWS flow forecasting system to generate deterministic forecasts for the river basins. The coupled model was run with DWD ICON forecast data from 01-01-2018 to 31-12-2021. The deterministic forecasts were obtained for each forecast simulation for 7 days lead time.

4.5.1   Evaluation of Forecast Performance

The deterministic streamflow predictions were evaluated against the observed discharge and later to a reference simulation which would use observed meteorological fields as input to the calibrated hydrological model. To emphasize distinct components of the forecast performance, three separate dimensionless skill scores (PBias, RMSE and MAE) were considered as listed in Table 1. Performance scores were shown in terms of forecast lead times and basin sizes.

4.5.2   Sensitivity Analysis of Forecasts to Hydrological Model Parameters

In order to understand the influence of the wflow_sbm model on the forecast results, sensitivity analysis of the forecasts was performed. To do this, forecasts were generated by changing the model parameter i.e., KsatHorFrac and the variation of the results for each change were compared to determine the sensitivity of the forecasts.

5   RESULTS AND DISCUSSIONS

At the beginning of his chapter, the results for the hydrological trend analysis in the study area are discussed. Later the selection of the KsatHorFrac value is deliberated in this chapter. Impact of parameters other than KsatHorFrac e.g maximum leakage, soil thickness was checked for the river gauges where the observed discharge didn't agree with the simulated discharge despite using a wide range of KsatHorFrac values. Water balance in each river gauge was also checked in order to see if the model is providing reasonable response corresponding to the input forcing parameters. Lastly, the results of the forecast evaluation and sensitivity analysis are discussed.

5.1   Hydrological Modelling Results for Rur Catchment

5.1.1   Hydrological Trend Analysis

For the Rur, 3 stations each for the upstream (Gemund), middle (Eschweiler) and downstream (Stah) part of the catchment were selected to observe the trend of the hydrological conditions along with their spatial variability. Figure 5 and Table 4 show the plots and the Mann-Kendall test analysis of the trend of annual average precipitation, sum of actual evapotranspiration and interception (AET+I), temperature and potential evapotranspiration (PET) at Eschweiler. Results for other gauges are provided in Appendix A.
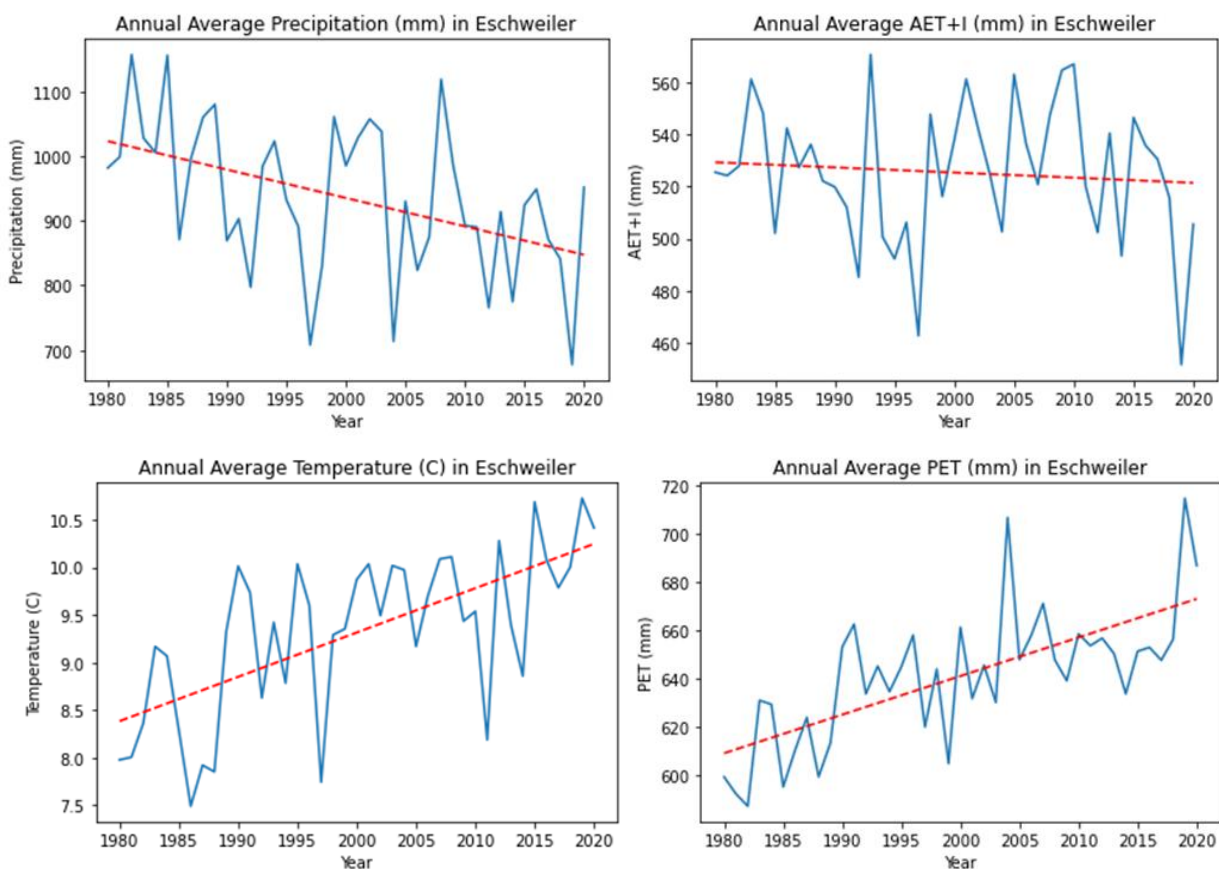
Figure 5 Trend of hydrological conditions in Eschweiler

Wasim, S.K. 2022. Predictability of flash flooding in sloping Dutch Catchments (Rur, Niers and Swalm Rivers)

Ljubljana, UL FGG, Masters of Science Thesis in Flood Risk Management.

19

Table 4 Mann-Kendall Test for hydrological conditions in Eschweiler

Analysis for	p-value	z-value	Tau	Sen slope	Score	Trend
Precipitation (mm)	0.00887	-2.61704	-0.28537	-4.340604952	-234	decreasing
AET+I (mm)	0.597568	-0.5279	-0.05854	-0.173125797	-48	no trend
PET (mm)	6.00E-06	4.526471	0.492683	1.470360317	404	increasing
Temperature (C)	1.25E-05	4.369224	0.47561	0.046445688	390	increasing

So, it is observed from this analysis that the precipitation in the middle of the Rur catchment is decreasing at an alarming rate. The Sen's slope value for precipitation indicates a decrease of 4.3 mm rainfall per year. Moreover, the temperature shows an increasing trend with a rate of 0.05°C/year and so the potential evapotranspiration also shows an increasing trend resulting from rising temperature. The p-values for both precipitation and temperature are quite low which indicates that the trends are significant enough. However, for this location, the sum of actual evapotranspiration and interception (AET+I) doesn't show any significant trend.

Additionally, the trend of annual mean, maximum and minimum discharge was also analysed to observe the impact of the precipitation and temperature as shown in Figure 6. The Mann-Kendall test was also performed for this analysis (Table 5).
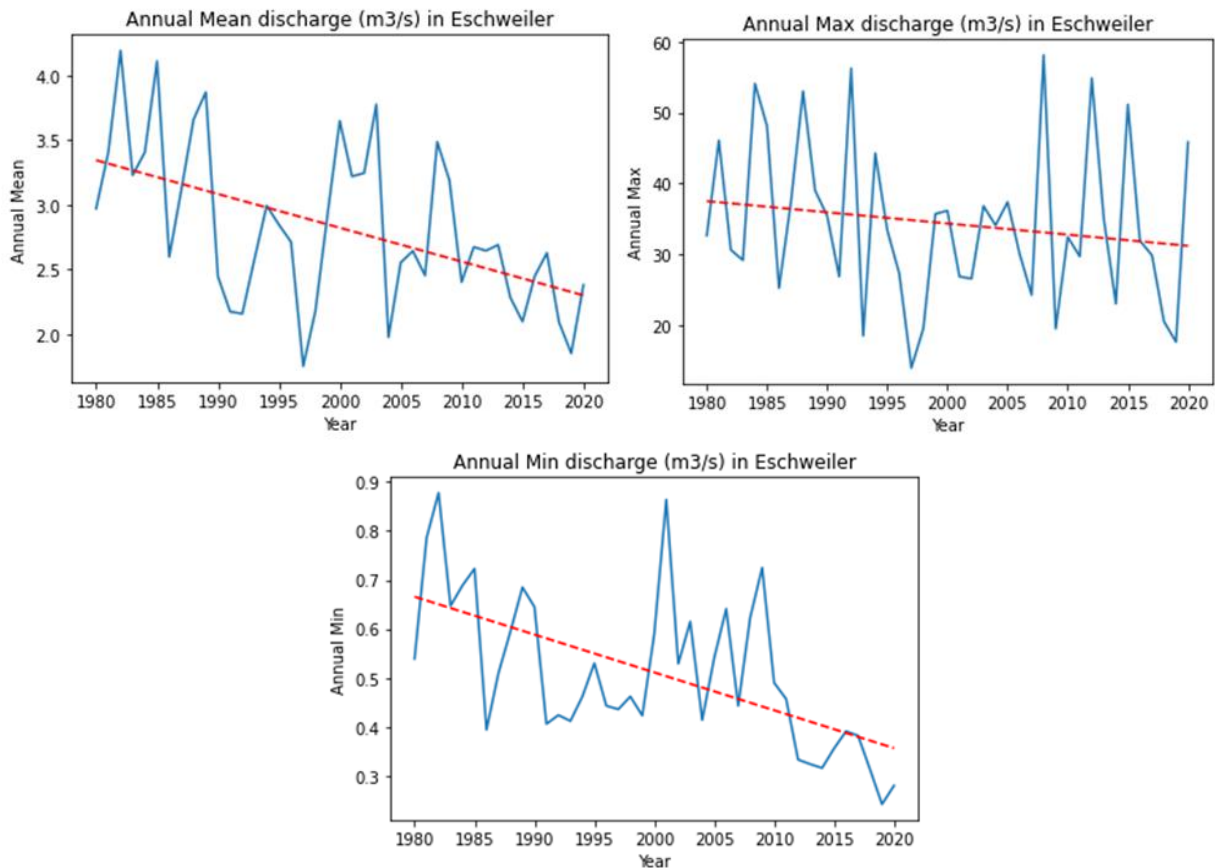
Figure 6 Trend analysis of annual mean, maximum and minimum discharges in Eschweiler

Table 5 Mann-Kendall Test for annual discharges in Eschweiler

Analysis for	p-value	z-value	Tau	Sen slope	Score	Trend
Annual Mean	0.001266	-3.22357	-0.35122	-0.0268548	-288	decreasing
Annual Max	0.181353	-1.3366	-0.14634	-0.212728	-120	no trend
Annual Min	6.06E-05	-4.01031	-0.43659	-0.00742222	-358	decreasing

It is observed from the above analysis that both the annual mean and annual minimum discharge is decreasing at a rate of 0.02 m^3/s per year and 0.007 m^3/s per year respectively. However, the annual maximum discharge shows no significant trend. The rising temperature and reducing precipitation are probable causes for the decrease in the annual mean discharge. Moreover, the seasonal variability of discharge has also been analysed as shown in Figure 7.
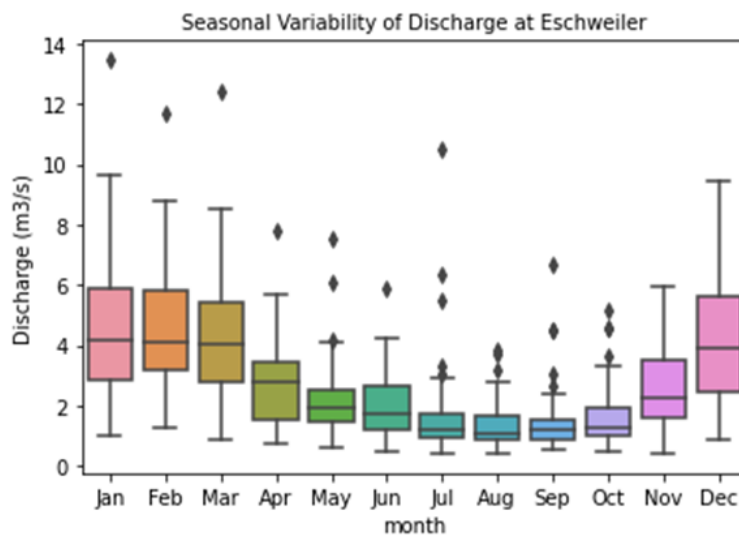
Figure 7 Seasonal variability of discharge at Eschweiler

The figure above indicates that the months from November to March have higher discharge during the year with a range of 3-7 m^3/s. From April to October the discharge is very low at Eschweiler. The lowest discharge is usually observed in August whereas the highest discharge occurs normally in December or January. Results of trend analysis and seasonal variability for the Niers and Swalm catchments can be found in Appendix A.

5.1.2   Hydrological Model Calibration

The Rur catchment was calibrated for 11-gauge stations. For the calibration, the horizontal hydraulic conductivity parameter (KsatHorFrac) was changed keeping the other parameters the same. For Rur catchment, the range of KsatHorFrac was chosen from 50 to 650 keeping an interval of 50. In this report, the calibration for the sub-catchment- Julich has been shown as it has one of the gauges on the Rur river which is situated downstream of the reservoir modeled in this study. Calibration of the other sub-catchments are provided in Appendix C. After determining the KsatHorfrac of the upstream sub-catchments of Julich (from Kall sportplatz to Eschweiler) the model was run again, and the results were obtained as presented below. Figure 8 shows the values of different indicators for different KsatHorFrac

Wasim, S.K. 2022. Predictability of flash flooding in sloping Dutch Catchments (Rur, Niers and Swalm Rivers)

21

Ljubljana, UL FGG, Masters of Science Thesis in Flood Risk Management.

in Julich from 2011 to 2019. From these plots, the best KsatHorFrac was chosen for each indicator as shown in Table 6.
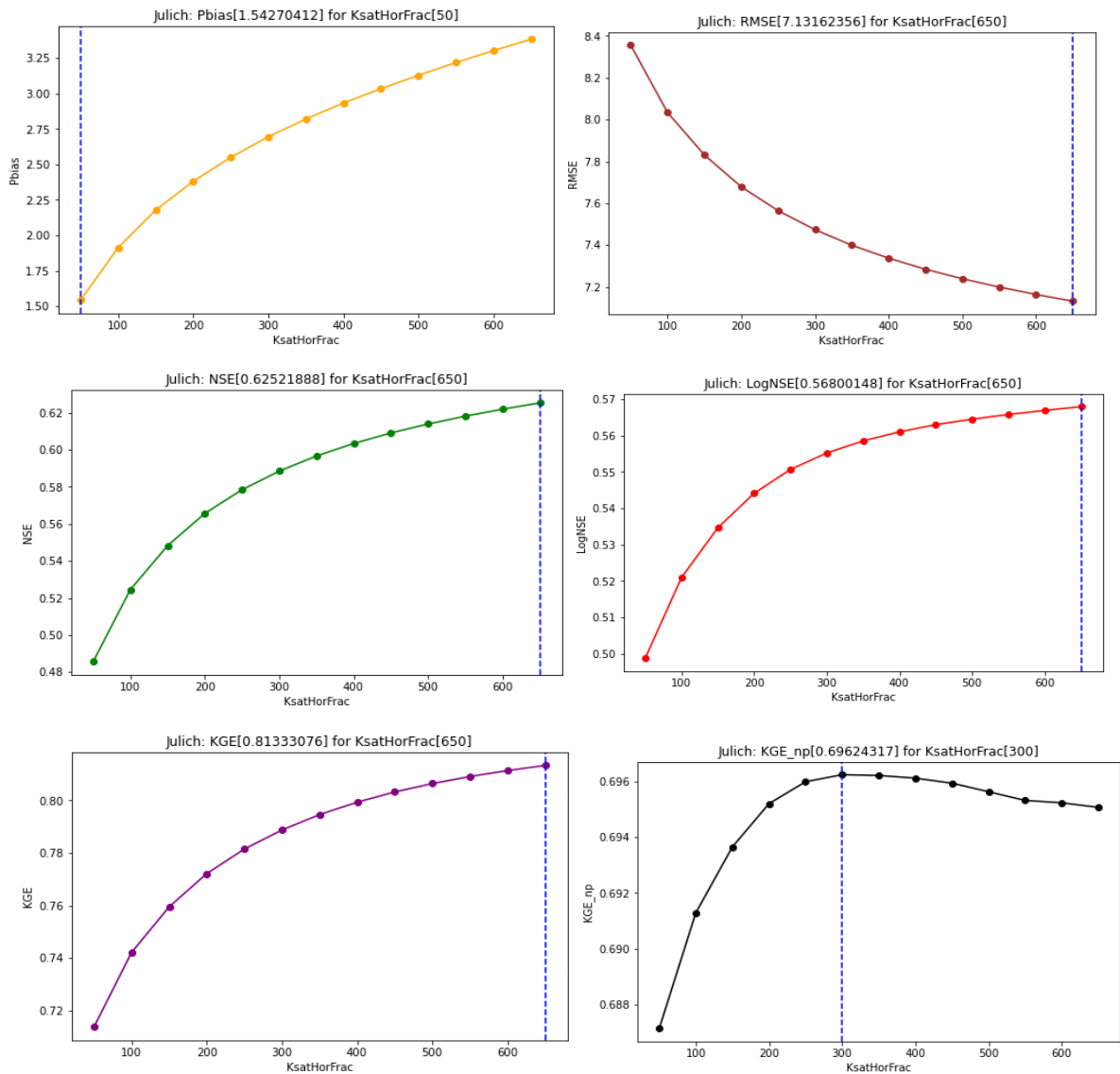
Figure 8 Indicators for Different KsatHorFrac in Julich from 2011 to 2019

Table 6 Indicator for best KsatHorFrac for different time period in Julich

| Station | Year | Indicators | | | | | | | | | | | | KsatHorFrac |
| | | Pbias | | RMSE | | NSE | | LogNSE | | KGE | | KGE_np | | Average |
		Value	Ksat	Value	Ksat	Value	Ksat	Value	Ksat	Value	Ksat	Value	Ksat	
Julich	1981-1990	15.5	50	9.26	650	0.58	650	0.54	500	0.74	650	0.7	650	520
	1991-2000	2.58	50	7.5	650	0.57	650	0.64	650	0.7	650	0.74	650	550
	2001-2010	1.54	50	7.13	650	0.63	650	0.57	650	0.81	650	0.7	300	490
	2011-2019	2.67	50	7.86	650	0.57	650	0.54	200	0.73	100	0.67	150	300

This way a range of possible KsatHorFrac values (300-550) was obtained. Using this range, the indicators were calculated again to observe the range of the indicator values for different time period in Table 7.

Table 7 Range of indicator values for different KsatHorFrac in Julich

KsatHorFrac	Pbias	RMSE	NSE	LogNSE	KGE	KGE_np
1981-1990						
300	16.42	9.91	0.45	0.53	0.64	0.69
400	16.61	9.66	0.48	0.54	0.66	0.69
500	16.77	9.47	0.50	0.55	0.67	0.70
550	16.84	9.39	0.51	0.55	0.68	0.70
1991-2000						
300	7.93	8.34	0.51	0.62	0.64	0.75
400	8.20	8.14	0.53	0.63	0.65	0.75
500	8.41	7.99	0.55	0.64	0.67	0.75
550	8.50	7.93	0.55	0.65	0.67	0.75
2001-2010						
300	2.70	7.47	0.59	0.56	0.79	0.70
400	2.93	7.34	0.60	0.56	0.80	0.70
500	3.13	7.24	0.61	0.56	0.81	0.70
550	3.22	7.20	0.62	0.57	0.81	0.70
2011-2019						
300	4.15	8.09	0.54	0.54	0.72	0.67
400	4.47	8.00	0.55	0.54	0.71	0.67
500	4.74	7.94	0.56	0.54	0.71	0.67
550	4.85	7.91	0.56	0.54	0.70	0.67

From this table it is observed that, although the range of KsatHorFrac is wide enough for Julich, the indicators- NSE, LogNSE, KGE and KGE_np do not show much variation. However, RMSE shows a little variation and PBias has a wide range of values with respect to both KsatHorFrac and the time period. Considering the changes of all the indicators and the KsatHorfrac value for the nearest sub-catchments, the value 400 was chosen as the optimum KsatHorFrac value for Julich.

For the Rur catchment, the driest and wettest (the year with the lowest and highest mean discharge) were found to be 2011 and 1984 respectively and their hydrographs are shown in Figure 9. Moreover, Figure 10 shows the annual mean, maximum and minimum hydrographs for KsatHorFrac =400 in Julich. The annual mean discharge is quite well represented by the simulated results. However, there are some overestimation of the peak discharges and the minimum discharges are not well simulated from 2003-2019. For the overall time period 1981-2019, the KsatHorFrac=400 gives PBias= 8.54, RMSE= 8.33, NSE= 0.54, LogNSE= 0.6, KGE= 0.74 and KGE_np= 0.74 as shown in Table 8 along with the values for the other sub-catchments.
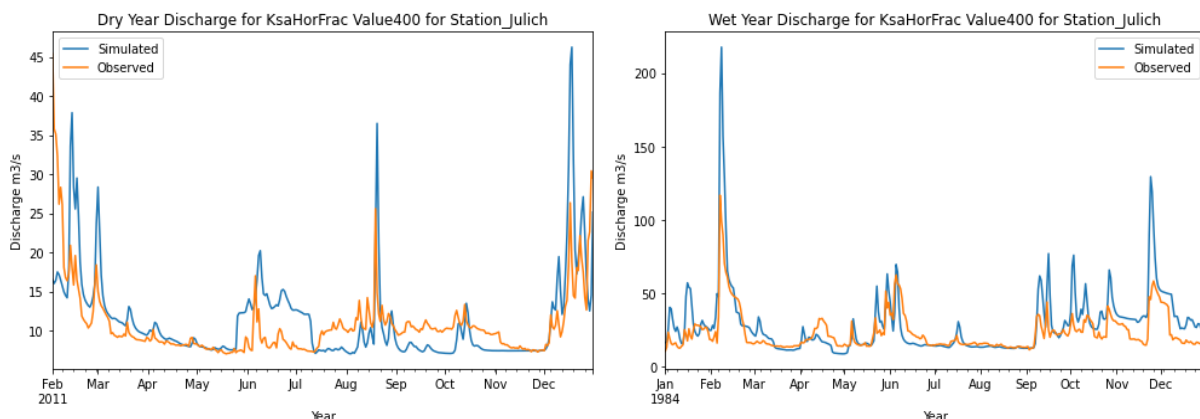
Figure 9 Hydrographs for the driest and wettest years corresponding to KsatHorFrac=400 in Julich

Wasim, S.K. 2022. Predictability of flash flooding in sloping Dutch Catchments (Rur, Niers and Swalm Rivers)

23

Ljubljana, UL FGG, Masters of Science Thesis in Flood Risk Management.
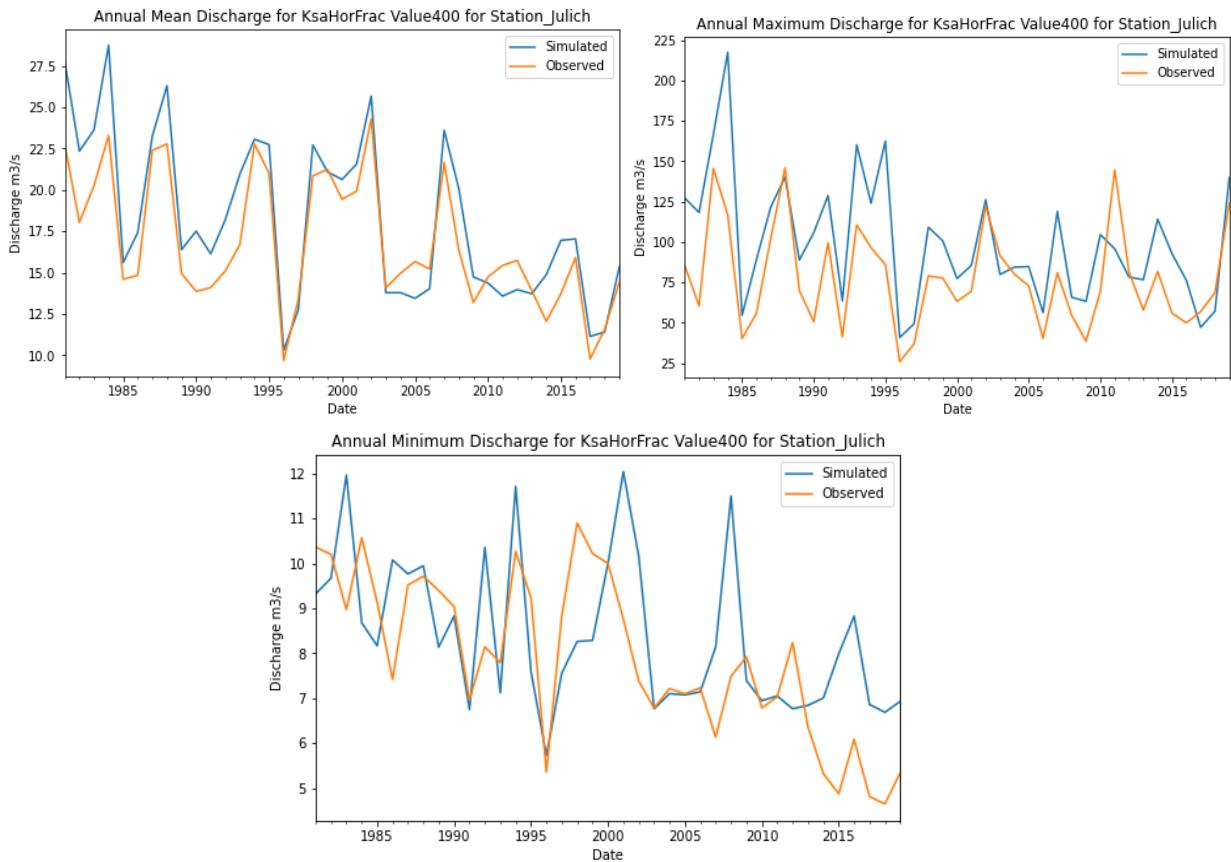
Figure 10 Annual mean, maximum and minimum discharges corresponding to KsatHorFrac=400 in Julich

Following the steps described above, the optimum KsatHorFrac for the other sub-catchments were selected. Figure 11 shows all the chosen values for the whole Rur Catchment. It can be observed that upstream part of the Rur river has lower KsatHorFrac compared to the part downstream of the reservoir. However, the tributaries of Rur- Urft, Inde and Wurm have much higher values of KsatHorFrac compared to the Rur river itself.

Station Name	River	KsatHorFrac
Kall_Sportplatz	Urft	450
Gemund	Urft	450
Monschau	Rur	200
Zerkall	Rur	350
Mulartshutte	Vichtbach	220
Kornelimunster	Inde	470
Eschweiler	Inde	450
Julich	Rur	400
Herzogenrath	Wurm	650
Randerath	Wurm	550
Stah	Rur	450
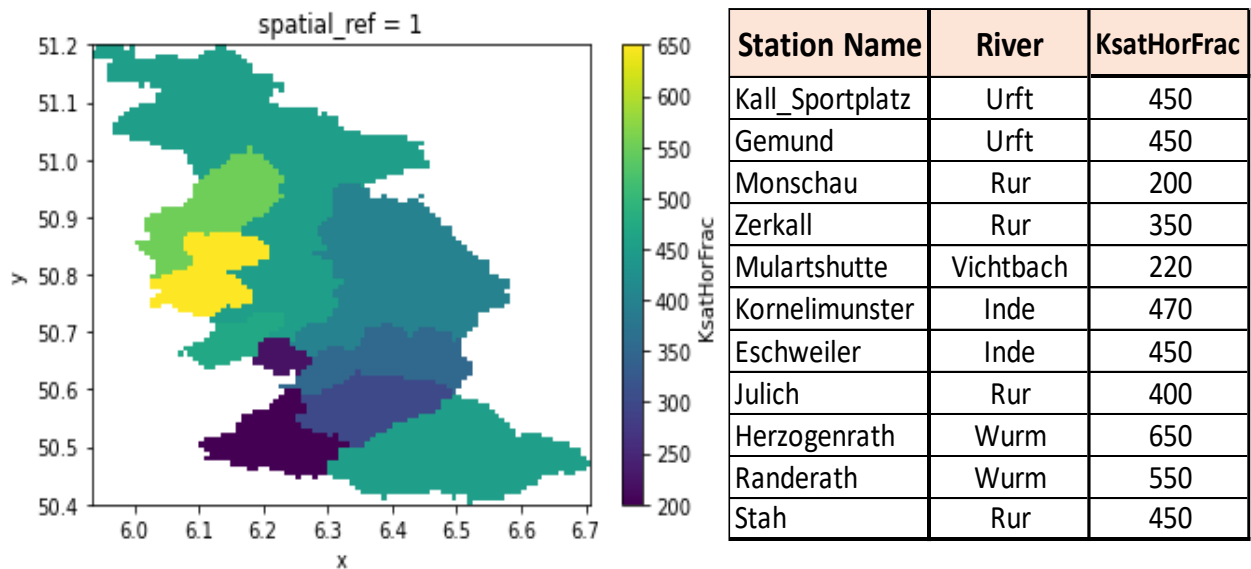
Figure 11 Selected KsatHorFrac values in the Rur catchment

Table 8 Indicators for the whole period for the selected KsatHorFrac in Rur Catchment

Station	KsatHorFrac	1981-2019					
		Pbias	RMSE	NSE	LogNSE	KGE	KGE_np
Kall_Sportplatz	450	0.20	1.16	0.67	0.80	0.82	0.90
Gemund	450	-9.68	3.05	0.76	0.70	0.82	0.85
Monschau	200	-27.99	3.25	0.60	0.73	0.45	0.67
Zerkall	350	-4.82	6.21	0.51	0.34	0.62	0.48
Mulartshutte	220	-26.18	0.66	0.51	0.65	0.44	0.69
Kornelimunster	470	11.72	0.70	0.64	0.64	0.76	0.82
Eschweiler	450	13.27	2.18	0.65	0.77	0.74	0.83
Julich	400	8.54	8.33	0.55	0.60	0.74	0.74
Herzogenrath	650	-22.96	1.67	-0.16	-2.17	0.38	0.57
Randerath	550	11.17	4.05	-2.07	-1.11	-0.32	0.55
Stah	450	18.90	16.04	-0.45	0.42	0.15	0.71

5.1.3   Water Balance Analysis

It was discovered that the discharge in the downstream sub-catchments, such as Herzogenrath, Randerath, and Stah, was not accurately simulated while calibrating the Rur catchment. As demonstrated in Table 8, the indicator values, in particular Pbias, NSE, and KGE, were not as good as compared to the catchment's upstream portion. In order to determine whether the model simulation and the input forcing parameters agree, a water balance analysis was done.
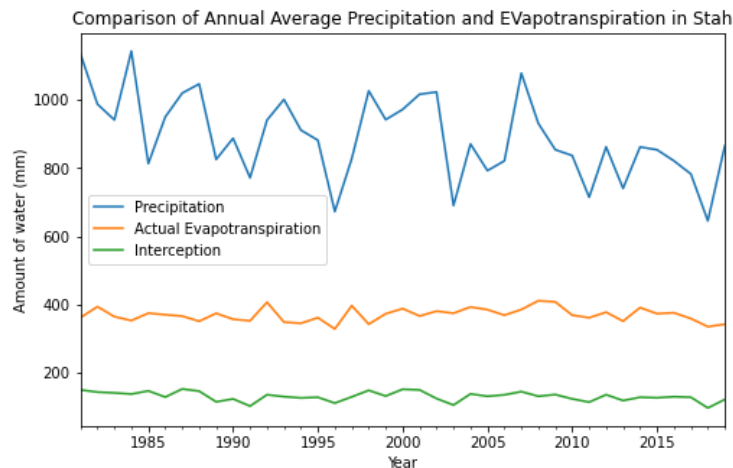
Figure 12 Precipitation, evapotranspiration and interception at Stah

The mean precipitation in the upstream area of Stah is around 890 mm as seen from Figure 12. Mean actual evapotranspiration and interception are 370 mm and 130 mm respectively. The comparison of the inflow and outflow for both simulated and observed discharges are presented in the next figures.

Wasim, S.K. 2022. Predictability of flash flooding in sloping Dutch Catchments (Rur, Niers and Swalm Rivers)

25

Ljubljana, UL FGG, Masters of Science Thesis in Flood Risk Management.
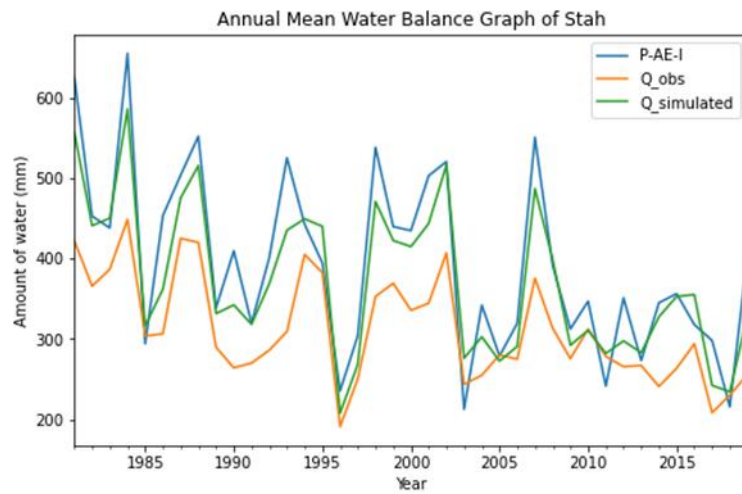
Figure 13 Annual mean water balance of Stah

From Figure 13 it is observed that the simulated discharge for KsatHorFrac = 450 in Stah well represents the water balance components of the region. However, the observed discharge seems to be significantly low. But both the observed and simulated discharge in the upstream sub-catchments incline with the water balance of the respective area (Appendix D). The observed discharges and the inflows of Stah and Julich (the adjacent upstream sub-catchment of Stah) are compared in Figure 14.
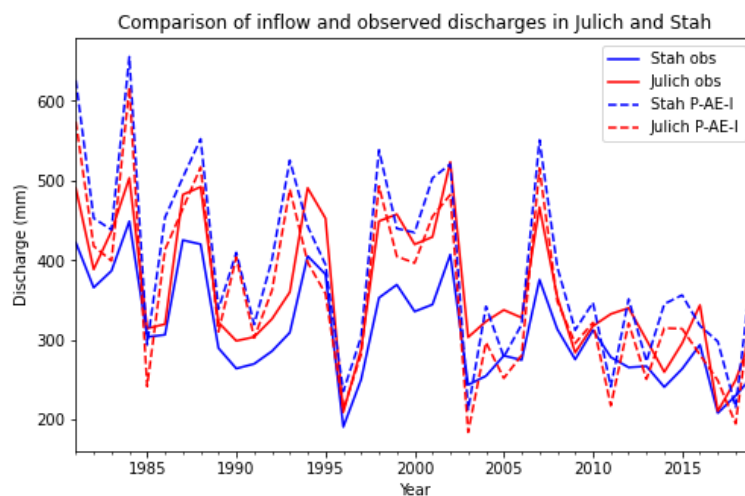
Figure 14 Comparison of inflow and observed discharges in Julich and Stah

Since Stah is located just at downstream of Julich, the sub-catchment is supposed to get more discharge compared to Julich. But Figure 14 shows that the annual mean discharge in Stah (solid blue line) is much lower than that of Julich (solid red line). It is also evident from the graph that the inflow for Julich (red dashed line) is lower than Stah (blue dashed line) as it is supposed to be and the observed discharge of Julich aligns with it. But the observed discharge of Stah is much lower than its inflow. Therefore, it can be assumed that the reason for such lower observed discharges in the downstream part of the Rur catchment might be caused by some external water abstraction activities. Figure 15 shows the locations where ground water is extracted near the study area.
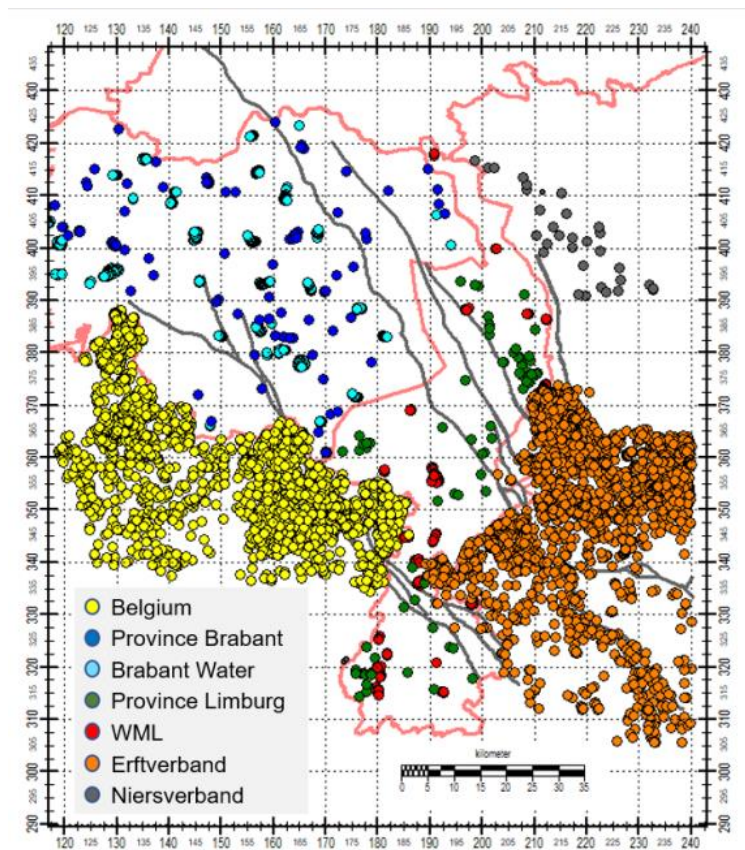
Figure 15 Location of ground water extractions near Limburg
(Vermeulen and op den Kelder, 2022)

It is observed that the intensity of the ground water extraction locations is very high at the near the Netherlands border as well as the downstream part of the Rur catchment. Vermeulen and op den Kelder (2022), analysed the impact of groundwater extractions in the Roer Valley Graben. They reported that, the total volume of groundwater extracted in 2017 was about 325 million m^3/year, of which the drinking water business in Germany (Erfverband) extracts 20%, the drinking water company in The Netherlands (WML and Brabant Water) extracts a combined 63%, and the remaining 17% is extracted by industry in The Netherlands and Belgium. Moreover, the order of ground water extraction from the open pit mines- Hambach and Inden, is about 100 million m^3/year.

According to Vermeulen and op den Kelder (2022), there was a significant impact along the rivers Rode Beek and the Saeffeler bach due to the drawdown of all extractions in the Roer Valley Graben. For example, the drainage capacity of Rode Beek and Saeffeler bach are reduced with 65% and 52% respectively since 1970. The reason for the reduction of flow in these rivers were identified in their report to be the presence of the extractions in Limburg and the lowering of ground water by the open pit mining. They also stated that according to a report from AHU AG Aachen published in 1995, external deficits of surface water discharge was 10 million m^3/year near the Rur Valley Graben. So, there is a possibility that these ground water extractions both directly or indirectly effect discharges in the Rur river and its tributaries. These external abstractions can be considered while Modeling the downstream part of the Rur catchment to see if the simulations improve.

Wasim, S.K. 2022. Predictability of flash flooding in sloping Dutch Catchments (Rur, Niers and Swalm Rivers)

27

Ljubljana, UL FGG, Masters of Science Thesis in Flood Risk Management.

5.2   Hydrological Modeling Results for Niers Catchment

For the Niers catchment, the hydrological analysis was done for the Goch and Oedt sub-catchments. The process of determining the best KsatHorFrac value (from 20 to 800) based on the indicators was also applied for this catchment. However, the values of the indicators for the Niers catchment were extremely poor (Appendix C). In order to observe the change in the simulated results with the KsatHorFrac, the annual mean, maximum, minimum, dry year and wet year discharges were compared for KsatHorFrac=20 and 800 (Figure 16).
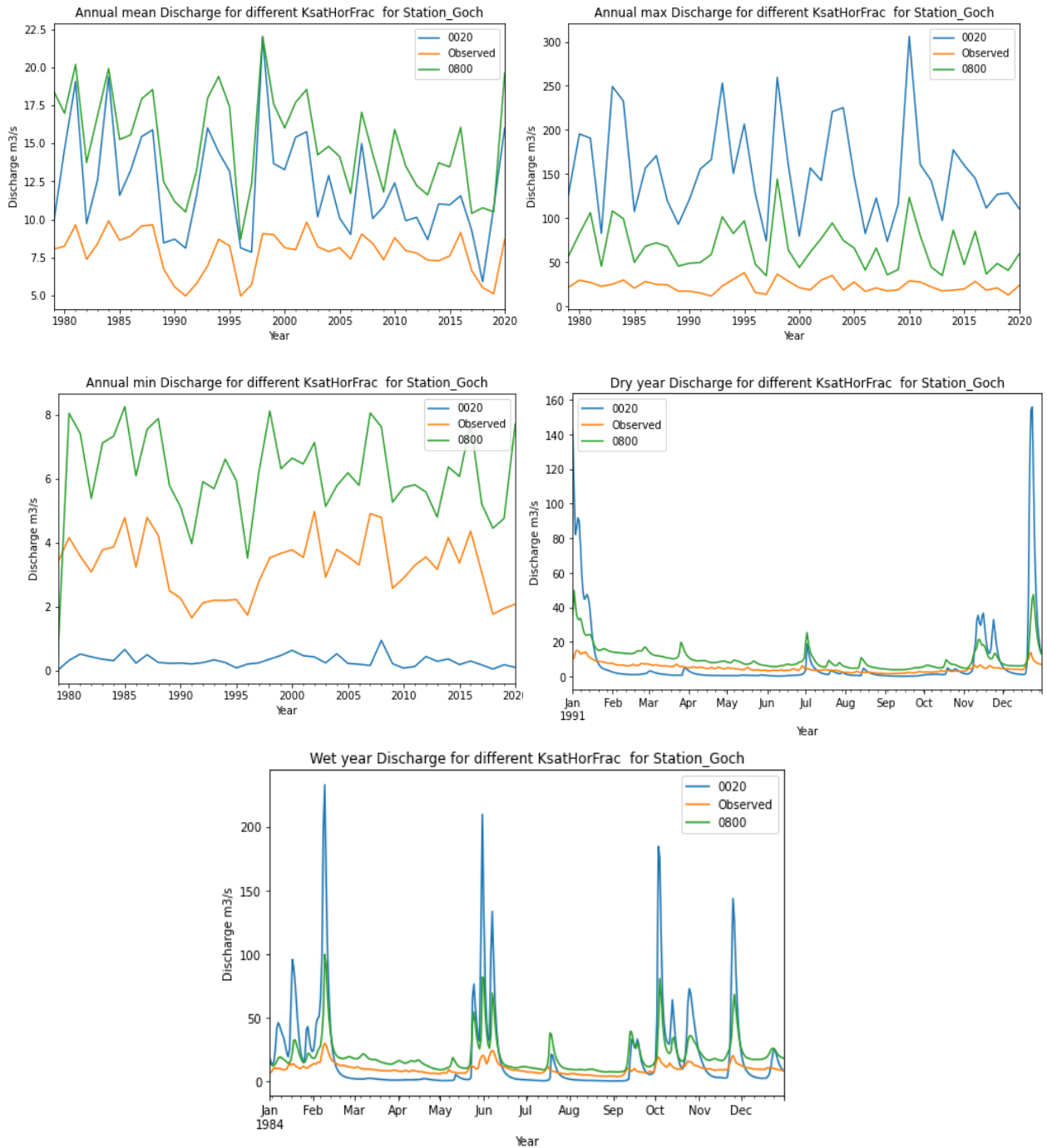
Figure 16 Comparing hydrographs in Goch for KsatHorFrac=20 and 800

In Figure 16 the orange line represents the observed discharge and the blue and green lines represent the simulated discharge for KsatHorFrac =20 and 800 respectively. It is evident that the observed discharge is extremely lower than both of the simulated discharges (KsatHorFrac=20 and 800) for annual mean (top left) and annual maximum (top right) values. Although the minimum or base flow (middle left) can be represented better with a KsatHorFrac value in between 300-500, the dry and wet year hydrographs (middle right and bottom) show that the peaks are very poorly simulated for both low and high values of KsatHorFrac.

With a view to improving the simulated values, some other parameters, such as- maximum leakage (infiltration) and soil thickness were changed, and the model was run again. The initial value of these two parameters were MaxLeakage= 0mm and Soil Thickness=2000mm. The model was run again for MaxLeakage [0.5mm, 1mm] and Soil Thickness [2500 mm, 3000mm] separately. Apparently, there was no change in the simulated results by changing the soil thickness (Appendix). On the other hand, increasing the maximum leakage to 1mm reduced the peak discharge which was better than the peaks of the initially simulated discharge for 0mm. However, the simulation of the base flow was significantly underestimated due to increasing the leakage. Figure 17 shows the hydrographs of the driest (left) and wettest (right) years for different maximum leakage values in Goch.
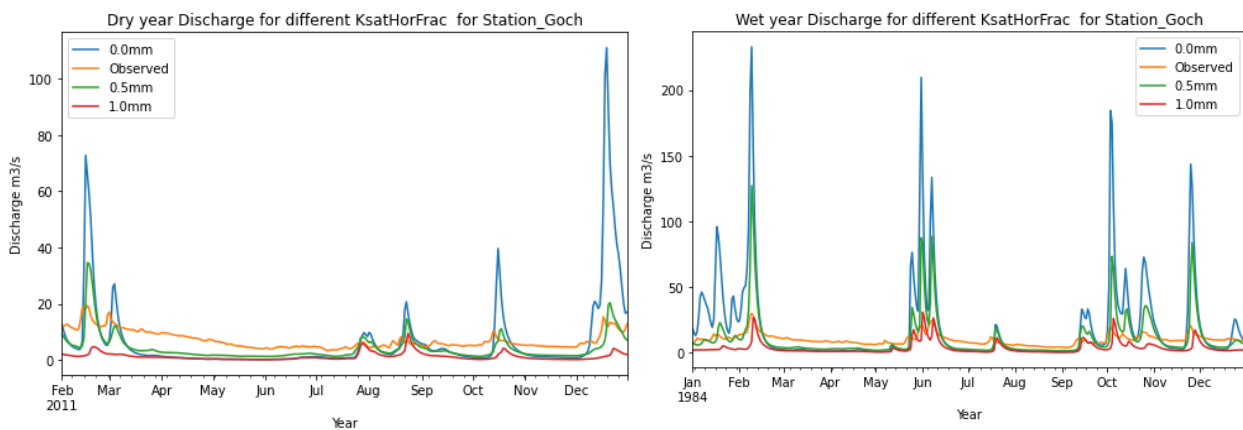
Figure 17 Hydrographs of Driest and Wettest years for different MaxLeakage Values in Goch

Since the simulation in the Niers catchment was poor for a wide range of KsatHorFrac values and it also didn't well represent the observed discharge by changing other parameters, the water balance analysis similar to the Rur catchment was done for Niers.
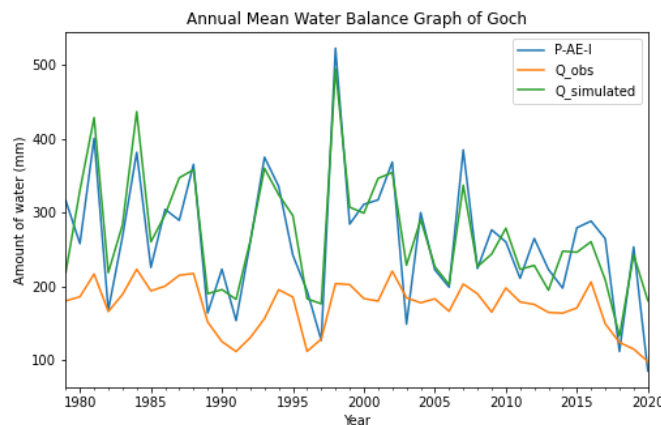
Figure 18 Annual mean water balance of Goch

Wasim, S.K. 2022. Predictability of flash flooding in sloping Dutch Catchments (Rur, Niers and Swalm Rivers)

29

Ljubljana, UL FGG, Masters of Science Thesis in Flood Risk Management.

Figure 18 shows that the simulated discharge for KsatHorFrac=20 (green line) closely aligns with the inflow of water, P-AE-I (blue line). But the annual mean observed discharge at Goch is almost half of this. It can be seen from Figure 15 that the density of ground water extraction locations is also very high in the Niers and Swalm catchments as well. Moreover, the coal mines- Garzweiler I and II are situated at the upstream part of the Niers catchment. And due to the water abstraction by the lignite industry, in summer the water level in the upper reaches becomes very low.

The catchment area of the Niers now counts more than 750,000 inhabitants, almost half of them in the cities Mönchengladbach and Viersen lives. As a result of the various hydraulic interventions and the intensification of land use and management, the water-retaining capacity (the sponge effect) of the entire Niers catchment area has been seriously affected. Moreover, due to the artificially accelerated discharge of the precipitation water into the Meuse, the ground water level has been structurally lowered, for which the Niers has dried up. In particular, frequent mowing management has led to a significant reduction in summer water levels in the Niers. Van Den Brink and Lanphen (1999), reported that after mowing the water vegetation, the water level in the Niers decreases by 0.3 to 0.4 meters. If it were no longer mowed at all, it is estimated that the water level in the Niers - as well as the groundwater level in the stream valley floor - would rise structurally by approximately 1 to 1.5 metres.

Due to the reasons mentioned above, the observed discharge is very low in the Niers catchment. Therefore, it is not possible to calibrate the discharge in the Niers Catchment without considering these external effects. So, the analysis for Niers catchment was not further continued due to the limitations of the hydrological model built for Niers.

5.3 Hydrological Modeling Results for Swalm Catchment

For Swalm catchment the hydrological analysis was done for Molzmuhle, Pannenmuhle and Landesgrenze. The values of the indicators were calculated for KsatHorFrac value from 5 to 700. Similar to the Niers catchment the indicator values were very poor for Swalm as shown in Table 9.

Table 9 Indicator for Best KsatHorFrac for Different Time Period in Swalm Catchment

Station	Year	Indicators												KsatHorFrac
		Pbias		RMSE		NSE		LogNSE		KGE		KGE_np		Average
		Value	Ksat	Value	Ksat	Value	Ksat	Value	Ksat	Value	Ksat	Value	Ksat	
Landesgrenze	1986-1990	13.44	5	1.26	500	-3.9	500	-0.98	250	-0.33	500	0.53	50	300
	1991-2000	25.16	5	1.5	500	-5.34	500	-1.18	250	-0.68	500	0.45	50	300
	2001-2010	10.03	5	1.2	500	-3.66	500	-1.01	250	-0.34	500	0.54	50	300
	2011-2020	0.36	20	0.91	500	-1.62	500	-0.08	250	0.03	500	0.66	250	330
Molzmuhle	1986-1990	64.8	5	0.7	700	-32.8	700	-5.12	500	-3.82	700	0.05	50	440
	1991-2000	50.14	5	0.7	700	-23.2	700	-3	500	-3.12	700	0.16	250	470
	2001-2010	15.44	5	0.62	700	-13.2	700	-3.02	500	-2.19	700	0.42	500	510
	2011-2020	0.3	5	0.49	700	-6.47	700	-1.73	500	-1.19	700	0.52	500	510
Pannenmuhle	1986-1990	32.53	5	0.99	700	-9.47	700	-1.76	500	-1.46	700	0.4	250	470
	1991-2000	22.14	5	0.94	500	-8.14	500	-1.31	500	-1.37	500	0.46	250	370
	2001-2010	-0.86	20	0.82	700	-3.88	700	-1.08	500	-0.63	700	0.6	500	520
	2011-2020	-3.38	50	0.62	500	-3.84	500	-0.72	500	-0.75	500	0.7	500	420

The plots for the annual mean, maximum, minimum, dry year and wet year discharges for different KsatHorFrac can be found in Appendix C. The water balance analysis was also done for Swalm (Appendix D) which shows that the observed discharge in Swalm is much lower than the inflow in the catchment. Figure 15 shows the high density of ground water extraction points in the Swalm catchment as well. Therefore, similar to the Niers catchment, the analysis for Swalm was not continued further.

5.4   Results of Forecast Analysis

5.4.1   Evaluation of Forecast Performance

The forecast with Delft-Fews was only generated for the Rur catchment as the hydrological model performance was very poor for both the Niers and Swalm catchments. After coupling the calibrated Rur model with Delft-FEWS, the hydrological deterministic forecast was generated from 01-01-2018 to 31-12-2021. However, due to lack of observed data after June 30, 2021, the forecast evaluation could not be done after that date. In order to evaluate the performance of the generated forecast, the outputs from Delft-FEWS were compared to the observed discharge of several river gauges in the Rur and the skill scores (PBias, RMSE and MAE) were calculated. Figure 19 shows the variation of these scores with lead time for the sub-catchment Stah. Plots for other sub-catchments are provided in Appendix E.
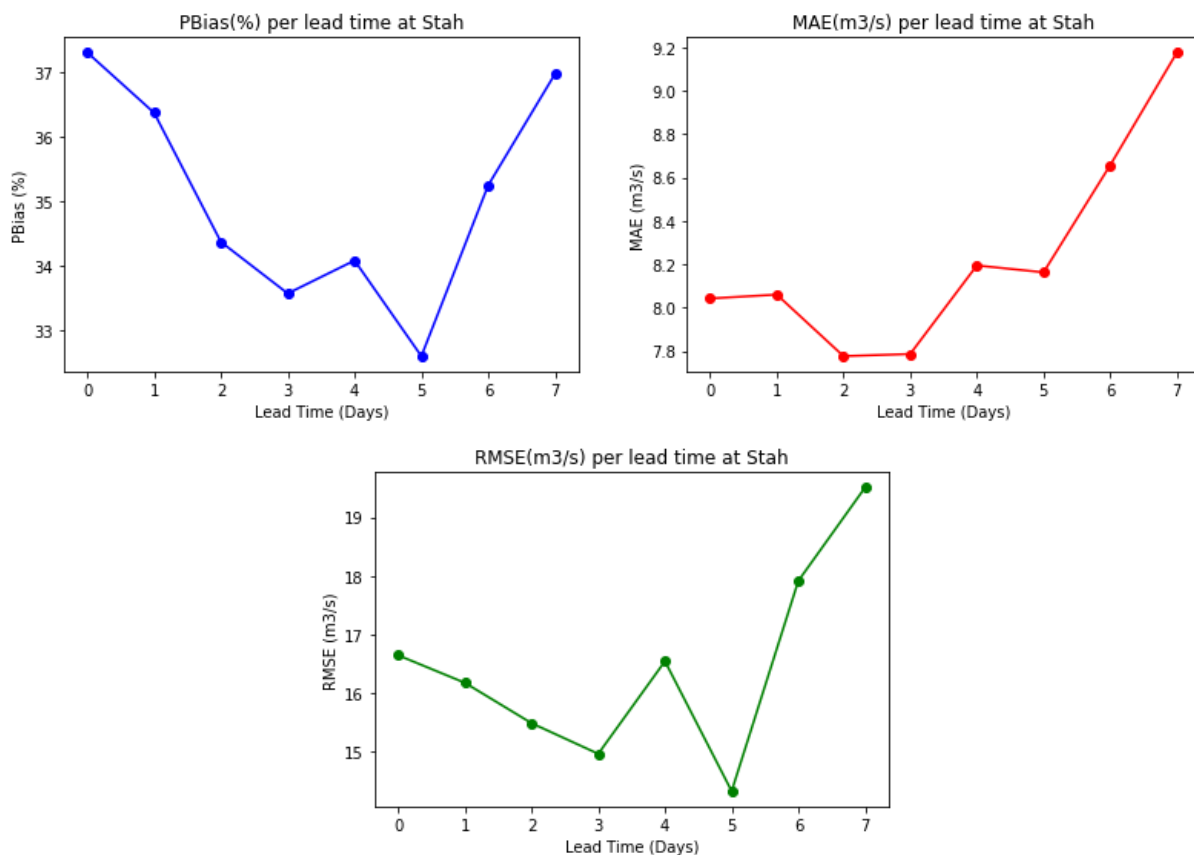
Figure 19 Forecast skill scores per lead time for Stah

It can be observed from Figure 19 that, skill scores are very high for 6- and 7-days lead time. The PBias and RMSE are both lowest for 5 days lead time. The range of MAE is 7.8 m^3/s-9.1 m^3/s and the range for RMSE is 14.3 m^3/s-19.1 m^3/s for 0-7 days lead time. Since the mean daily discharge at Stah is around

Wasim, S.K. 2022. Predictability of flash flooding in sloping Dutch Catchments (Rur, Niers and Swalm Rivers)

31

Ljubljana, UL FGG, Masters of Science Thesis in Flood Risk Management.

21 m^3/s, these errors are considered to be very significant. The reason for the high quantity of error in Stah could be the large difference between the observed and simulated discharges as discussed in section 5.1.3. Summary of all the scores in five sub-catchments in the Rur basin is provided in Table 10.

Table 10 Forecast skill scores per lead time in the Rur catchment

Station	Area	Mean Daily	Lead Time (Days)							
	sq.km	Discharge (m3/s)	0	1	2	3	4	5	6	7
Pbias (%)										
Kall-Sportplatz	133.5	1.36	0.67	-0.88	-3.22	-1.90	-1.55	-3.16	-1.63	1.13
Eschweiler	251.18	2.8	33.10	28.38	23.82	24.47	21.50	20.16	23.45	24.27
Gemund	345.61	4.82	-16.85	-18.83	-20.19	-19.98	-19.82	-21.18	-20.82	-19.36
Zerkall	791.99	11.65	-4.75	-4.77	-5.09	-4.93	-4.74	-4.57	-4.25	-3.69
Stah	2151.73	21.2	37.31	36.38	34.37	33.58	34.09	32.60	35.25	36.98
RMSE (m3/s)										
Kall-Sportplatz	133.5	1.36	0.66	0.90	0.93	1.14	1.25	1.23	1.31	1.41
Eschweiler	251.18	2.8	2.11	2.33	2.26	2.74	2.86	2.89	3.33	3.64
Gemund	345.61	4.82	2.31	2.82	3.02	3.35	3.64	3.68	3.79	4.00
Zerkall	791.99	11.65	7.37	7.44	7.51	7.56	7.55	7.48	7.42	7.38
Stah	2151.73	21.2	16.65	16.18	15.49	14.97	16.55	14.33	17.92	19.51
MAE (m3/s)										
Kall-Sportplatz	133.5	1.36	0.31	0.36	0.38	0.43	0.46	0.49	0.50	0.54
Eschweiler	251.18	2.8	0.96	0.97	1.02	1.11	1.16	1.26	1.38	1.46
Gemund	345.61	4.82	1.40	1.55	1.62	1.70	1.77	1.83	1.87	1.91
Zerkall	791.99	11.65	4.44	4.47	4.50	4.51	4.50	4.47	4.44	4.41
Stah	2151.73	21.2	8.04	8.06	7.78	7.79	8.19	8.16	8.66	9.18

To easily interpret Table 10, PBias is plotted against the sub-catchments to visualize the variation with their basin size since PBias is a unitless measurement of the error (Figure 20).
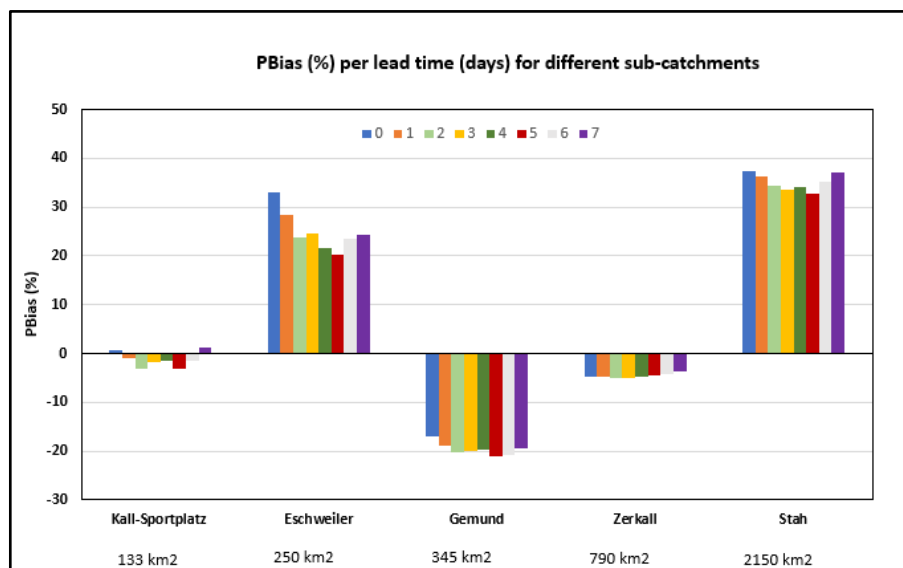
Figure 20 PBias per lead time for different sub-catchments in the Rur

Figure 20 shows the performance of the forecast is better for Zerkall than the other sub-catchments. The PBias is around -3.7% for 7 days lead time in Zerkall. The bias is maximum for Stah. Apparently, there

is no pattern of the PBias value associated with the area of the sub-catchments. In order to understand the predictability of flooding in the Rur catchment, the forecast was compared with the wflow simulation (with EOBS dataset) from 13-07-2021 to 23-07-2021 (Figure 21) along with observed peak values on 16-07-2021. Since Stah is the closest to the outlet of the Rur catchment, this analysis was conducted for Stah.
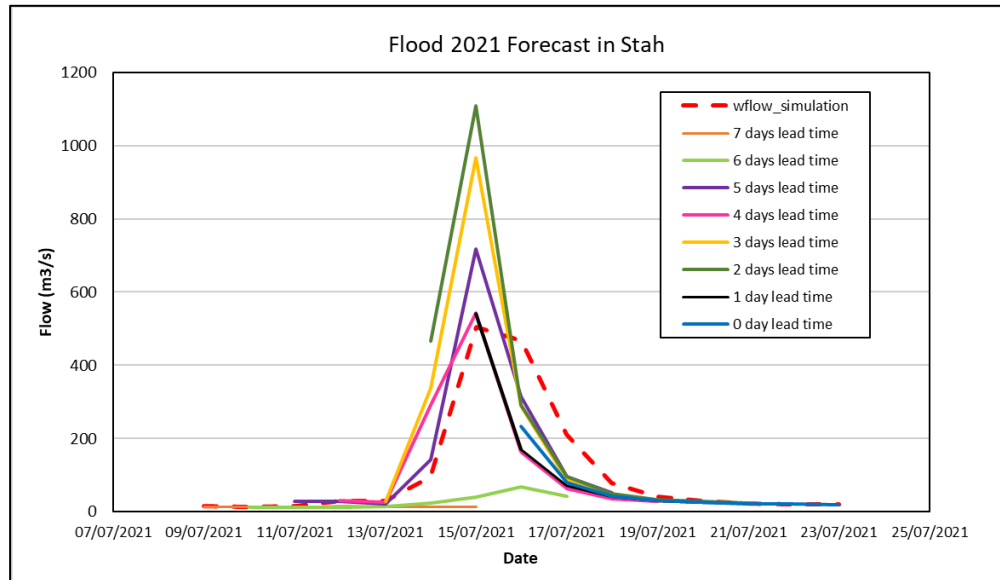
Figure 21 Comparison of forecast and wflow_simulation for the July, 2021 flood event in Stah

Considering 16 July 2021 as the day of the event, the forecasts have been plotted in Figure 21. Due to lack of observed data during that event, it was not possible to compare the forecast by plotting the observed discharge in this graph. However, there are different sources which provide an idea of the peak discharge at Stah on 16 July. According to Geertsema & Asselman (2022), the discharge at Stah was 230 (+/- 10) to 258 (+/- 10) m^3/s around 5PM on 16 July. Moreover, the maximum discharge measured in Rur was around 270 m^3/s (Hoogwater, 2021) on 16 July around 8PM (Bottema et al., 2022). According to Figure 21 the flood peak occurred on 15 July which means the discharge peak in the model simulations occurs before the measured discharge peak. This could suggest that the peak wave experienced more resistance than is currently modeled.

Compared to the measured range of peak flow on 16 July, it can be said that the forecasts have extremely overestimated the peak discharge of the flood. However, the model predicted around 40-60 m^3/s discharge in Stah from 10 July; 6 days ahead of the flood. On the next day it predicted around 717 m^3/s of flood on 15 July which is almost three times the actual flood peak on 16 July. The wflow simulation (red dotted line) provides a significant overestimation of the flood discharge (around 500 m^3/s on 15 July). The reason for this overestimation of the model could be the lowering of observed flow in the river due to external abstractions as discussed in section 5.1.3. But the forecasts with 3 days and 2 days lead time are almost as double as the wflow simulation. To investigate this, forecasts in the most upstream gauge in the Rur basin, Kall-Sportplatz (Figure 23) and the immediate downstream gauge of the reservoir, Zerkall (Figure 22) were compared to the wflow simulations.

Wasim, S.K. 2022. Predictability of flash flooding in sloping Dutch Catchments (Rur, Niers and Swalm Rivers)

33

Ljubljana, UL FGG, Masters of Science Thesis in Flood Risk Management.
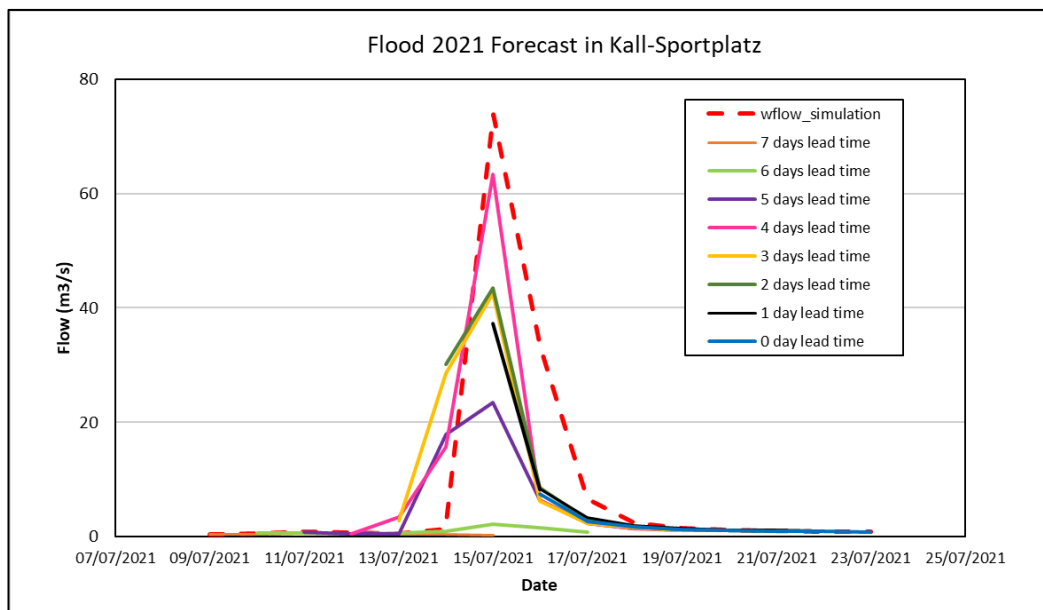
Figure 23 Comparison of forecast and wflow_simulation for the July, 2021 flood event in Kall-Sportplatz
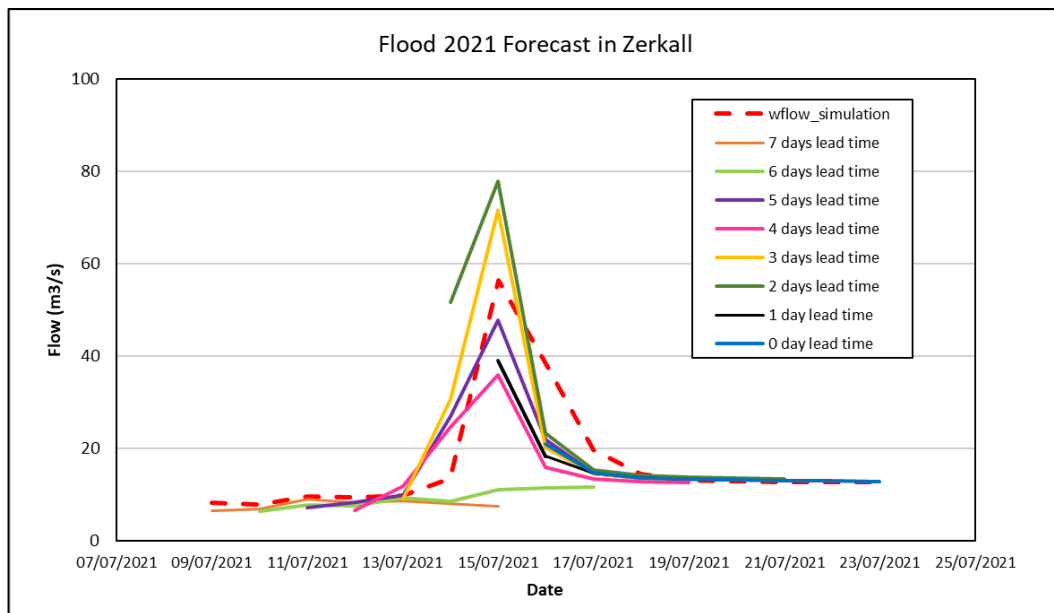
Figure 22 Comparison of forecast and wflow_simulation for the July, 2021 flood event in Zerkall

The forecasts do not overestimate the flow compared to the wflow simulation in Kall-Sportplatz as can be seen from Figure 23 but they do overestimate the flow downstream of the reservoir as shown in Figure 21and Figure 22. From Table 8 it can be seen that the scores for Kall-Sportplatz were comparatively good and the sub-catchment was calibrated for KsatHorFrac=450. For this particular flood event, the forecast predicts high flow in Kall-Sportplatz 5 days ahead of the flood and the forecast with 4 days lead time is closest to the wflow simulation. However, for Zerkall the forecasts with 2- and 3-days lead time show large overestimation which was also the case for Stah. As the reservoir operations in the Rur catchment were not adequately modeled, this is a likely cause for the forecast model's high overestimation in the downstream gauges of the reservoir. In Stah the forecast performance is better for

a longer time period as discussed in this section earlier, but the pattern of the performance does not remain same for an individual event due to the frequent fluctuations in the meteorological data in a small-time range. Although the performance of the forecast model is not satisfactory considering this particular event, it predicted the high flows 5-6 days ahead of the flood which could be useful for disaster preparedness and management.

5.4.2   Sensitivity Analysis of Forecasts

The forecast was run again by changing the KsatHorFrac parameters values of the hydrological model to check the sensitivity of the forecast to this parameter. KsatHorFrac = 100, 350 and 450 was used for this sensitivity analysis. Figure 24, Figure 25 and Figure 26 shows the PBias, RMSE and MAE respectively for different KsatHorFrac for the sub-catchment Stah.
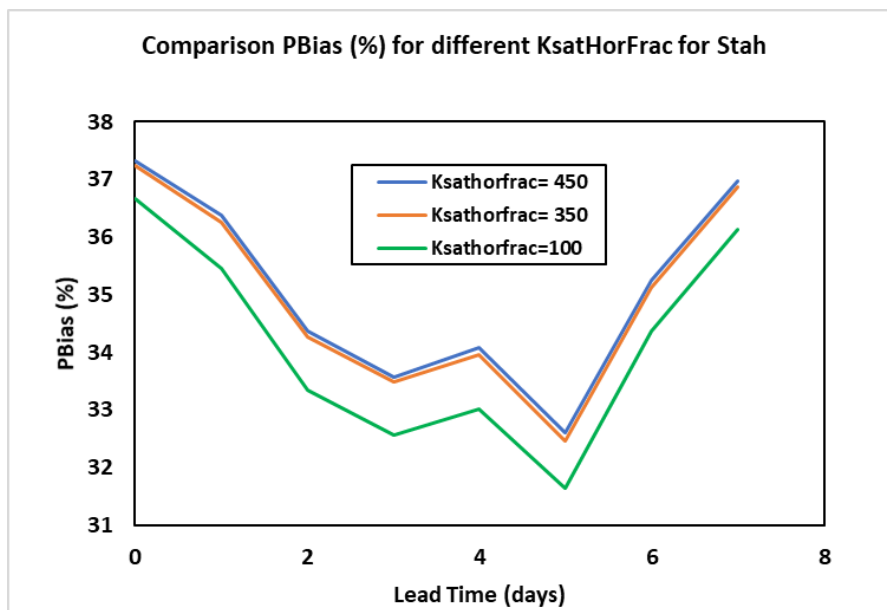
Figure 24 Comparison of PBias for different KsatHorFrac values in Stah
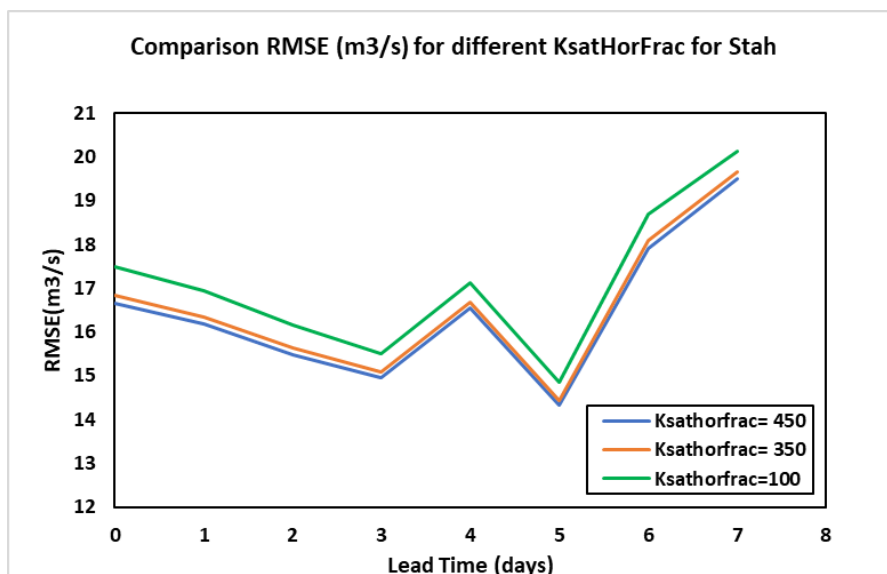
Figure 25 Comparison of RMSE for different KsatHorFrac values in Stah

Wasim, S.K. 2022. Predictability of flash flooding in sloping Dutch Catchments (Rur, Niers and Swalm Rivers)

35

Ljubljana, UL FGG, Masters of Science Thesis in Flood Risk Management.
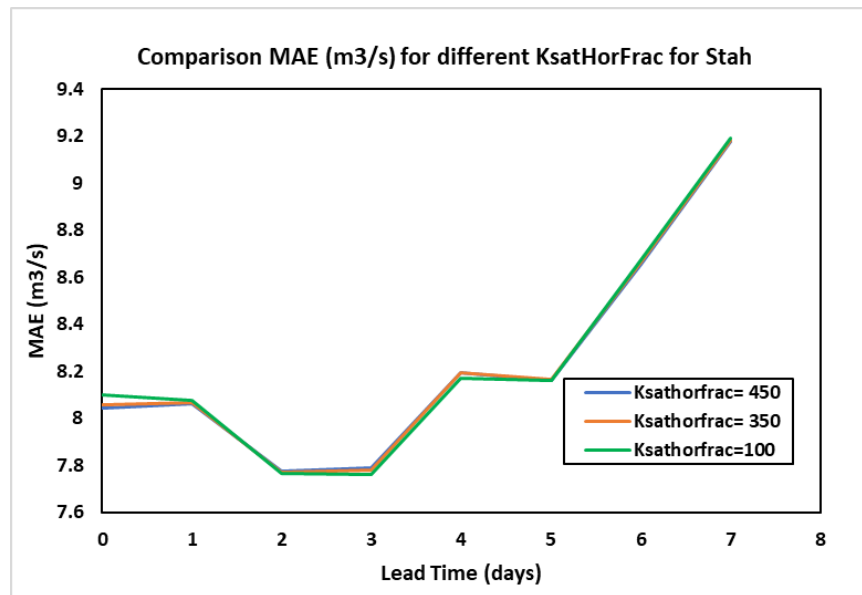
Figure 26 Comparison of MAE for different KsatHorFrac values in Stah

It is evident from Figure 24 that the PBias values are better for smaller KsatHorFrac in Stah. In Table 6 the smallest KsatHorFrac value corresponded to the best PBias value for Julich, which is also the case for Stah as can be found in Appendix C. For RMSE, KsatHorFrac=450 (selected value for Stah) shows the best result but the sensitivity of the score is very low to the changing parameter. Besides, the MAE shows almost no sensitivity to the KsatHorFrac values. Therefore, to reduce the overestimation by the model, the KsatHorFrac in Stah can be reduced without compromising the overall performance of the model.

6   CONCLUSIONS AND RECOMMENDATIONS

6.1   Summary and Conclusions

The trend analysis shows an increase in temperature in all three catchments. The annual rise in temperature in the study area varies between 0.03-0.05ºC which leads to increasing evapotranspiration. Although the precipitation in the Rur catchment is decreasing, there is no significant trend in the Niers and Swalm. As a result, the annual mean discharge in Rur had a declining trend, whereas there was no trend in annual discharges in Niers and Swalm.

According to the results of the calibration of the Rur catchment, the calibrated wflow model provides satisfactory simulations for most parts of the catchment. However, the values of the indicators were very poor for the three most downstream sub-catchments- Herzogenrath, Randerath and Stah. Water balance analysis results show that the wflow simulations align quite well with the inflow coming into the catchment but the observed discharge in the downstream part is very low compared to the inflow. Ground water abstractions by drinking water companies, industries or for open pit minings could be a possible reason for such lowering of river flow in the Rur catchment. As for the upstream part, it was found that the average value of the horizontal hydraulic conductivity (KsatHorFrac) ranges from 220-450.

Similar to the downstream part of the Rur catchment, the observed flows of the Niers and Swalm catchments were also found to be very low compared to the wflow simulation. The results did not improve by changing parameters other than KsatHorFrac, such as- maximum leakage and soil thickness. Water balance analysis for Niers and Swalm indicated similar results as for the downstream part of Rur. The ground water extraction points cover most of the parts of these catchments. Another important reason for such low discharge in the Niers river could be the frequent mowing management in the catchment area. Since the simulated discharge showed poor results for all the river gauges analysed for the Niers and Swalm rivers, the hydrological models could not be calibrated for these rivers and so the forecast was not possible to generate.

Forecast analysis results for the Rur catchment showed that the forecast skill scores MAE and RMSE increase with lead time. However, the PBias values did not show any particular pattern of change with lead time or sub-catchment size. The values of the skill scores were significantly high for most sub-catchments which indicates poor forecast performance. Since the DWD ICON forecast has a low resolution (approx. 27km), the forecast results generated using this dataset were not satisfactory. Using a dataset with a higher resolution e.g. ECMWF reforecast dataset can improve the forecast performance.

Forecasts generated for the time period of July 2021 flood showed that the model provided prediction of the flood 6 days ahead. According to the model, the flood peak occurs on 15 July whereas the actual flood peak occurred on 16 July. This indicates that the peak wave encountered greater resistance than predicted by the current model. Since the external water abstractions were not incorporated and the reservoirs were not adequately represented in the wflow model, the forecast generated using this hydrological model extremely overestimated the flood peak downstream of the reservoir. For a small

Wasim, S.K. 2022. Predictability of flash flooding in sloping Dutch Catchments (Rur, Niers and Swalm Rivers)

37

Ljubljana, UL FGG, Masters of Science Thesis in Flood Risk Management.

time period such as this flood event, the pattern of the forecast performance was not similar to the overall forecast period due to frequent fluctuations in the meteorological forecast dataset.

Sensitivity of the percent bias to the model parameter KsatHorFrac showed that for smaller values of KsatHorFrac in Stah the overestimation of the flow could be reduced. However, for higher KsatHorFrac, the forecasts fit slightly better to the observed dataset and the mean absolute error remains almost constant with the changing of the parameter.

6.2   Study Limitations/Future Study Recommendations

For this study only one source of dataset was used for the input forcing dataset (EOBS for precipitation and ERA5 for temperature and evapotranspiration) and discharge (ELWAS). For future studies, data from more sources can be used to calibrate the hydrological model and the results can be compared to prepare a better set of observed data.

The Olef, Urft and Rur reservoirs could not be Modeled separately in wflow rather they were combined as one reservoir. So, the dependency of the reservoirs on one another could not be Modeled. The results of the forecasts could have been better if the reservoir operations were accurately Modeled in wflow.

For the calibration of the wflow model, only the spatial variation of the horizontal hydraulic conductivity parameter (KsatHorFrac) was considered. Although the effects of maximum leakage and soil thickness parameter were analysed for the Niers and Swalm catchment, their values were kept constant over the whole catchment. It was observed from the effects of the maximum leakage parameter that, higher value of MaxLeakage reduces the discharge significantly which led to underestimation of the base flow. Therefore, it is recommended to use a spatial variability of these parameters to check if this improves the simulation results.

The DWD ICON forecast dataset which has a very low resolution (0.25°) was used for generating the deterministic forecasts. It is recommended to use a forecast dataset with higher resolution e.g. ECMWF HRES dataset (9km resolution) in order to get satisfactory forecast performance. Moreover, the results from using different sources of forecast dataset can be compared to check the extent of variation in the FEWS model results. Another scope for future studies in this study area could be generating ensemble forecasts using ECMWF medium range forecasts.

Due to lack of recent discharge measurement data, it was not possible to compare the forecast results for the July 2021 flood event with the observed dataset. Therefore, it is crucial to make the river data accessible for research in order to improve forecasts and prepare for catastrophes like the one that occurred on July 16, 2021.

The sentivity analysis for the other sub-catchmets in Rur was not conducted in this study. To properly understand the response of the forecast model to the hydrological model parameters, analysis for other sub-catchments should be included in future studies. Moreover, sensitivity of the forecast to other parameters of the hydrological model could also be conducted in future studies.

REFERENCES

Alfieri, L., Pappenberger, F., Wetterhall, F., Haiden, T., Richardson, D., & Salamon, P. (2014). Evaluation of ensemble streamflow predictions in Europe. *Journal of Hydrology*, *517*, 913-922.

Bottema, M., Sprokkereef, E., Teunis, B. & Slomp, R. (2022). A summer flood, what was different? https://doi.org/10.13140/RG.2.2.21213.28647.

Dabney, S. M., & Selim, H. M. (1987). Anisotropy of a fragipan soil: Vertical vs. horizontal hydraulic conductivity. *Soil Science Society of America Journal*, *51*(1), 3-6.

De Wit, M. J. M., Van Den Hurk, B. J. J. M., Warmerdam, P. M. M., Torfs, P. J. J. F., Roulin, E., & Van Deursen, W. P. A. (2007). Impact of climate change on low-flows in the river Meuse. *Climatic change*, *82*(3), 351-372.

Delft-FEWS (2022). "About Delft-FEWS". Retrieved from https://oss.deltares.nl/web/delft-fews/about-delft-fews

Drogue, G., Fournier, M., Bauwens, A., Buiteveld, H., Commeaux, F., Degre, A., ... & Vanneuville, W. (2010). Analysis of climate change, high-flows and low-flows scenarios on the Meuse basin: WP1 report-Action 3.

Eilander, D., van Verseveld, W., Yamazaki, D., Weerts, A., Winsemius, H., & Ward, P. (2020). A hydrography upscaling method for scale invariant parametrization of distributed hydrological models. *Hydrology and Earth System Sciences Discussions*, *November* 1–34. https://doi.org/10.5194/hess-2020-582

ERA5: data documentation. (2022, June 23). Retrieved from https://confluence.ecmwf.int/display/CKB/ERA5%3A+data+documentation

Garzweiler surface mine. (2022). Retrieved July 12, 2022, from https://en.wikipedia.org/wiki/Garzweiler_surface_mine.

Gash, J. (1979). An analytical model of rainfall interception by forests. Q. J. R. Meteorol. Soc. 105, 43–55. https://doi.org/10.1002/qj.49710544304

Geertsema, T. & Asselman, N. (2022, May 5). Analyse hoogwater Roermonding. (Report no. 11207700-000-ZWS-0020). Deltares, Delft.

Gupta, H. V., Sorooshian, S., & Yapo, P. O. (1999). Status of automatic calibration for hydrologic models: Comparison with multilevel expert calibration. *Journal of hydrologic engineering*, *4*(2), 135-143.

Haggett, C. (1998). An integrated approach to flood forecasting and warning in England and Wales. *Water and Environment Journal*, *12*(6), 425-432.

Hartgring, S. (2022). *Flood prediction in the Rur catchment.* [Unpublished Manuscript]. Civil Engineering, Hydraulic Engineering, Delft University of Technology.

Hallouin, T. (2021). hydroeval: an evaluator for streamflow time series in Python. https://doi.org/10.5281/zenodo.2591217

Hussain et al., (2019). pyMannKendall: a python package for non-parametric Mann Kendall family of trend tests. *Journal of Open Source* Software, 4(39), 1556, https://doi.org/10.21105/joss.01556

Wasim, S.K. 2022. Predictability of flash flooding in sloping Dutch Catchments (Rur, Niers and Swalm Rivers)

39

Ljubljana, UL FGG, Masters of Science Thesis in Flood Risk Management.

Hyndman, R. J., & Koehler, A. B. (2006). Another look at measures of forecast accuracy. *International Journal of Forecasting*, *22*(4), 679–688. https://doi.org/10.1016/j.ijforecast.2006.03.001

Hoogwater, T. F. F. F. (2021). Hoogwater 2021 Feiten en Duiding. *ENW report*. Task Force Fact Finding Hoogwater, Limburg.

Houska, T., Kraft, P., Chamorro-Chavez, A., & Breuer, L. (2015). SPOTting model parameters using a ready-made python package. *PLoS ONE*, *10*(12), 1–22. https://doi.org/10.1371/journal.pone.0145180

Imhoff, R. O., van Verseveld, W. J., van Osnabrugge, B., & Weerts, A. H. (2020). Scaling Point-Scale (Pedo)transfer Functions to Seamless Large-Domain Parameter Estimates for High-Resolution Distributed Hydrologic Modeling: An Example for the Rhine River. *Water Resources Research*, *56*(4), 1–28. https://doi.org/10.1029/2019WR026807

Knoben, W. J. M., Freer, J. E., & Woods, R. A. (2019). Technical note: Inherent benchmark or not? Comparing Nash-Sutcliffe and Kling-Gupta efficiency scores. *Hydrology and Earth System Sciences*, *23*(10), 4323–4331. https://doi.org/10.5194/hess-23-4323-2019

Krause, P., Boyle, D. P., & Bäse, F. (2005). Comparison of different efficiency criteria for hydrological model assessment. *Advances in geosciences*, *5*, 89-97.

Kreienkamp, F., Philip, S. Y., Tradowsky, J. S., Kew, S. F., Lorenz, P., Arrighi, J., ... & Wanders, N. (2021). Rapid attribution of heavy rainfall events leading to the severe flooding in Western Europe during July 2021. Department of Physics and Astronomy, Ghent University.

Legates, D. R., & McCabe Jr, G. J. (1999). Evaluating the use of "goodness-of-fit" measures in hydrologic and hydroclimatic model validation. *Water resources research*, *35*(1), 233-241.

Limburg flood was beyond worst case scenario. (2022, January 24). Retrieved from https://nltimes.nl/2022/01/24/limburg-flood-beyond-worst-case-scenario-report

Lindström, G., Johansson, B., Persson, M., Gardelin, M., & Bergström, S. (1997). Development and test of the distributed HBV-96 hydrological model. *Journal of hydrology*, *201*(1-4), 272-288.

Mann-Kendall Test for Trend Overview. (2021). Retrieved from https://help.healthycities.org/hc/en-us/articles/233420187-Mann-Kendall-Test-for-Trend-Overview

Meiners, D. (2002, November). Monitoring Garzweiler II based on the Water Frame Directive–Quantitative Condition of the Groundwater in the Partial Catchment Area of the Niers. In *First International Scientific Symposium on the River Meuse* (p. 32).

Moriasi, D. N., Arnold, J. G., Van Liew, M. W., Bingner, R. L., Harmel, R. D., & Veith, T. L. (2007). Model evaluation guidelines for systematic quantification of accuracy in watershed simulations. *Transactions of the ASABE*, *50*(3), 885-900.

Nash, J. E., & Sutcliffe, J. V. (1970). River flow forecasting through conceptual models part I—A discussion of principles. *Journal of hydrology*, *10*(3), 282-290.

Reinert, D., Frank, H., & Prill, F. (2016). *ICON database reference manual*. Deutscher Wetterdienst. Retrieved August 5, 2022 from https://d-nb.info/1081305452/34

Report Task Force Fact Finding on the High Water & Flooding in NL. (2021, September 16). Retrieved from https://vu.nl/en/news/2021/report-task-force-fact-finding-on-the-high-water-and-flooding-in-the-netherlands-ivm

Rutter, A., Kershaw, K., Robins, P., Morton, A., 1971. A predictive model of rainfall interception in forests, 1. Derivation of the model from observations in a plantation of Corsican pine. Agric. Meteorol. 9, 367–384. https://doi.org/10.1016/0002-1571(71)90034-3

Schellekens, J., Verseveld, W. van, Visser, M., Winsemius, H., Euser, T., Bouaziz, L., Thiange, C., Vries, S. de, Boisgontier, H., Eilander, D., Tollenaar, D., Weerts, A., Baart, F., Hazenberg, P., Lutz, A., Velden, C. ten, Jansen, M., & Benedict, I. (2021). *Openstreams. wflow* (unstable-master, obtained: 17/02/2021). https://github.com/openstreams/wflow

Score definitions and requirements. (2018, April 13). Retrieved from https://confluence.ecmwf.int/display/WLD/Score+definitions+and+requirements

Sharma, P. (2021, September 7). *Flood disaster in Limburg*. Retrieved from https://www.hollandtimes.nl/2021-edition-7-september/flood-disaster-in-limburg/

Van Den Brink, F., & Lanphen, B. (1999). De Niers: grensoverschrijdende beekdalontwikkeling van een laaglandrivier. *Natuurhistorisch Maandblad*, *88*(7), 148-154.

Van Verseveld, W. J., Weerts, A. H., Visser, M., Buitink, J., Imhoff, R. O., Boisgontier, H., ... & Russell, B. (2022). Wflow_sbm v0. 6.1, a spatially distributed hydrologic model: from global data to local applications. *Geoscientific Model Development Discussions*, 1-52.

Vandenberghe, J., De Moor, J. J. W., & Spanjaard, G. (2012). Natural change and human impact in a present-day fluvial catchment: The Geul River, Southern Netherlands. *Geomorphology*, *159*, 1-14.

Vermeulen, P. & op den Kelder, T. (2022, January 22). The Impact of Groundwater Extractions in the Roer Valley Graben. (Report No. 11204053-002-BGS-0001). Deltares, Delft.

Vertessy, R. A., & Elsenbeer, H. (1999). Distributed modeling of storm flow generation in an Amazonian rain forest catchment: Effects of model parameterization. *Water Resources Research*, *35*(7), 2173-2187.

Vidaurre, R., Stein, U., Browne, A., Lordkipanidze, M., Furusho, C., Goedeking, A., ... & Homann, C. (2016). Eifel-Rur: Old Water Rights and Fixed Frameworks for Action. In *Governance for Drought Resilience* (pp. 67-82). Springer, Cham.

Vogel, R. M., & Fennessey, N. M. (1995). Flow duration curves II: A review of applications in water resources planning 1. *JAWRA Journal of the American Water Resources Association*, *31*(6), 1029-1039.

Wannasin, C., Brauer, C. C., Uijlenhoet, R., van Verseveld, W. J., & Weerts, A. H. (2021). Daily flow simulation in Thailand Part I: Testing a distributed hydrological model with seamless parameter maps based on global data. *Journal of Hydrology: Regional Studies*, *34*, 100794.

Werner, M., Schellekens, J., Gijsbers, P., van Dijk, M., van den Akker, O., & Heynert, K. (2013). The Delft-FEWS flow forecasting system. *Environmental Modelling & Software*, *40*, 65-77.

Wasim, S.K. 2022. Predictability of flash flooding in sloping Dutch Catchments (Rur, Niers and Swalm Rivers)

41

Ljubljana, UL FGG, Masters of Science Thesis in Flood Risk Management.

LIST OF APPENDICES

Appendix A   Hydrological Trend Analysis

A.1 Station Gemund (Rur):
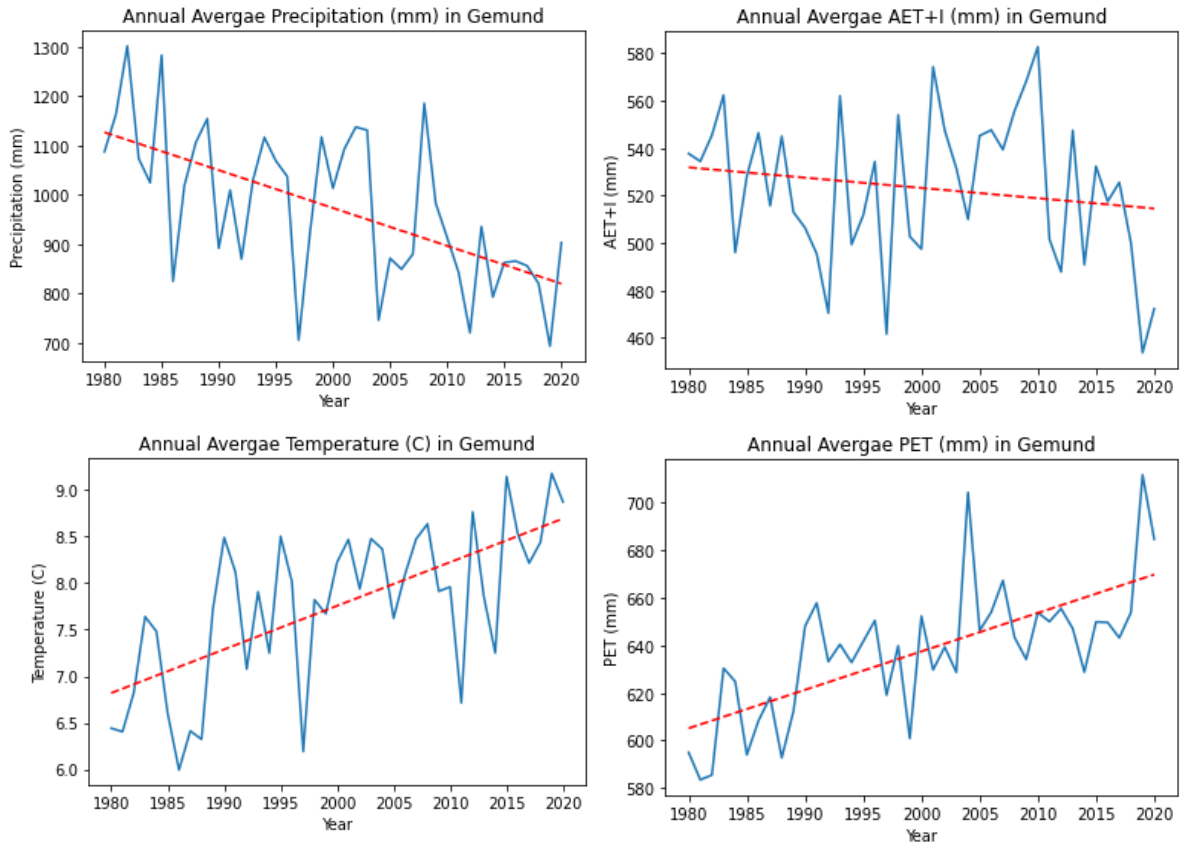
Mann-Kendall test for Annual average analysis:

Analysis for	p-value	z-value	Tau	Sen's slope	Score	Trend
Precipitation (mm)	0.00024	-3.67284	-0.4	-7.913032323	-328	decreasing
AET+I (mm)	0.328481	-0.97718	-0.10732	-0.430200144	-88	no trend
PET (mm)	3.91E-06	4.616327	0.502439	1.447304529	412	increasing
Temperature (C)	1.87E-05	4.279368	0.465854	0.046601368	382	increasing
Observed Discharge (m3/s)	0.003625	-2.90907	-0.31707	-0.041491495	-260	decreasing
Simulated Discharge (m3/s)	0.00022	-3.69531	-0.40244	-0.074742893	-330	decreasing
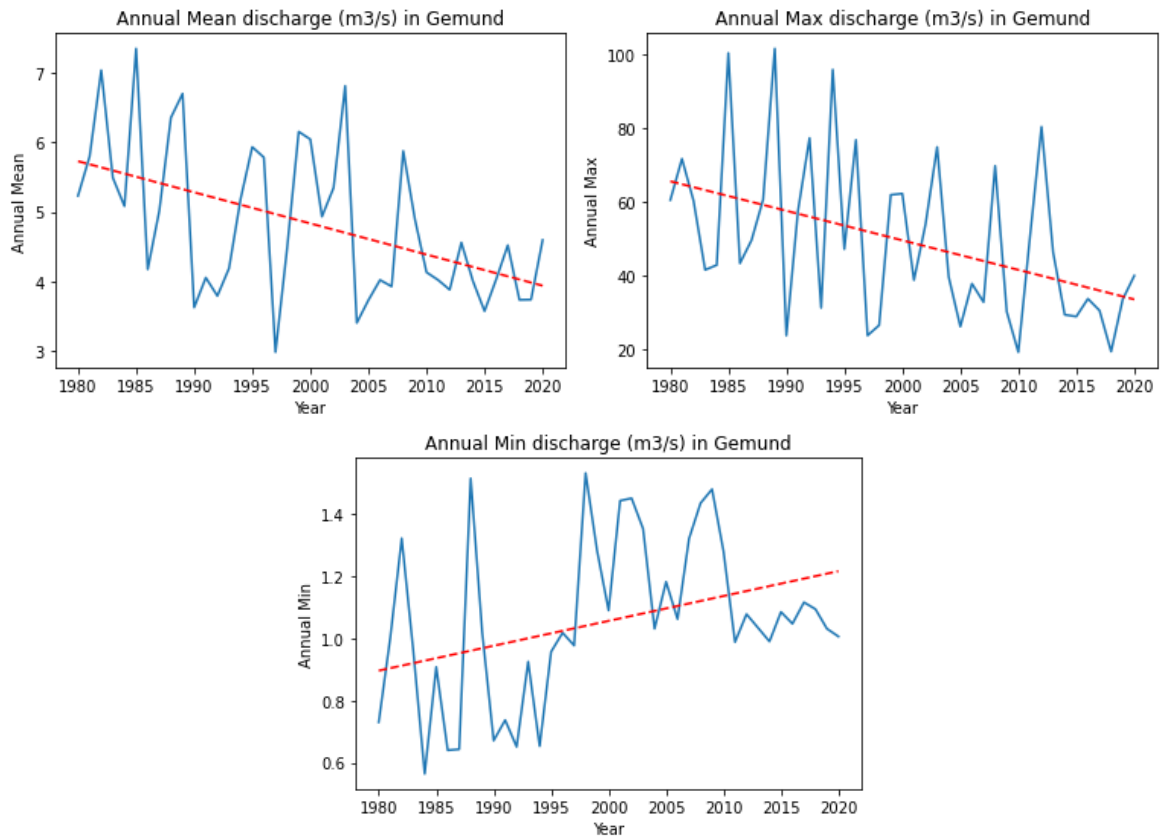
Wasim, S.K. 2022. Predictability of flash flooding in sloping Dutch Catchments (Rur, Niers and Swalm Rivers)

43

Ljubljana, UL FGG, Masters of Science Thesis in Flood Risk Management.

Mann-Kendall test for Observed discharge:

Analysis for	p-value	z-value	Tau	sen slope	score	trend
Annual Mean	0.003625	-2.90907	-0.31707	-0.041491495	-260	decreasing
Annual Max	0.00887	-2.61704	-0.28537	-0.743185185	-234	decreasing
Annual Min	0.01113	2.538578	0.276829	0.006384211	227	increasing

Seasonal Variability of Discharge:
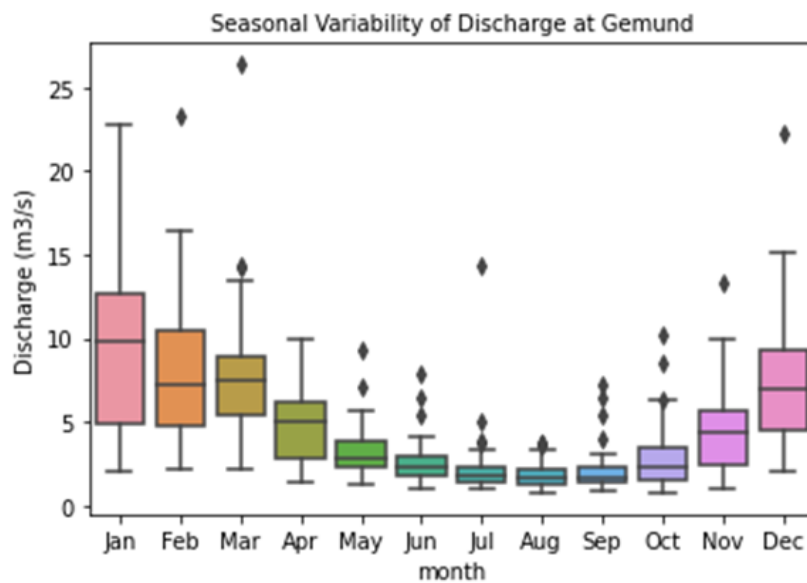
A.2 Station Stah (Rur):
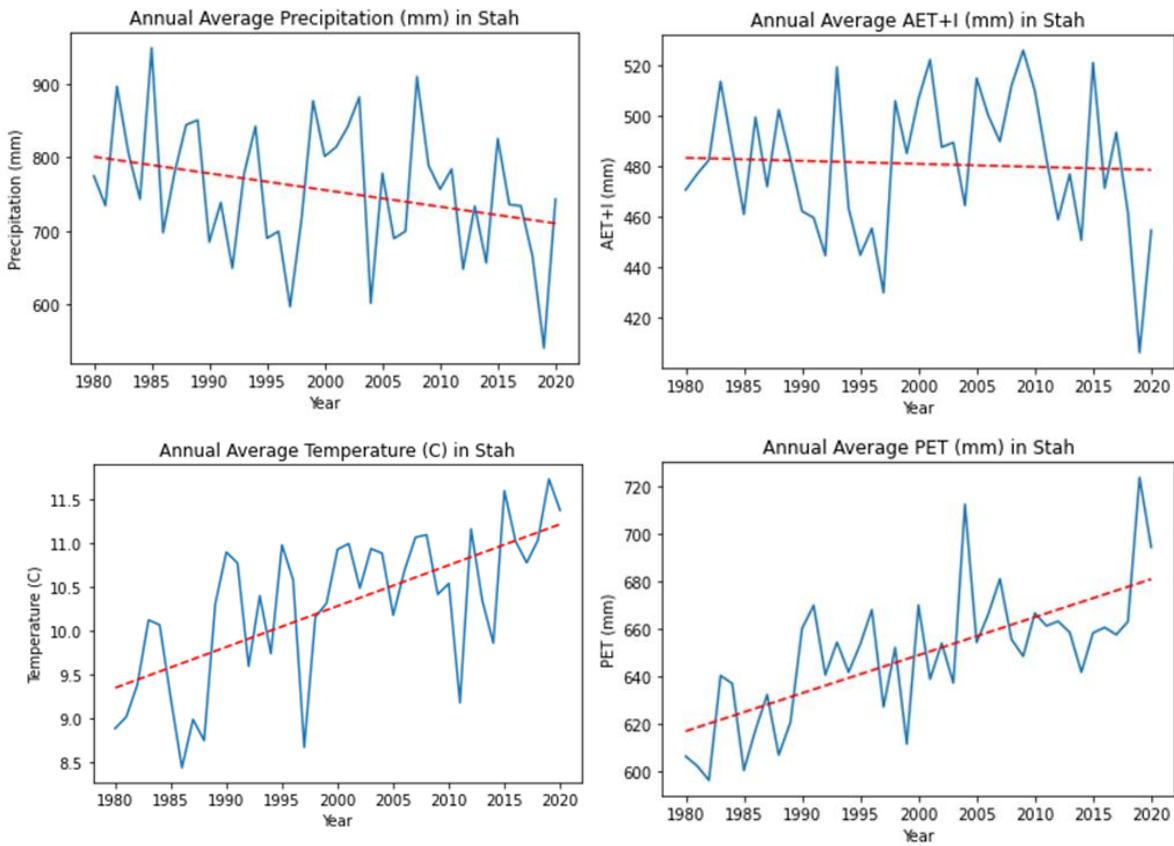
Mann-Kendall test for Annual average analysis:

Analysis for	p-value	z-value	Tau	Sen slope	Score	Trend
Precipitation (mm)	0.098719	-1.65109	-0.18049	-2.214587438	-148	no trend
AET+I (mm)	0.97312	-0.0337	-0.00488	-0.020396663	-4	no trend
PET (mm)	6.00E-06	4.526471	0.492683	1.485540526	404	increasing
Temperature (C)	5.39E-06	4.548935	0.495122	0.047473449	406	increasing
Observed Discharge (m3/s)	0.000168	-3.7627	-0.40976	-0.202095173	-336	decreasing
Simulated Discharge (m3/s)	0.00201	-3.08878	-0.33659	-0.265418682	-276	decreasing
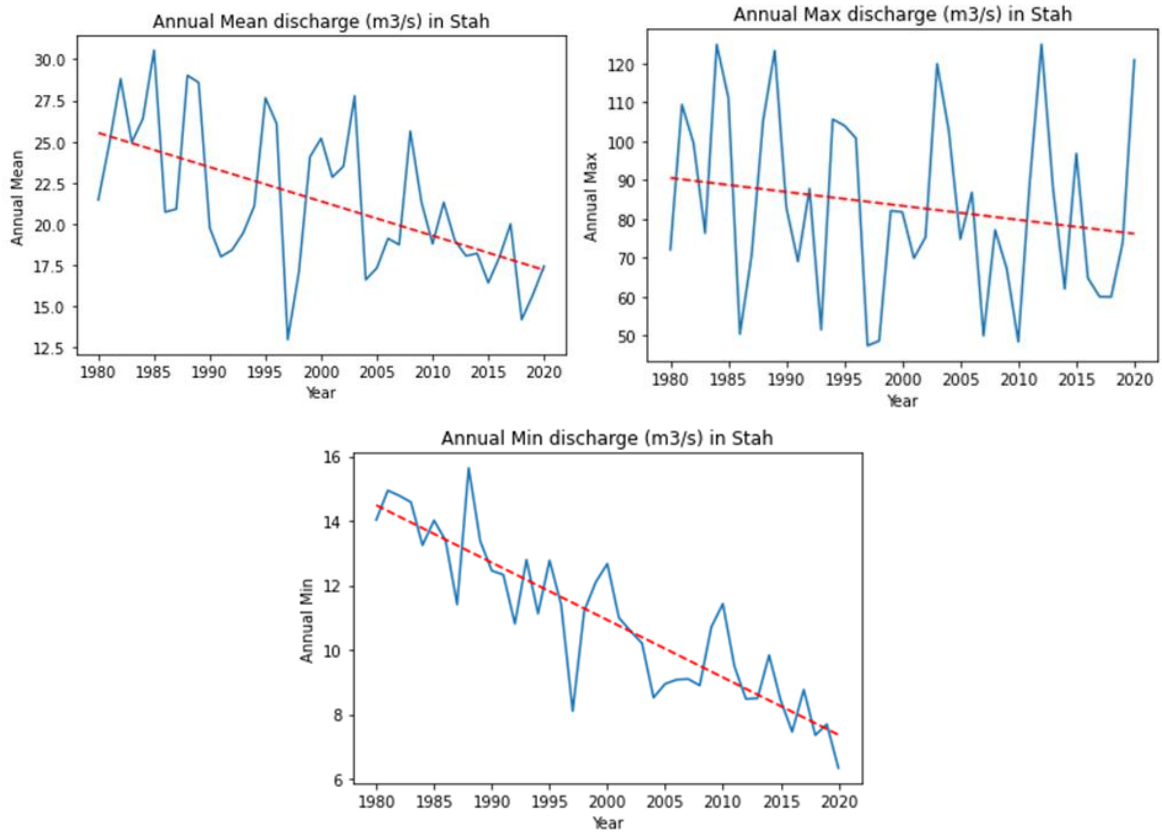
Wasim, S.K. 2022. Predictability of flash flooding in sloping Dutch Catchments (Rur, Niers and Swalm Rivers)

45

Ljubljana, UL FGG, Masters of Science Thesis in Flood Risk Management.

Mann-Kendall test for Observed discharge:

Analysis for	p-value	z-value	Tau	Sen slope	Score	Trend
Annual Mean	0.000168	-3.7627	-0.40976	-0.202095173	-336	decreasing
Annual Max	0.14736	-1.44892	-0.15854	-0.376417457	-130	no trend
Annual Min	2.73E-11	-6.66054	-0.72439	-0.181923701	-594	decreasing

Seasonal Variability of Discharge:
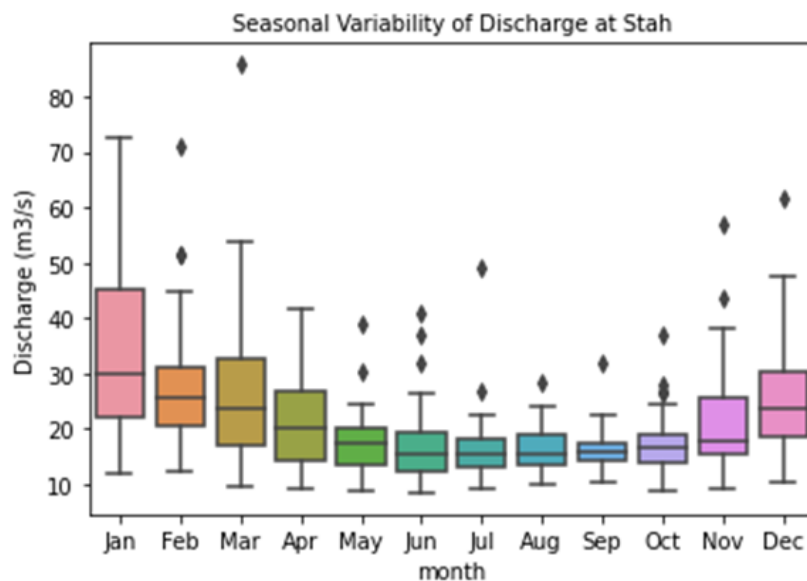
A.3 Station Goch (Niers):
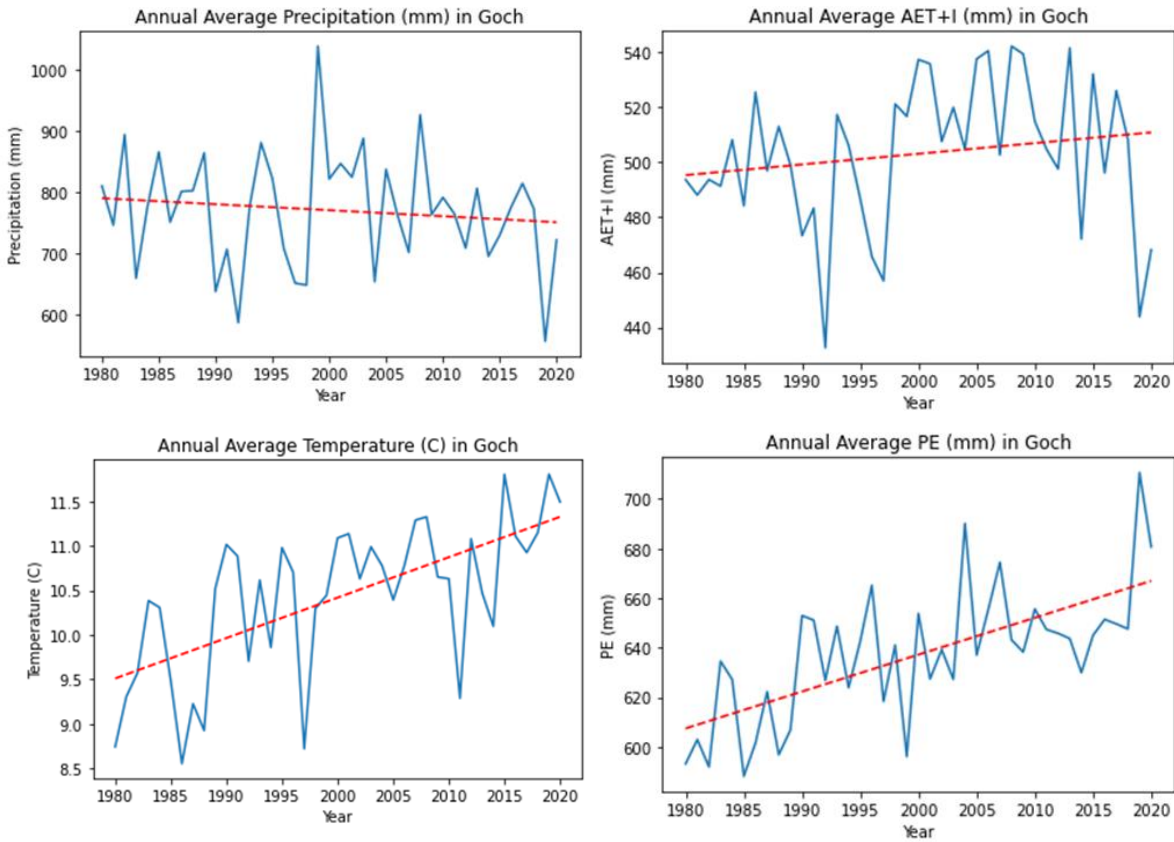
Mann-Kendall test for Annual average analysis:

Analysis for	p-value	z-value	Tau	Sen slope	Score	Trend
Precipitation (mm)	0.451726	-0.75254	-0.08293	-0.959148042	-68	no trend
AET+I (mm)	0.14736	1.44892	0.158537	0.499981784	130	no trend
PE (mm)	1.69E-05	4.301832	0.468293	1.424095659	384	increasing
Temperature (C)	1.12E-05	4.391688	0.478049	0.04435418	392	increasing
Observed Discharge (m3/s)	0.060692	-1.87573	-0.20488	-0.032102345	-168	no trend
Simulated Discharge (m3/s)	0.042054	-2.03298	-0.22195	-0.098597069	-182	decreasing
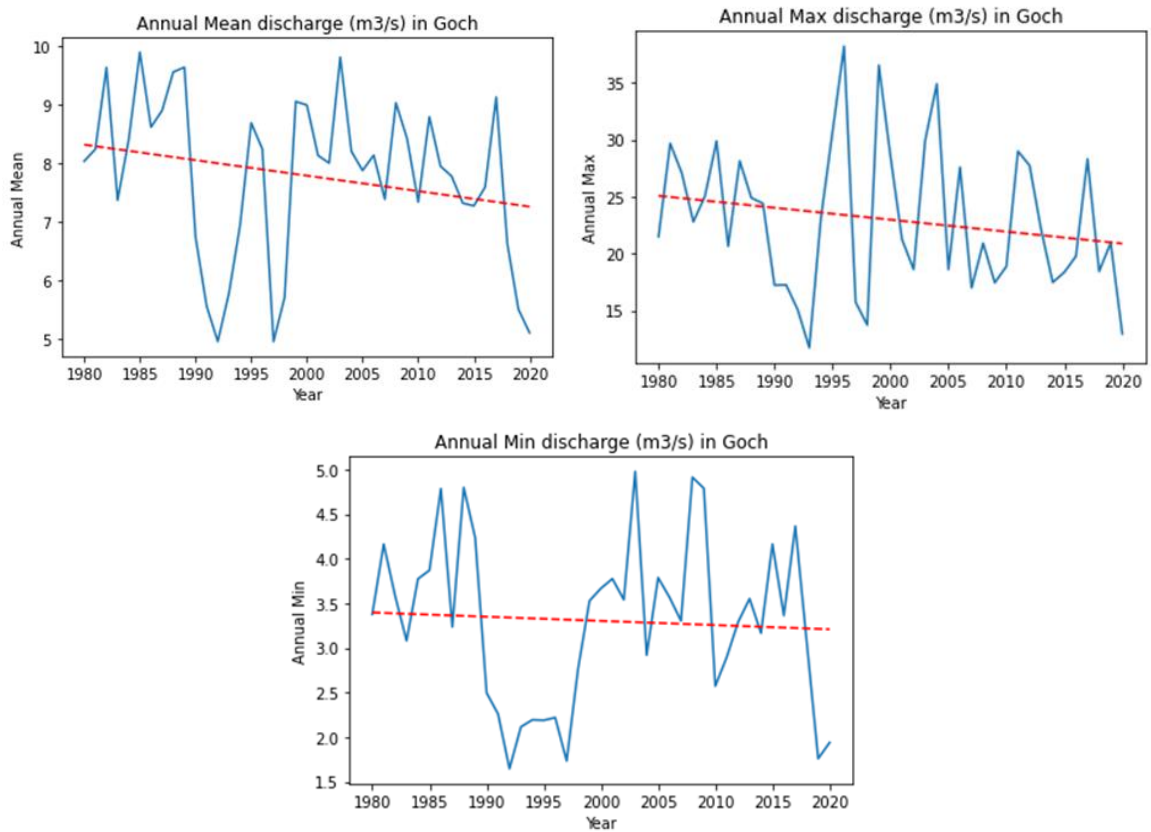
Wasim, S.K. 2022. Predictability of flash flooding in sloping Dutch Catchments (Rur, Niers and Swalm Rivers)

47

Ljubljana, UL FGG, Masters of Science Thesis in Flood Risk Management.

Mann-Kendall test for Observed discharge:

Analysis for	p-value	z-value	Tau	Sen slope	Score	Trend
Annual Mean	0.060692	-1.87573	-0.20488	-0.032102345	-168	no trend
Annual Max	0.19647	-1.29167	-0.14146	-0.11544	-116	no trend
Annual Min	7.28E-01	-0.34819	-0.03902	-0.005274194	-32	no trend

Seasonal Variability of Discharge:
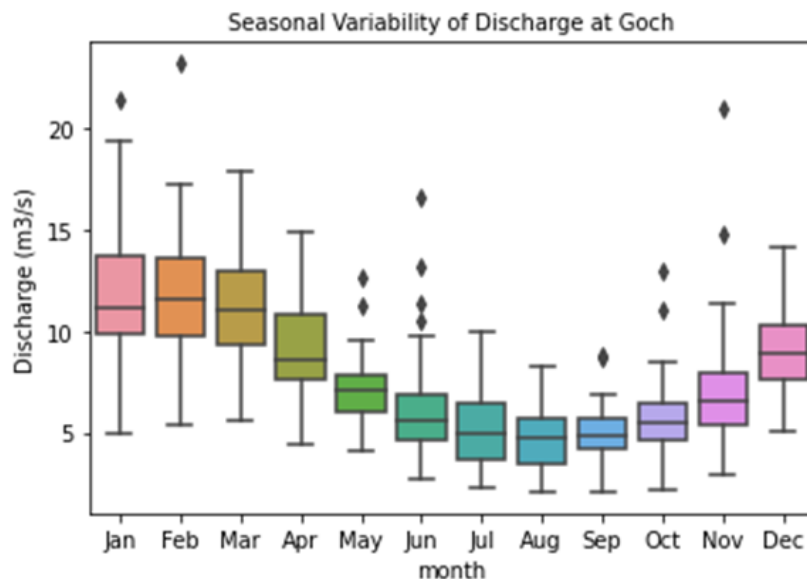
A.4 Station Landesgrenze (Swalm):
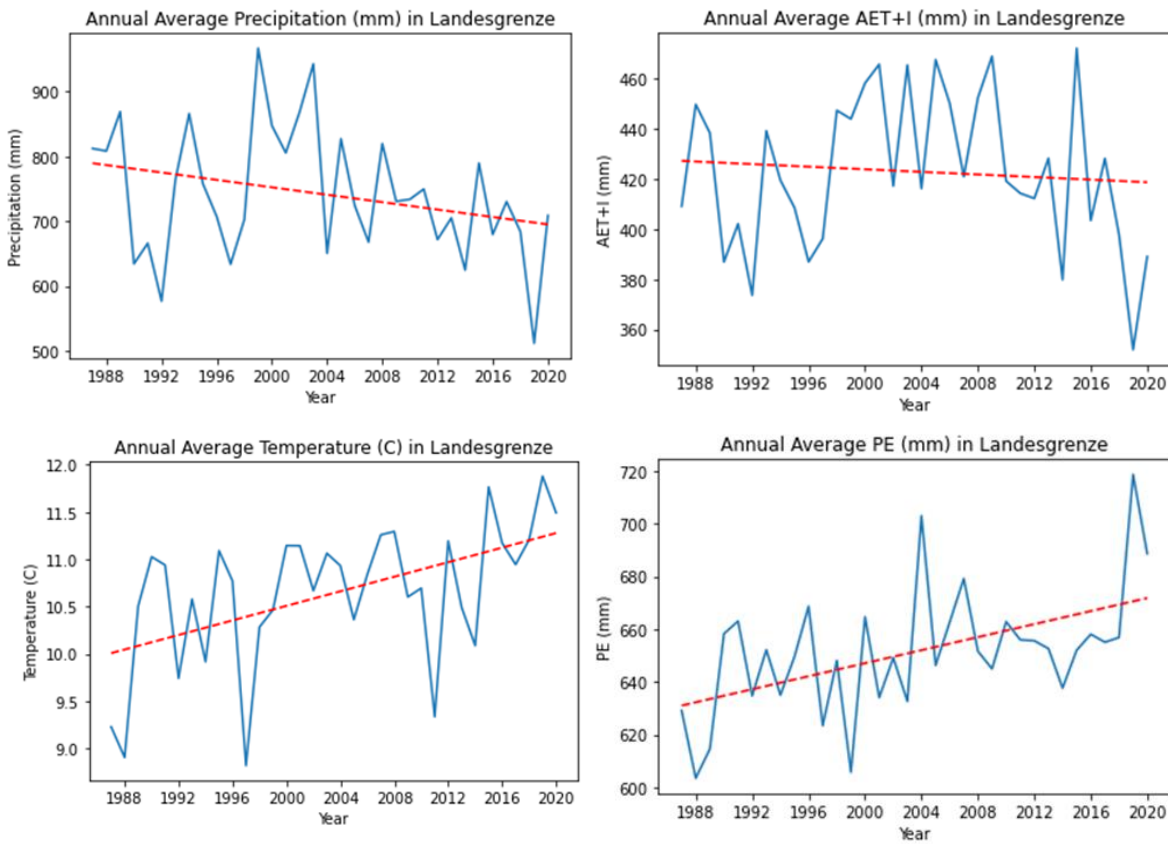
Mann-Kendall test for Annual average analysis:

Analysis for	p-value	z-value	Tau	Sen slope	Score	Trend
Precipitation (mm)	0.123136	-1.54174	-0.18717	-3.11119216	-105	no trend
AET+I (mm)	0.905596	-0.1186	-0.01604	-0.159019521	-9	no trend
PE (mm)	7.62E-03	2.6684	0.322638	1.007545296	181	increasing
Observed Discharge (m3/s)	9.06E-01	-0.1186	-0.01604	-0.0006	-9	no trend
Temperature (C)	0.001674	3.142782	0.379679	0.034295084	213	increasing
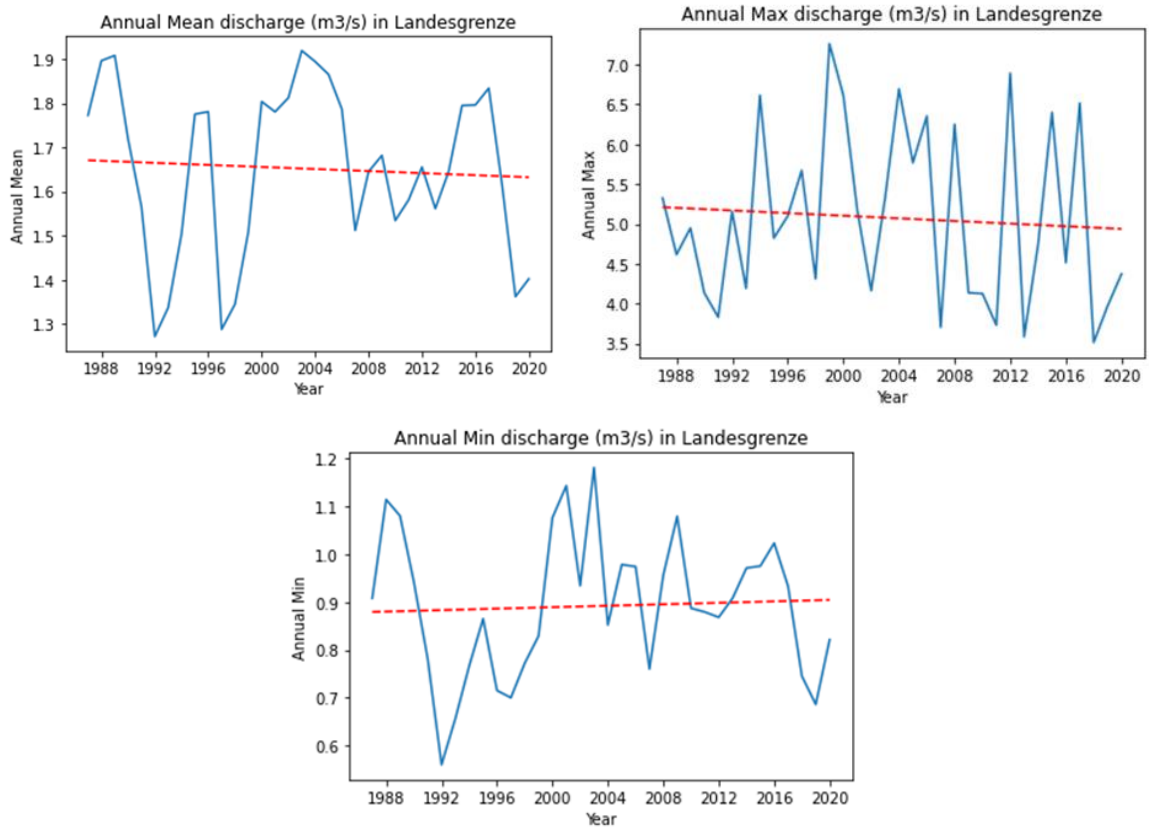
Wasim, S.K. 2022. Predictability of flash flooding in sloping Dutch Catchments (Rur, Niers and Swalm Rivers)

49

Ljubljana, UL FGG, Masters of Science Thesis in Flood Risk Management.

Annual Mean discharge (m3/s) in Landesgrenze

Annual Max discharge (m3/s) in Landesgrenze

Annual Min discharge (m3/s) in Landesgrenze

Mann-Kendall test for Observed discharge:

Analysis for	p-value	z-value	Tau	Sen slope	Score	Trend
Annual Mean	0.905596	-0.1186	-0.01604	-0.0006	-9	no trend
Annual Max	0.53353	-0.62263	-0.07665	-0.011294118	-43	no trend
Annual Min	8.01E-01	0.252043	0.032086	0.00125	18	no trend

Seasonal Variability of Discharge:

Seasonal Variability of Discharge at Landesgrenze
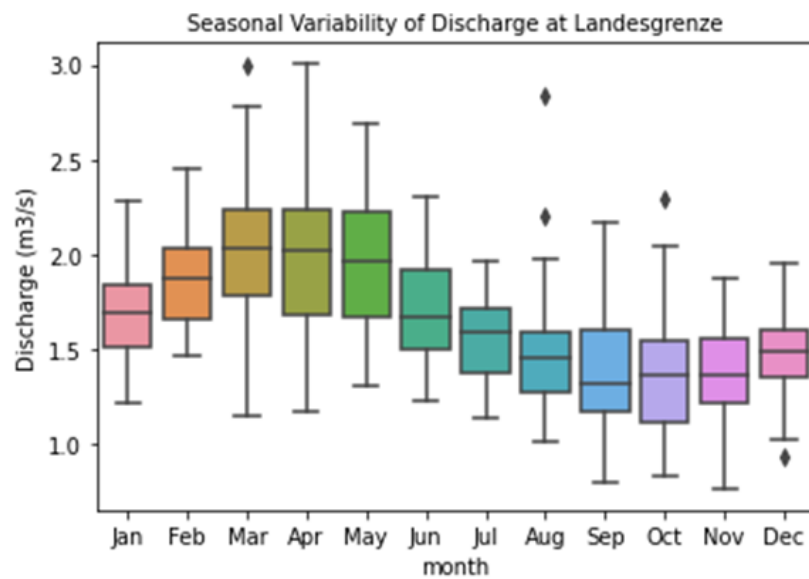
Appendix B   Hydrological Model Parameters

B.1 Niers:

Parameter ID	Parameter Name	Units	Value	Variation
Physiography				
dem	Terrain Elevation	m	[28.9, 100.53]	Spatial
Slope	Terrain Slope	-	[0.003, 0.0486]	Spatial
RiverSlope	River Slope	-	[0, 0.006]	Spatial
riverlength	River Length	m	[75.3, 1968.625]	Spatial
RiverDepth	River Depth	m	[1, 2.108]	Spatial
riverwidth	River Width	m	[30, 108.5]	Spatial
Land use and soil properties				
landuse	Land use	-	class	Spatial
soil	Soil Type	-	class	Spatial
N	Manning parameter for overland flow	$s/m^{1/3}$	[0.01,0.6]	Spatial
N_River	Manning parameter for river flow	$s/m^{1/3}$	[0.03,0.05]	Spatial
SoilMinThickness	Minimum soil depth	mm	[600, 2000]	Spatial
SoilThickness	maximum soil depth	mm	[600, 2000]	Spatial
KsatVer	Vertical saturated conductivity at the surface	mm/day	[83.9, 7788.87]	Spatial
M	decrease of KsatVer with depth	mm	[133, 10,000]	Spatial
thetaR	Residual water content	mm/mm	[0.054, 0.135]	Spatial
thetaS	Water content saturation	mm/mm	[0.406, 0.431]	Spatial
KsatHorFrac*	Horizontal saturated conductivity fraction	-	[20, 800]	Constant/Spatial
Infiltration				
c	Brooks-Corey power co-efficient	-	[7.37, 9.57]	Spatial
cf_soil	Infiltration reduction factor	-	0.038	Constant
InfiltCapPath	Infiltration capacity of compacted soil fraction	mm/day	5	Constant
InfiltCapSoil	Infiltration capacity of non-compacted soil fraction	mm/day	600	Constant
MaxLeakage	Maximum Leakage	mm/day	0	Constant
PathFrac	Fraction of compacted area	-	[0, 0.999]	Spatial
Evaporation				
EoverR	Average wet canopy evaporation over precipitation	-	0.11	Constant
LAI	Monthly leaf area index	-	[0, 2.13]	Spatial/Temporal
SI	Specific leaf storage	mm	[0.02, 0.127]	Spatial
Kext	Light extinction coefficient	-	[0.6,0.8]	Spatial
Swood	"Canopy" capacity of vegetation woody fraction	-	[0, 0.5]	Spatial
RootingDepth	Rooting depth of the vegetation	mm	[46.97, 427.96]	Spatial
rootdistpar	Root connection with the groundwater table	mm	-500	Constant
Snow				
Cfmax	Ice Melting Factor	$mm/(^{o}C/day)$	3.75	Constant
TT	Temperature threshold for snow precipitation	^{o}C	0	Constant
TTI	Temperature range for rain and snow mixing	^{o}C	2	Constant
TTM	Temperature threshold for ice melting	^{o}C	0	Constant
WHC	Fraction of water stored in snow volume	-	0.1	Constant
WaterFrac	Water fraction	-	[0, 0.248]	Spatial

Wasim, S.K. 2022. Predictability of flash flooding in sloping Dutch Catchments (Rur, Niers and Swalm Rivers)

51

Ljubljana, UL FGG, Masters of Science Thesis in Flood Risk Management.

B.2 Swalm

Parameter ID	Parameter Name	Units	Value	Variation
Physiography				
dem	Terrain Elevation	m	[9.8, 116.88]	Spatial
Slope	Terrain Slope	-	[0.001, 0.068]	Spatial
RiverSlope	River Slope	-	[0, 0.0034]	Spatial
riverlength	River Length	m	[75.3, 1968.625]	Spatial
RiverDepth	River Depth	m	[1, 1.47]	Spatal
riverwidth	River Width	m	[30, 108.5]	Spatial
Land use and soil properties				
landuse	Land use	-	class	Spatial
soil	Soil Type	-	class	Spatial
N	Manning parameter for overland flow	$s/m^{1/3}$	[0.011,0.58]	Spatial
N_River	Manning parameter for river flow	$s/m^{1/3}$	[0.03,0.05]	Spatial
SoilMinThickness	Minimum soil depth	mm	[600, 2000]	Spatial
SoilThickness	maximum soil depth	mm	[600, 2000]	Spatial
KsatVer	Vertical saturated conductivity at the surface	mm/day	[122.86, 7024.79]	Spatial
M	decrease of KsatVer with depth	mm	[134, 1446.9]	Spatial
thetaR	Residual water content	mm/mm	[0.064, 0.161]	Spatial
thetaS	Water content saturation	mm/mm	[0.407, 0.451]	Spatial
KsatHorFrac*	Horizontal saturated conductivity fraction	-	[5, 700]	Constant/Spatial
Infiltration				
c	Brooks-Corey power co-efficient	-	[7.47, 8.96	Spatial
cf_soil	Infiltration reduction factor	-	0.038	Constant
InfiltCapPath	Infiltration capacity of compacted soil fraction	mm/day	5	Constant
InfiltCapSoil	Infiltration capacity of non-compacted soil fraction	mm/day	600	Constant
MaxLeakage	Maximum Leakage	mm/day	0	Constant
PathFrac	Fraction of compacted area	-	[0, 0.88]	Spatial
Evaporation				
EoverR	Average wet canopy evaporation over precipitation	-	0.11	Constant
LAI	Monthly leaf area index	-	[0, 2.363]	Spatial/Temporal
SI	Specific leaf storage	mm	[0, 0.127]	Spatial
Kext	Light extinction coefficient	-	[0.6,0.8]	Spatial
Swood	"Canopy" capacity of vegetation woody fraction	-	[0, 0.5]	Spatial
RootingDepth	Rooting depth of the vegetation	mm	[0, 429.8]	Spatial
rootdistpar	Root connection with the groundwater table	mm	-500	Constant
Snow				
Cfmax	Ice Melting Factor	mm/(^{o}C/day)	3.75	Constant
TT	Temperature threshold for snow precipitation	^{o}C	0	Constant
TTI	Temperature range for rain and snow mixing	^{o}C	2	Constant
TTM	Temperature threshold for ice melting	^{o}C	0	Constant
WHC	Fraction of water stored in snow volume	-	0.1	Constant
WaterFrac	Water fraction	-	[0, 0.72]	Spatial

Appendix C   Hydrological Model Calibration

C.1 Rur

C.1.1 Indicator for best KsatHorFrac for different time period

Station	Year	Pbias Value	Pbias Ksat	RMSE Value	RMSE Ksat	NSE Value	NSE Ksat	LogNSE Value	LogNSE Ksat	KGE Value	KGE Ksat	KGE_np Value	KGE_np Ksat	KsatHorFrac Average
Kall Sportplatz	1981-1990	0.31	200	1.35	650	0.65	650	0.78	650	0.82	650	0.9	570	560
	1991-2000	1.21	50	1.13	650	0.7	650	0.78	650	0.77	650	0.85	370	500
	2001-2010	-8.52	650	1.05	350	0.71	350	0.8	570	0.8	300	0.85	570	460
	2011-2019	-0.07	600	0.83	320	0.71	320	0.85	370	0.83	250	0.9	350	360
Gemund	1981-1990	0.05	500	3.53	370	0.76	370	0.84	350	0.88	350	0.91	300	370
	1991-2000	-0.63	650	2.76	350	0.83	350	0.73	500	0.9	470	0.9	350	440
	2001-2010	-14.36	650	2.57	250	0.79	250	0.63	550	0.79	250	0.8	400	390
	2011-2019	-22.89	650	2.53	200	0.74	200	0.53	600	0.69	150	0.73	450	370
Monschau	1981-1990	-29.76	650	3.18	120	0.7	120	0.76	220	0.64	50	0.66	250	230
	1991-2000	-19.17	650	2.31	100	0.82	100	0.84	150	0.74	50	0.76	200	200
	2001-2010	-23.03	650	2.43	120	0.73	120	0.81	200	0.69	50	0.72	200	220
	2011-2019	-38.52	650	2.85	50	0.65	50	0.74	220	0.5	50	0.58	200	200
Zerkall	1981-1990	6.3	50	6.3	300	0.67	300	0.41	350	0.72	50	0.53	450	250
	1991-2000	1.18	50	4.78	350	0.66	350	0.47	600	0.8	50	0.55	650	340
	2001-2010	-11.67	650	5.82	200	0.47	200	0.23	250	0.58	50	0.43	50	230
	2011-2019	-22.07	650	7.69	100	0.15	100	0.21	200	0.16	50	0.42	100	200
Mulartshutte	1981-1990	-8.1	650	0.53	150	0.62	150	0.65	220	0.74	100	0.78	120	230
	1991-2000	-17.99	650	0.54	100	0.63	100	0.64	300	0.69	50	0.72	220	230
	2001-2010	-29.04	650	0.7	50	0.54	50	0.68	250	0.5	50	0.64	150	200
	2011-2019	-33.95	650	0.65	50	0.54	50	0.63	250	0.43	50	0.59	200	200
Kornelimunster	1981-1990	3.67	50	0.74	650	0.68	650	0.57	650	0.82	650	0.8	600	540
	1991-2000	6.96	50	0.58	650	0.72	650	0.74	650	0.76	650	0.84	520	520
	2001-2010	13.22	50	0.64	650	0.66	650	0.69	650	0.75	650	0.77	470	520
	2011-2019	9.14	50	0.67	650	0.61	650	0.72	650	0.76	570	0.8	320	480
Eschweiler	1981-1990	11.48	50	2.37	650	0.66	650	0.75	650	0.71	650	0.8	550	530
	1991-2000	13.02	50	2.05	650	0.63	650	0.76	650	0.65	650	0.79	300	490
	2001-2010	2.4	50	1.93	650	0.73	650	0.78	650	0.85	500	0.87	450	490
	2011-2019	7.35	50	1.99	650	0.69	650	0.8	450	0.8	550	0.84	250	430
Herzogenrath	1981-1990	-22.25	650	1.88	650	-3.88	650	-1.99	650	0.29	650	0.53	650	650
	1991-2000	-25.94	650	1.62	650	-0.18	650	-3.09	650	0.37	650	0.56	650	650
	2001-2010	-24.11	650	1.55	650	0.003	650	-2.2	650	0.48	650	0.56	650	650
	2011-2019	-19.76	650	1.64	650	-0.18	650	-1.97	650	0.36	650	0.63	650	650
Julich	1981-1990	15.5	50	9.26	650	0.58	650	0.54	500	0.74	650	0.7	650	520
	1991-2000	2.58	50	7.5	650	0.57	650	0.64	650	0.7	650	0.74	650	550
	2001-2010	1.54	50	7.13	650	0.63	650	0.57	650	0.81	650	0.7	300	490
	2011-2019	2.67	50	7.86	650	0.57	650	0.54	200	0.73	100	0.67	150	300
Randerath	1981-1990	0.06	250	4.09	650	-2.42	650	-2.19	650	-0.46	650	0.59	650	580
	1991-2000	0.22	250	3.81	650	-1.99	650	-1.85	650	-0.31	650	0.57	650	580
	2001-2010	6.6	50	3.72	650	-1.46	650	-0.54	650	-0.1	650	0.59	650	550
	2011-2019	12.69	50	3.67	650	-1.88	650	-0.45	650	0.26	650	0.58	650	550
Stah	1981-1990	19.8	50	18.27	650	-0.6	650	0.32	650	0.09	650	0.68	650	550
	1991-2000	19.48	50	16.42	650	-0.62	650	0.35	650	0.04	650	0.69	650	550
	2001-2010	15.63	50	14.24	650	-0.34	650	0.37	650	0.2	650	0.69	650	550
	2011-2019	16.42	50	13.42	650	-0.14	650	0.47	650	0.36	650	0.7	250	480

Wasim, S.K. 2022. Predictability of flash flooding in sloping Dutch Catchments (Rur, Niers and Swalm Rivers)

53

Ljubljana, UL FGG, Masters of Science Thesis in Flood Risk Management.

C.1.2 Range of indicator values for different KsatHorFrac from 1981-1990

Station	KsatHorFrac for	1981-1990					
		Pbias	RMSE	NSE	LogNSE	KGE	KGE_np
Kall Sportplatz	550	3.80	1.38	0.64	0.77	0.78	0.89
	500	3.44	1.40	0.62	0.76	0.83	0.90
	450	3.05	1.44	0.60	0.73	0.82	0.90
	370	2.35	1.52	0.56	0.67	0.79	0.89
Gemund	370	-0.75	3.50	0.76	0.84	0.85	0.85
	450	-0.22	3.54	0.75	0.83	0.83	0.85
	400	-0.53	3.50	0.76	0.84	0.84	0.85
Monschau	220	-31.11	3.14	0.68	0.78	0.55	0.68
	200	-31.26	3.11	0.69	0.78	0.56	0.68
Zerkall	250	5.17	0.90	0.51	0.01	0.65	0.77
	350	5.69	0.83	0.58	0.28	0.72	0.79
	200	4.85	0.94	0.46	-0.23	0.61	0.76
Mulartshutte	220	-10.27	0.54	0.60	0.65	0.45	0.69
	200	-10.48	0.53	0.61	0.65	0.46	0.69
Kornelimunster	550	6.48	0.76	0.65	0.51	0.79	0.80
	520	6.38	0.77	0.64	0.49	0.77	0.81
	470	6.19	0.78	0.63	0.45	0.76	0.81
Eschweiler	550	15.16	2.43	0.61	0.74	0.69	0.80
	500	14.97	2.47	0.59	0.73	0.67	0.80
	450	14.76	2.51	0.58	0.73	0.66	0.80
Herzogenrath	650	-22.38	1.86	-0.36	-2.02	0.38	0.57
Julich	300	16.42	9.91	0.45	0.53	0.64	0.69
	400	16.61	9.66	0.48	0.54	0.66	0.69
	500	16.77	9.47	0.50	0.55	0.67	0.70
	550	16.84	9.39	0.51	0.55	0.68	0.70
Randerath	570	3.45	4.28	-2.66	-2.97	-0.32	0.55
	550	3.30	4.32	-2.73	-3.10	-0.34	0.54
Stah	400	20.47	18.67	-0.67	0.29	0.06	0.68
	450	20.53	18.58	-0.65	0.30	0.07	0.68
	500	20.58	18.50	-0.64	0.30	0.07	0.68
	550	20.64	18.42	-0.63	0.31	0.08	0.68

54   Wasim, S.K. 2022. Predictability of flash flooding in sloping Dutch Catchments (Rur, Niers and Swalm Rivers).

Ljubljana, UL FGG, Masters of Science Thesis in Flood Risk Management.

C.1.3 Range of indicator values for different KsatHorFrac from 1991-2000

Station	KsatHorFrac for	1991-2000					
		Pbias	RMSE	NSE	LogNSE	KGE	KGE_np
Kall Sportplatz	550	9.34	1.14	0.70	0.79	0.76	0.86
	500	8.81	1.15	0.70	0.78	0.83	0.90
	450	8.20	1.17	0.69	0.76	0.82	0.90
	370	7.04	1.22	0.66	0.72	0.79	0.89
Gemund	370	-4.60	2.76	0.83	0.72	0.85	0.85
	450	-3.88	2.83	0.82	0.73	0.83	0.85
	400	-4.31	2.78	0.83	0.72	0.84	0.85
Monschau	220	-21.30	2.52	0.79	0.82	0.55	0.68
	200	-21.52	2.47	0.79	0.83	0.56	0.68
Zerkall	250	9.03	0.73	0.57	0.31	0.61	0.82
	350	9.96	0.67	0.64	0.53	0.67	0.84
	200	8.47	0.77	0.52	0.12	0.57	0.81
Mulartshutte	220	-20.34	0.58	0.59	0.66	0.45	0.69
	200	-20.65	0.57	0.60	0.65	0.46	0.69
Kornelimunster	550	11.38	0.60	0.71	0.72	0.75	0.85
	520	11.19	0.61	0.70	0.70	0.77	0.81
	470	10.85	0.62	0.69	0.67	0.76	0.81
Eschweiler	550	18.92	2.09	0.61	0.76	0.63	0.78
	500	18.64	2.12	0.60	0.75	0.62	0.78
	450	18.33	2.15	0.59	0.74	0.61	0.79
Herzogenrath	650	-25.00	1.62	-0.15	-2.85	0.38	0.57
Julich	300	7.93	8.34	0.51	0.62	0.64	0.75
	400	8.20	8.14	0.53	0.63	0.65	0.75
	500	8.41	7.99	0.55	0.64	0.67	0.75
	550	8.50	7.93	0.55	0.65	0.67	0.75
Randerath	570	5.69	3.91	-2.07	-1.92	-0.32	0.55
	550	5.51	3.94	-2.12	-2.01	-0.34	0.54
Stah	400	20.36	16.77	-0.69	0.33	0.02	0.69
	450	20.44	16.70	-0.67	0.33	0.02	0.69
	500	20.52	16.62	-0.66	0.34	0.03	0.69
	550	20.59	16.55	-0.64	0.34	0.03	0.69

Wasim, S.K. 2022. Predictability of flash flooding in sloping Dutch Catchments (Rur, Niers and Swalm Rivers)

55

Ljubljana, UL FGG, Masters of Science Thesis in Flood Risk Management.

C.1.4 Range of indicator values for different KsatHorFrac from 2001-2010

Station	KsatHorFrac for	2001-2010					
		Pbias	RMSE	NSE	LogNSE	KGE	KGE_np
Kall Sportplatz	550	-9.51	1.09	0.68	0.80	0.74	0.85
	500	-10.08	1.08	0.69	0.80	0.83	0.90
	450	-10.73	1.06	0.70	0.79	0.82	0.90
	370	-11.93	1.05	0.71	0.75	0.79	0.89
Gemund	370	-16.38	2.71	0.77	0.59	0.85	0.85
	450	-15.64	2.86	0.74	0.62	0.83	0.85
	400	-16.08	2.77	0.76	0.61	0.84	0.85
Monschau	220	-25.19	2.55	0.70	0.81	0.55	0.68
	200	-25.41	2.52	0.71	0.81	0.56	0.68
Zerkall	250	16.00	0.76	0.52	0.35	0.68	0.76
	350	16.92	0.71	0.58	0.53	0.72	0.77
	200	15.44	0.80	0.48	0.19	0.65	0.75
Mulartshutte	220	-32.08	0.76	0.46	0.67	0.45	0.69
	200	-32.35	0.75	0.47	0.66	0.46	0.69
Kornelimunster	550	18.29	0.65	0.65	0.67	0.75	0.77
	520	18.11	0.66	0.64	0.66	0.77	0.81
	470	17.78	0.67	0.63	0.63	0.76	0.81
Eschweiler	550	8.52	1.93	0.72	0.77	0.84	0.86
	500	8.27	1.94	0.71	0.77	0.84	0.86
	450	7.99	1.95	0.71	0.76	0.83	0.86
Herzogenrath	650	-24.12	1.55	0.00	-2.21	0.38	0.57
Julich	300	2.70	7.47	0.59	0.56	0.79	0.70
	400	2.93	7.34	0.60	0.56	0.80	0.70
	500	3.13	7.24	0.61	0.56	0.81	0.70
	550	3.22	7.20	0.62	0.57	0.81	0.70
Randerath	570	17.00	3.84	-1.63	-0.68	-0.32	0.55
	550	16.80	3.87	-1.68	-0.73	-0.34	0.54
Stah	400	16.45	14.59	-0.41	0.36	0.17	0.69
	450	16.52	14.52	-0.39	0.36	0.18	0.69
	500	16.59	14.44	-0.38	0.36	0.18	0.69
	550	16.66	14.37	-0.37	0.37	0.19	0.69

C.1.5 Range of indicator values for different KsatHorFrac from 2011-2019

Station	KsatHorFrac for	2011-2019					
		Pbias	RMSE	NSE	LogNSE	KGE	KGE_np
Kall Sportplatz	550	-0.78	0.88	0.67	0.82	0.69	0.88
	500	-1.57	0.86	0.69	0.83	0.83	0.90
	450	-2.46	0.85	0.70	0.85	0.82	0.90
	370	-4.13	0.83	0.71	0.85	0.79	0.89
Gemund	370	-25.02	2.75	0.69	0.47	0.85	0.85
	450	-24.21	2.90	0.65	0.51	0.83	0.85
	400	-24.69	2.81	0.68	0.49	0.84	0.85
Monschau	220	-40.44	3.15	0.57	0.74	0.55	0.68
	200	-40.63	3.10	0.58	0.73	0.56	0.68
Zerkall	250	12.59	0.78	0.51	0.44	0.70	0.80
	350	13.71	0.74	0.56	0.60	0.73	0.80
	200	11.95	0.80	0.47	0.28	0.68	0.79
Mulartshutte	220	-37.22	0.71	0.44	0.62	0.45	0.69
	200	-37.55	0.71	0.46	0.60	0.46	0.69
Kornelimunster	550	15.38	0.70	0.60	0.71	0.76	0.80
	520	15.17	0.70	0.60	0.70	0.77	0.81
	470	14.80	0.71	0.59	0.69	0.76	0.81
Eschweiler	550	13.62	2.00	0.69	0.80	0.80	0.83
	500	13.31	2.01	0.69	0.80	0.80	0.83
	450	12.97	2.02	0.69	0.80	0.80	0.83
Herzogenrath	650	-19.76	1.64	-0.18	-1.97	0.38	0.57
Julich	300	4.15	8.09	0.54	0.54	0.72	0.67
	400	4.47	8.00	0.55	0.54	0.71	0.67
	500	4.74	7.94	0.56	0.54	0.71	0.67
	550	4.85	7.91	0.56	0.54	0.70	0.67
Randerath	570	24.84	4.01	-2.21	-0.54	-0.32	0.55
	550	24.63	4.05	-2.27	-0.58	-0.34	0.54
Stah	400	17.31	13.80	-0.20	0.46	0.33	0.70
	450	17.39	13.72	-0.19	0.46	0.34	0.70
	500	17.46	13.64	-0.18	0.46	0.34	0.70
	550	17.54	13.56	-0.16	0.46	0.35	0.70

Wasim, S.K. 2022. Predictability of flash flooding in sloping Dutch Catchments (Rur, Niers and Swalm Rivers)

57

Ljubljana, UL FGG, Masters of Science Thesis in Flood Risk Management.

C.1.6 Comparison of Annual mean discharge with the calibrated model
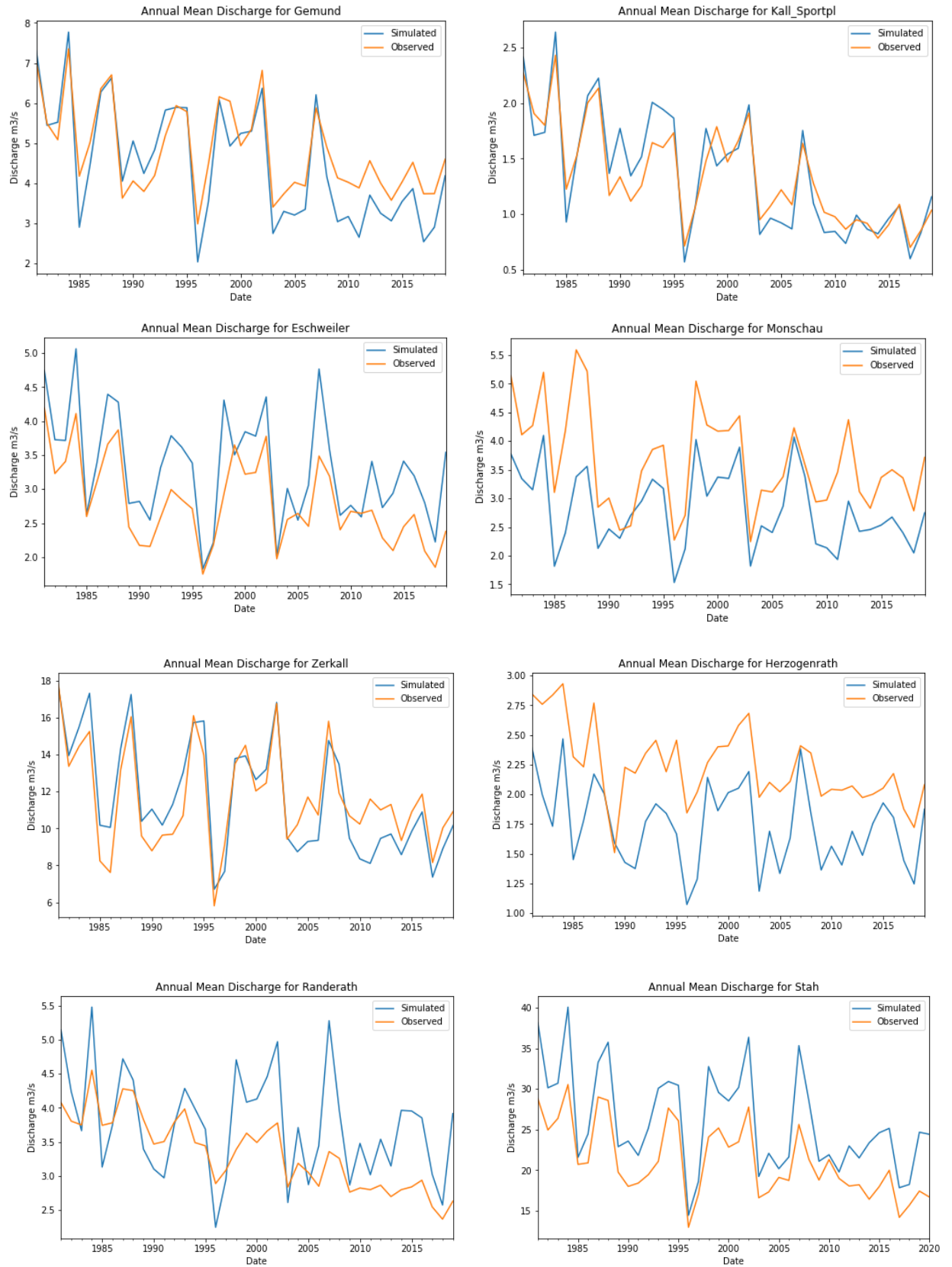
C.2 Niers

C.2.1 Indicator for Best KsatHorFrac for Different Time Period

| Station | Year | Indicators | | | | | | | | | | | | KsatHorFrac |
| | | Pbias | | RMSE | | NSE | | LogNSE | | KGE | | KGE_np | | Average |
		Value	Ksat	Value	Ksat	Value	Ksat	Value	Ksat	Value	Ksat	Value	Ksat	
Goch	1981-1990	56.8	5	10.45	800	-5.68	800	-0.69	350	-0.7	800	0.23	50	460
	1991-2000	0.08	5	11.6	800	-5.65	800	-0.73	350	-0.98	800	0.08	5	460
	2001-2010	44.04	5	9.28	800	-5.27	800	-0.92	350	-0.66	800	0.3	50	460
	2011-2029	34.7	5	7.13	800	-2.72	800	-0.14	350	0.27	800	0.39	50	460
Oedt	1981-1990	90.84	5	5.45	800	-24	800	-3.7	500	-2.76	800	-0.12	5	480
	1991-2000	81.37	5	5.13	800	-21.1	800	-2.92	500	-2.6	800	-0.04	5	480
	2001-2010	38.78	5	4.53	800	-17.1	800	-3.15	800	-2.33	800	0.21	350	590
	2011-2019	23.89	5	3.22	800	-9.67	800	-1.33	800	-1.52	800	0.36	350	590

C.2.2 Comparison of hydrographs for KsatHorFrac=20 and 800 in Oedt

Wasim, S.K. 2022. Predictability of flash flooding in sloping Dutch Catchments (Rur, Niers and Swalm Rivers)

59

Ljubljana, UL FGG, Masters of Science Thesis in Flood Risk Management.
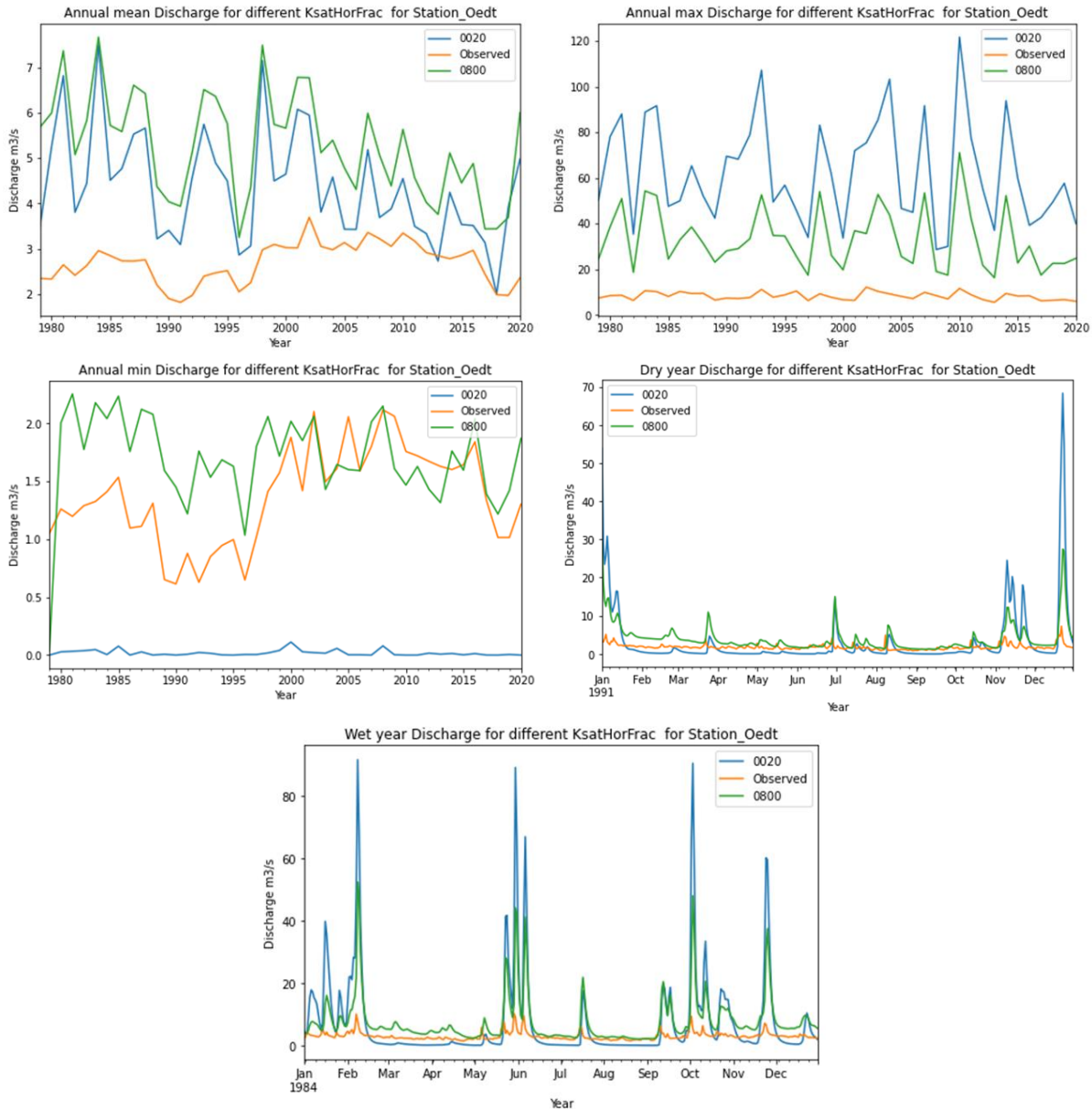
C.3 Swalm

C.3.1 Comparison of hydrographs for KsatHorFrac=20,250 and 500 in Landesgrenze
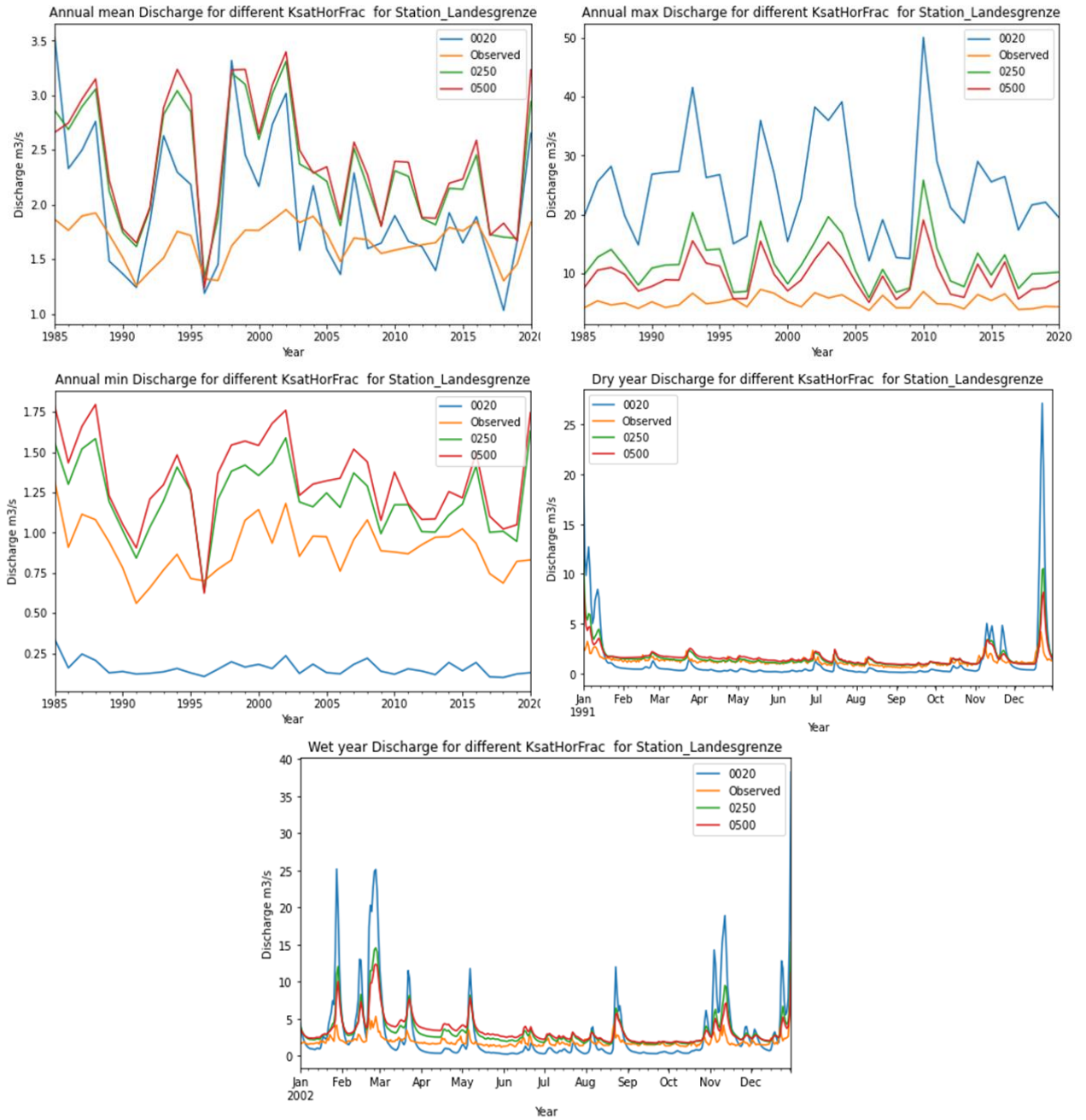
C.3.2 Comparison of hydrographs for KsatHorFrac=20,250 and 500 in Pannenmuhle

Wasim, S.K. 2022. Predictability of flash flooding in sloping Dutch Catchments (Rur, Niers and Swalm Rivers)

61

Ljubljana, UL FGG, Masters of Science Thesis in Flood Risk Management.
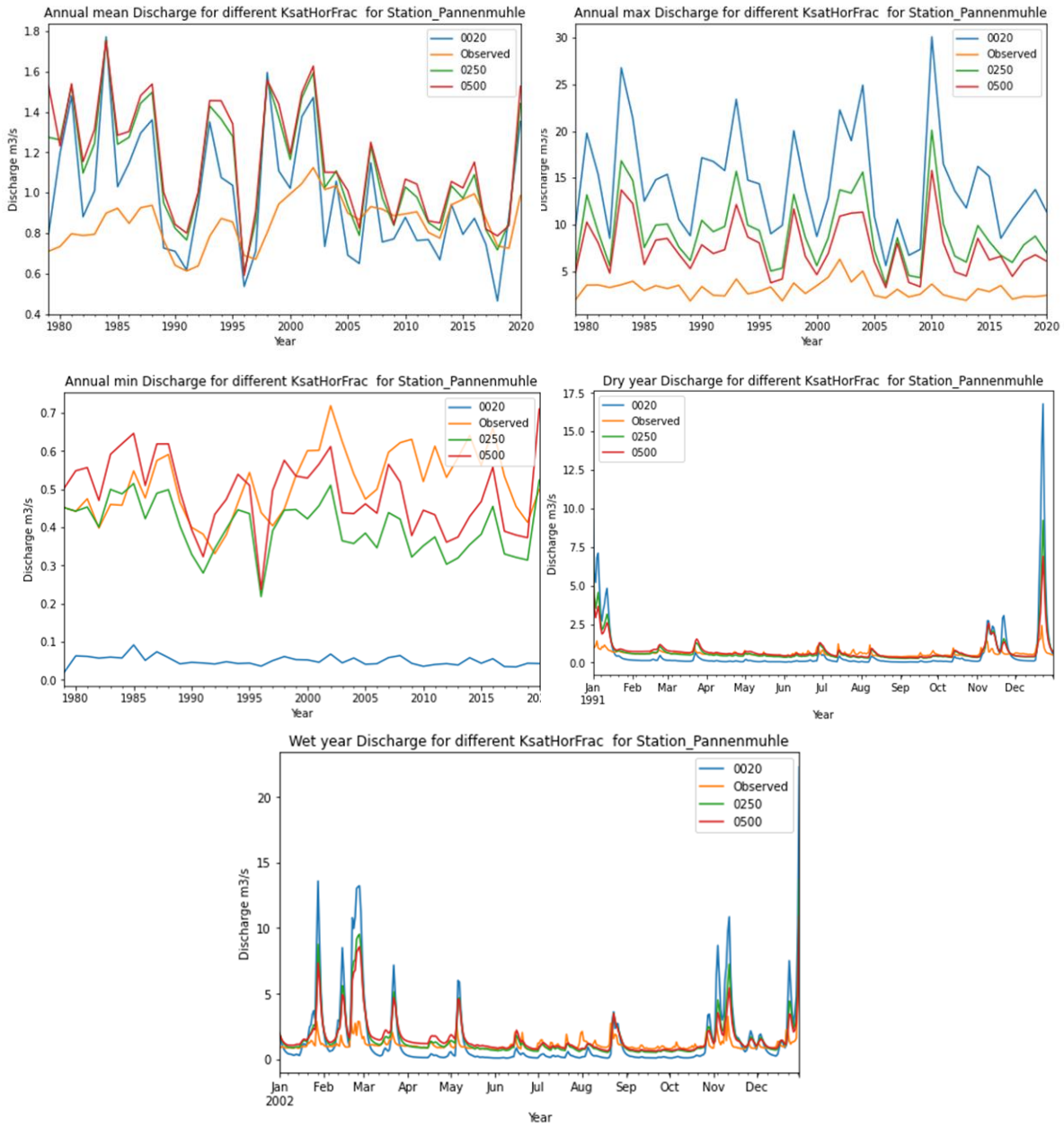
C.3.3 Comparison of hydrographs for KsatHorFrac=20,250 and 500 in Molzmuhle
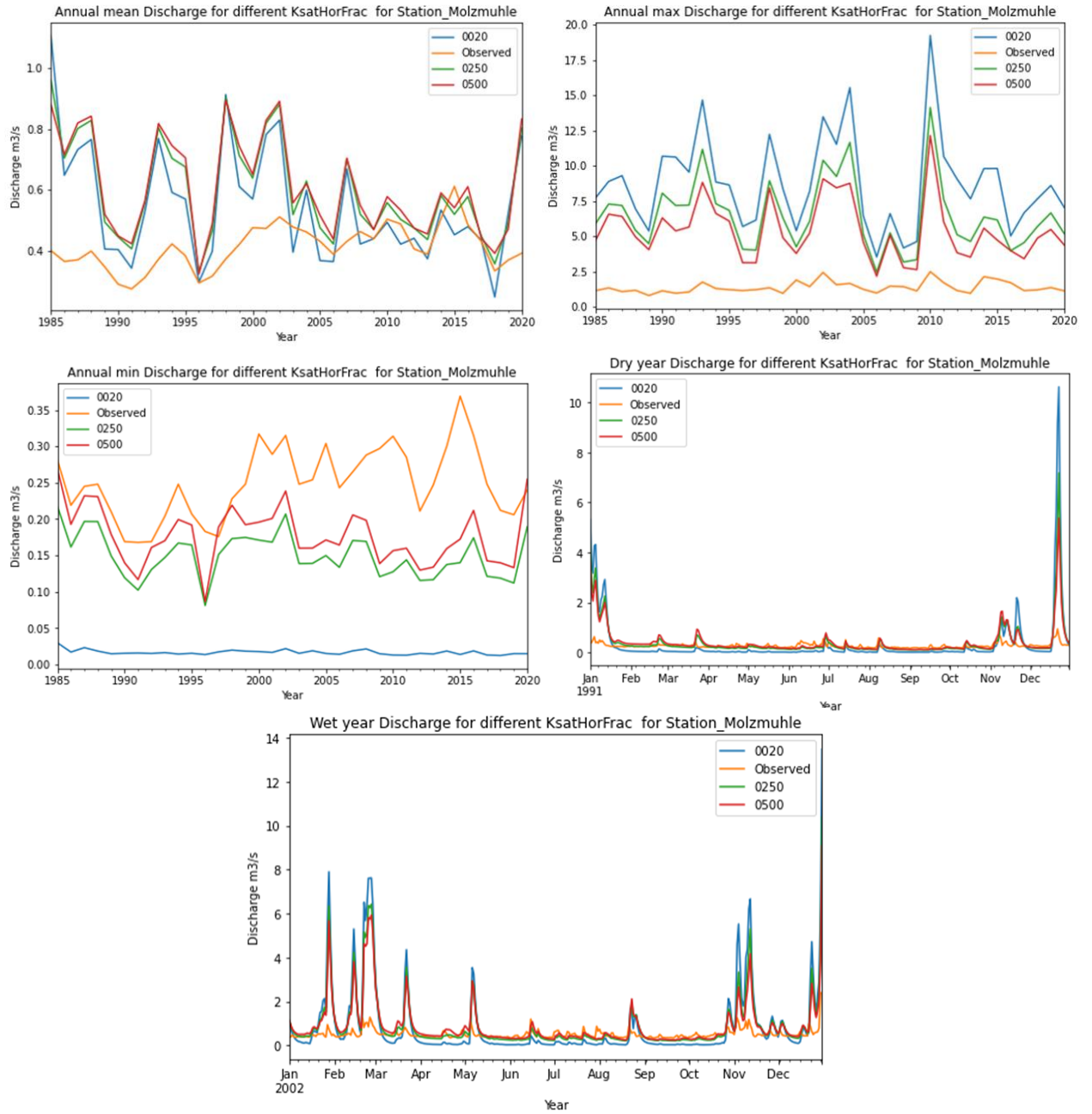
Appendix D   Water Balance Analysis

D.1 Rur

D.2 Swalm

Wasim, S.K. 2022. Predictability of flash flooding in sloping Dutch Catchments (Rur, Niers and Swalm Rivers)

63

Ljubljana, UL FGG, Masters of Science Thesis in Flood Risk Management.
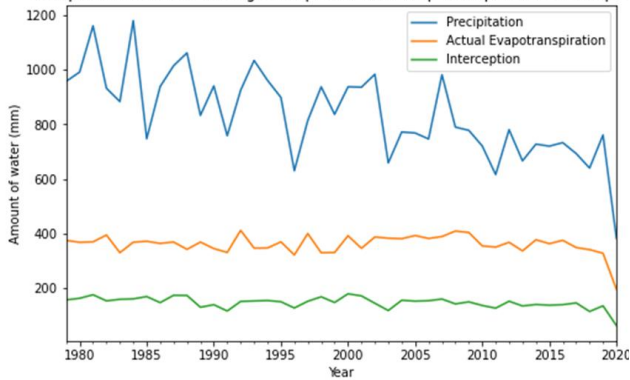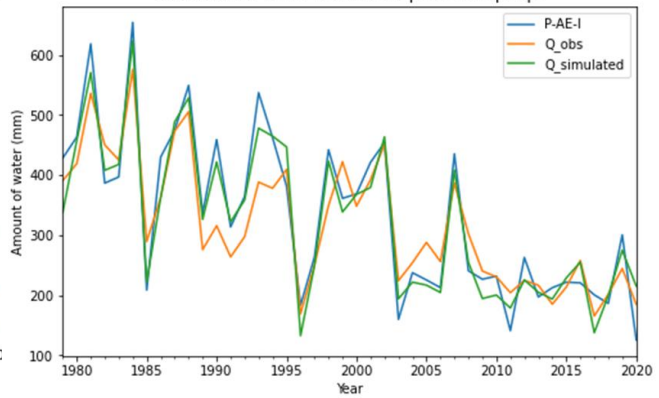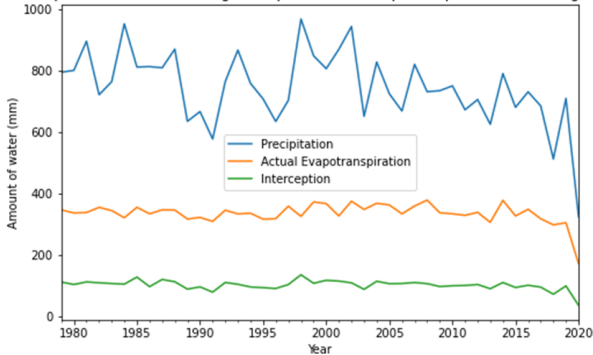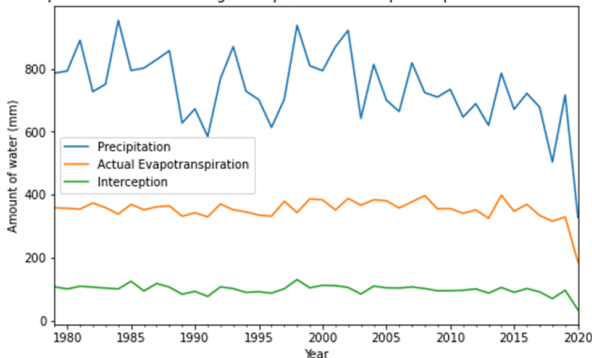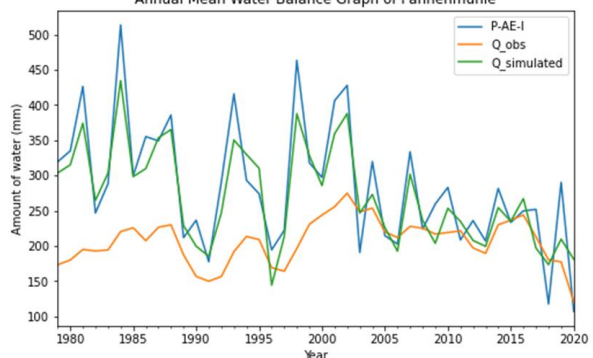
Appendix E   Evaluation of Forecast Performance

E.1 Gemund (Rur)
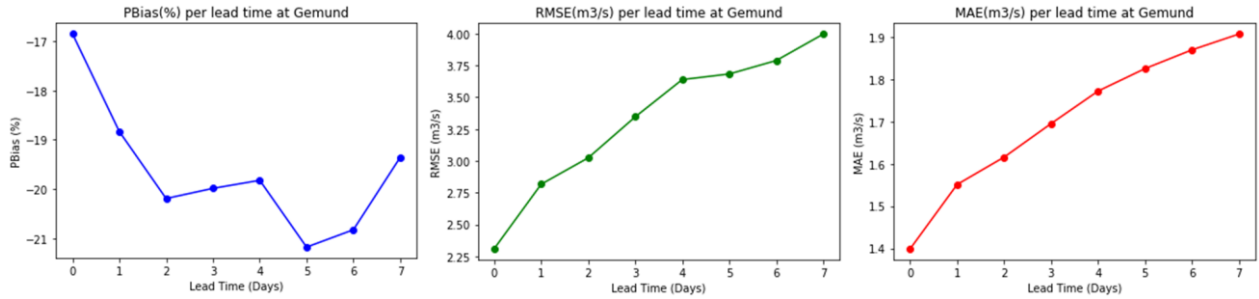
E.2 Kall-Sportplatz (Rur)
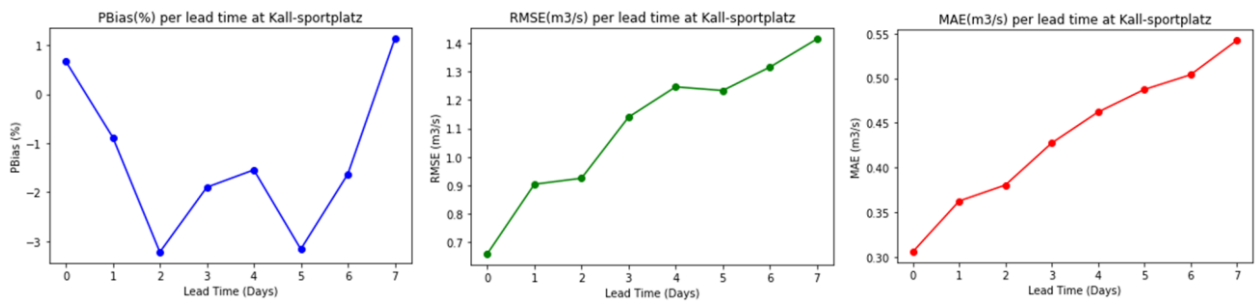
E.3 Eschweiler (Rur)

E.4 Zerkall (Rur)